CHAPTER 6

MODELS OF *C. BIMACULATA* DEVELOPMENT AND PHENOLOGY

6.1 INTRODUCTION

The main purpose of the models described in this chapter is to allow forest managers or entomologists to predict the time of peak occurrence of each of the *C. bimaculata* larval instars for a given compartment. Of particular interest in the Leaf Beetle IPM program is the time of this peak for each of the L1 to L3 larval instars. The time interval between the peaks of the L1 and L2 larvae is the critical period in which the population can be controlled before the L3 and L4 larvae feed. This is because there is little benefit in carrying out insecticidal control after the peak of the L2 stage if it fails to prevent the last two larval instars from feeding since together they consume almost 90% of the foliage (Greaves, 1966). In addition, if insecticidal control is to be used, for example using the broad-spectrum insecticide cypermethrin (Elliott *et al*. 1992; Greener and Candy, 1994), it should be delayed until after the majority of eggs have hatched to allow the population to be re-assessed (Fig. 1.4). This is because control is only required if this pre-control population assessment indicates that predation levels, or other natural mortality factors, have not been sufficient to reduce the population below the ‘action threshold‘ (Section 7.2). Since the majority of predation occurs at the egg stage (de Little *et al*., 1990) population assessments of later (i.e. L2 to L4) instars are unlikely to change the control decision and, importantly, may reduce the ‘control window’. The ‘control window’ can be considered the period starting from the time the decision is made to control up to the time of peak occurrence of L2 larvae (Section 7.9). In addition, application of the biotic insecticide, *Bacillus thuringiensis*, must be applied before larvae develop to less susceptible instars, (i.e. L2 or later), and ideally should coincide with peak occurrence of the L1 larvae (Greener and Candy, 1994; Elek and Beveridge, 1999).

From a pest management perspective, these important milestones in population development are defined above in terms of peak occurrence. However, occurrence can be defined in terms of relative or absolute population size. Time of peak *relative* occurrence of a stage is defined as the time, in either Julian days or physiological time units such as day-degrees, at which that stage represents the highest proportion of population relative to the other stages. Peak (absolute) occurrence for a stage, on

the other hand, is the time when the absolute number of individuals in that stage is greatest. Once recruitment of eggs is completed, the effect of mortality is to reduce the total population as time progresses. However, the number of individuals recruited to a larval stage will increase during this time up until the time of the stage's peak relative occurrence. The net effect is that the time of the peak in absolute numbers for a larval stage will occur before the time of peak relative occurrence. The difference in the time of these peaks depends on the relative rate of mortality compared to stage recruitment.

Phenology models that simultaneously incorporate sub-models of mortality and stage duration time allow the time of peak absolute occurrence to be predicted (e.g. Munholland and Dennis, 1992). However, mortality is a much 'noisier' stochastic process than temperature-driven development so that the accuracy of predictions of mortality over time in different seasons and sites to those of the calibration data sets may be so poor as to be irrelevant or even misleading. Further, these simultaneously fitted mortality/stage-duration-time models can usually only estimate a simple, stage-independent, constant mortality rate (Manly, 1990, Table 4.2; Munholland and Dennis, 1992). This approach is unrealistic if natural mortality factors are highly specific to different stages which is the case for populations of *C. bimaculata*. Mortality from oviposition to 'mid-first instar larvae' was reported by de Little *et al*. (1990) for two sites in Tasmania to represent between 66 and 84% of losses compared to total losses over all stages of between 95 and 97%. Therefore, predictive models that incorporate a stage-specific mortality function are required.

To avoid the difficulty in modelling mortality while still providing a description of population development of practical interest, relative occurrence, or the probability of observing a stage conditional on population size (Candy, 1991) was modelled. However, the effect of mortality on the difference between times of peak relative and peak absolute numbers in each stage was investigated using the mortality data reported by de Little *et al*. (1990).

To construct a model to predict the time of peak relative occurrence of each larval instar, given inputs that are easily and cheaply obtained by scouts, involves : (a) developing a model of development rate as a function of temperature that can be used

to construct a physiological time scale using ambient temperatures in the field (e.g. day-degrees) and, using this time scale, (b) fit a model of the field phenology of the successive development stages of interest. For *C. bimaculata* these are egg to final instar (L4) larval stages.

Models of the development rate/temperature relationship were calibrated from a study of development time for individual cohorts under constant temperature regimes (Greaves, 1966; de Little *et al*., 1990) where the cohorts were individual egg batches. Gilbert and Raworth (1996) estimate that similar studies have been published for over 300 species. The models in (b) were calibrated using stage-frequency data (Manly, 1990) collected from a population of (egg batch) cohorts recruited over a period that was short relative to the total development period. To accomplish (a) two simple models of development rate as a function of temperature were fitted; the familiar linear or day-degree model and a 3-parameter nonlinear model. These models were validated using a small sample of 'total' development times (i.e. the time from oviposition to initiation of the pre-pupal stage) for a sample of individual cohorts observed in the field. Corresponding candidate physiological time scales were then constructed and these used as the main input to predict field phenology (b) using the continuation ratio (CR) models described by Candy (1991).

Some of the statistical methods/results described have not been used previously in this type of application. These include : (i) maximum likelihood estimation of development rate/temperature response models for development times observed under fluctuating temperatures in the field and (ii) further developments to the method of modelling stage-frequency data using continuation ratios introduced by Candy (1991). The theory described in (i) is a generalisation of the distribution theory of Sharpe *et al*. (1977) for development times obtained in constant temperature studies to those obtained under ambient temperatures in the field. The developments in (ii) include a method to predict time to peak relative occurrence of each of L1 to L3 larval stages.

6.2 MODELS OF DEVELOPMENT RATE AS A FUNCTION OF TEMPERATURE : CONSTANT TEMPERATURE

6.2.1 The linear model and a nonlinear model

Most of the work on insect development rates as a function of temperature has concentrated on laboratory studies where each of a number of cohorts of each developmental stage is exposed to a given temperature and observations made on the time taken for individuals to complete development. The development time for the particular cohort/temperature regime is taken as the mean or median of the individual development times, where this mean or median time is denoted *l* and given in relevant time units such as Julian days. For the following *l* will refer to the mean development time. The empirical rate of development for the particular cohort/temperature regime is taken as $r = l^{-1}$ with units 'the proportion of development per unit time' (e.g. proportion per day). There have been many different model forms used for the development rate/temperature relationship $r = F(T, \boldsymbol{\theta})$, where T is temperature and $\boldsymbol{\theta}$ is a vector of unknown parameters, from the simple linear (or day-degree model) (Howe, 1967) to complex multi-parameter nonlinear models (Sharpe and DeMichele, 1977; Schoolfield *et al*., 1981). Two simple models were considered here. Firstly, the linear model given by

$$\begin{aligned} F_D(T, \boldsymbol{\theta}) &= \theta_1 (T - \theta_2) \qquad T > \theta_2 \\ &= 0 \qquad\qquad\quad T \leq \theta_2 \end{aligned} \tag{6.1}$$

where the parameter defining the lower developmental threshold temperature is θ_2 while θ_1 is a rate parameter (Howe, 1967). Alternatively, the simple nonlinear model used by Berry *et al*. (1977) and Vogt *et al*. (1990) is given by

$$F_N(T, \boldsymbol{\theta}) = \theta_1 \exp(\theta_2 T + \theta_3 T^2) \tag{6.2}$$

where a lower development threshold is not specified as in (6.1) but instead development rate is defined to reach a peak or optimum rate of $\theta_1 \exp\left(-\frac{\theta_2^2}{4\theta_3}\right)$ at

temperature $T_{opt} = -\frac{\theta_2}{2\theta_3}$ given the constraints $\theta_2 > 0$ and $\theta_3 < 0$. The quadratic term in *T* within the exponential in (6.2) allows development rate to decrease for $T > T_{opt}$ given $\theta_3 < 0$. If the quadratic term is excluded by setting θ_3 to zero then development rate increases exponentially with *T*. Such a model can only be realistic for temperatures below T_{opt} since at sufficiently high temperatures the health of the insect will deteriorate until finally a lethal temperature is reached. The parameter θ_2 in model (6.1) and parameters (θ_2, θ_3) in model (6.2) are temperature response parameters, denoted in general by the vector $\boldsymbol{\theta}^*$, since they control the 'shape' of the rate versus temperature response curve while θ_1 is the rate parameter in each case. Model (6.1) is a step function so that the change in 'shape' can be interpreted as the change in development rate as temperature passes through the change-point defined by θ_2.

Following Stinner *et al*. (1974), if the cohort is observed over time *t* then integrating (6.1) or (6.2) to mean time to completion of development (i.e. $t = l$) for fluctuating temperatures gives

$$1 = \int_0^l F\{T(t), \boldsymbol{\theta}\}\, dt \qquad (6.3).$$

If temperature is held constant so that $T(t) = T$ then from (6.1) the following relation is obtained for $T > \theta_2$

$$1 = \theta_1 (T - \theta_2) l \ .$$

This gives $(T - \theta_2) l$ as the day-degrees, or heat sum, required for completion of development for an average development time, *l*, with lower threshold, or base, temperature of θ_2 and rate parameter $\theta_1 = \{(T - \theta_2) l\}^{-1}$. The parameter θ_1 can be interpreted as the proportion of development per unit of day-degrees. For model (6.2) the above relation becomes

$$1 = \theta_1 \exp\left(\theta_2 T + \theta_3 T^2\right) l$$

so that the analogous nonlinear heat sum of $\left(\theta_2 T + \theta_3 T^2\right) l$ can be defined and similarly $\theta_1 = \left\{\exp\left(\theta_2 T + \theta_3 T^2\right) l\right\}^{-1}$.

6.2.2 DATA AND ESTIMATION METHODS

To provide initial estimates of parameters for (6.1) and (6.2), these models were fitted to constant temperature data (Greaves, 1966; de Little[1] *et al*., 1990; Clarke, 1998). These data were mean development periods for each of the egg, and L1 to L4 stages at temperatures of 8, 15, 20, 24, and 27^{o}C for *C. bimaculata* reared on *E. regnans* foliage (Greaves, 1966). The usual approach in the case of the linear model (6.1) is to fit a simple linear regression separately for each stage to the observed mean rate, *r*, the reciprocal of the mean development time at each temperature. Here, the 'linear' model was fitted in its nonlinear (i.e. in θ_2) form, given by (6.1), simultaneously to all stages with factors (or dummy variables) allowing specification of separate parameters for each stage. This allows the use of the F-statistic using the extra sum of squares principle (Draper and Smith, 1981, p.97; Ratkowsky, 1983, p.135) to test for a common lower threshold parameter across *s* stages (i.e. $\boldsymbol{\theta}^* = \theta_{2j}$, $j = 1...s$). The same approach can be used for the nonlinear model (6.2) with the test for common $\boldsymbol{\theta}^* = \left(\theta_{2j}, \theta_{3j}\right)$ carried out in two stages, that is : (a) test for common θ_3 and if (a) is accepted then (b) test if both $\left(\theta_2, \theta_3\right)$ are common to the stages. Here, since only mean and not individual development times were available, testing the fit of each model by application of the lack-of-fit test using pure error (Draper and Smith, 1981, p.33) was not available and examination of residuals was not very informative.

Although it is usual practice to use *r* as the response value in the regression, the time to completion of development, *l* (or its inverse, *r*), is not observed exactly. Rather, the experimenter observes the number of individuals, say n_i, that have emerged as

---

[1] These constant temperature data were recorded by Greaves but Greaves (1966) gave a combined, total development time for L1 to L3 stages. The development times for each larval instar were obtained by de Little *et al*. (1990) by personal communication with Greaves.

adults (or that have moulted to the next stage if progression of each stage is observed) between sampling times, t_i and t_{i+1} where t_0 is the start of development and the first emergents appear between t_1 and t_2. The midpoint of the time interval between two sampling points is then used as an approximation to the observed development time for all individuals emerging in that interval (Howe, 1967) and the regression is weighted by the number of individuals, n_i, for each (Dallwitz and Higgins, 1992). More rigorously, the observed response variable is not this approximate development time but rather the n_i. Given the total over all *m* observation periods of the n_i, $N = \sum_{i=1}^{m} n_i$, then the n_i can be assumed to be multinomially distributed. However, this distribution cannot be exploited for estimation using the constant temperature data of Greaves since the n_i are not known but they are known for a small data set of observations made in the field described in Section 6.3.4.

6.2.3 RESULTS

The hypothesis of a stage-independent θ_2 parameter for (6.1) (Table 6.1) was accepted. Table 6.2 gives the parameter estimates for the fit of (6.1) with common θ_2. Note that the data for total development, that is the total of the five stages, was not used in the above fit. The inverse of the estimate of θ_1 gives the estimated day-degrees, denoted simply by *DD* with dependence on θ_2 implicit, or more specifically by $DD[\hat{\theta}_2]$. Table 6.2 gives the *DD* and its approximate standard error for each stage. The approximate standard error was calculated from the variance of the estimate of θ_1, the inverse functional relationship, and its first-order Taylor series expansion (Bickel and Doksum, 1977, p.31) giving $Var(DD) \cong Var(\hat{\theta}_1) DD^4$.

Note that the sum of the *DD* across the five stages does not exactly equal *DD* calculated from the total development time due to the inverse relationship between mean rate (*r*) and mean development time (*l*) (Table 6.2). The standard error of the sum of the individual stage estimates of *DD* can be calculated from the sum of their variances. However, this standard error is not given in Table 6.2 because it would be misleading due to the positive correlation between development times for individual insects as they progress through the stages.

Table 6.1 Fit statistics for development rate models to constant temperature data

Model	Pooled Parameters	Error df	EMS[a] x 10^{-3}	F-statistic	Prob[b]
Linear (6.1)	None	15	2.869		
	θ_2	19	2.388	0.2023	>0.10
Nonlinear (6.2a) $\theta_3 = 0$	None	15	2.586		
	θ_2	19	2.413	0.5375	>0.10

[a] Error mean square

[b] Probability that the null hypothesis of a common θ_2 is true.

Figure 6.1 shows the fit of (6.1) from which it can be seen that the linear model appears adequate for the range of temperatures in the constant temperature study. There is no apparent slow down in development rate at the upper end of this temperature range. When model (6.2) was fitted, the hypothesis of common-across stage value for each of (θ_2, θ_3) was accepted (P>0.1 in each case). However, θ_3 for (6.2) was also found not significantly different from zero (P>0.1) due to the lack of nonlinearity mentioned above. However, the highest temperature regime of $27^{o}\mathrm{C}$ is not extreme for field conditions, so extrapolation of the linear model above $27^{o}\mathrm{C}$ is likely to result in over-estimation of development rate. Shaded field temperatures can, depending on altitude, occasionally reach $40^{o}\mathrm{C}$ but more commonly reach daily maxima of up to $35^{o}\mathrm{C}$ in the peak of summer. These problems with extrapolation are even more extreme with model (6.2) when the $\theta_3 T^2$ term excluded. Without more data on development time under temperature regimes up to al least $35^{o}\mathrm{C}$ it is not possible to address this problem in a rigorous manner. However, in the absence of such data a reasonable approach is to assume or guess the optimum temperature for development, T_{opt} and refit (6.2) in the following form

$$F_N(T,\boldsymbol{\theta}) = \theta_1 \exp\left(\theta_2 T - \frac{\theta_2 T^2}{2T_{opt}}\right) \qquad (6.2a)$$

where T_{opt} was fixed for all stages at $30^{o}\mathrm{C}$. For model (6.2a) a common across-stage estimate for θ_2 did not result in a significant increase in the residual variance (Table 6.1).

Table 6.2 Parameter estimates and standard errors for development rate models (6.1) and (6.2a) fitted to constant temperature data

Model	Stage /Instar	Parameter (s.e.)		
		θ_2 [b]	θ_1	θ_1^{-1}=*DD* or *NDD*
Linear (6.1)	Egg	5.08 (1.09)	0.01127 (0.00160)	88.7 (12.6)
	L1		0.01952 (0.00190)	51.2 (5.0)
	L2		0.02485 (0.00214)	40.2 (3.5)
	L3		0.02333 (0.00207)	42.9 (3.8)
	L4		0.01958 (0.00190)	51.1 (5.0)
	Total[c]			274.1
	Total[d]		0.00360 (0.00013)	277.5 (10.0)
Nonlinear [a] (6.2a)	Egg	0.2549 (0.0266)	0.00560 (0.00222)	178.5 (70.6)
	L1		0.00972 (0.00372)	102.9 (39.4)
	L2		0.01241 (0.00472)	80.6 (30.7)
	L3		0.01161 (0.00442)	86.1 (32.8)
	L4		0.00974 (0.00373)	102.7 (39.3)
	Total[c]			550.8
	Total[d]		0.00179 (0.00006)	557.7 (18.7)

[a] Modified model with T_{opt}=30.

[b] Estimated with assumed common parameter value across stages.

[c] Total of stage-specific estimates.

[d] Total development period from egg to L4. Response parameter, θ_2, taken as common estimate from individual stages.

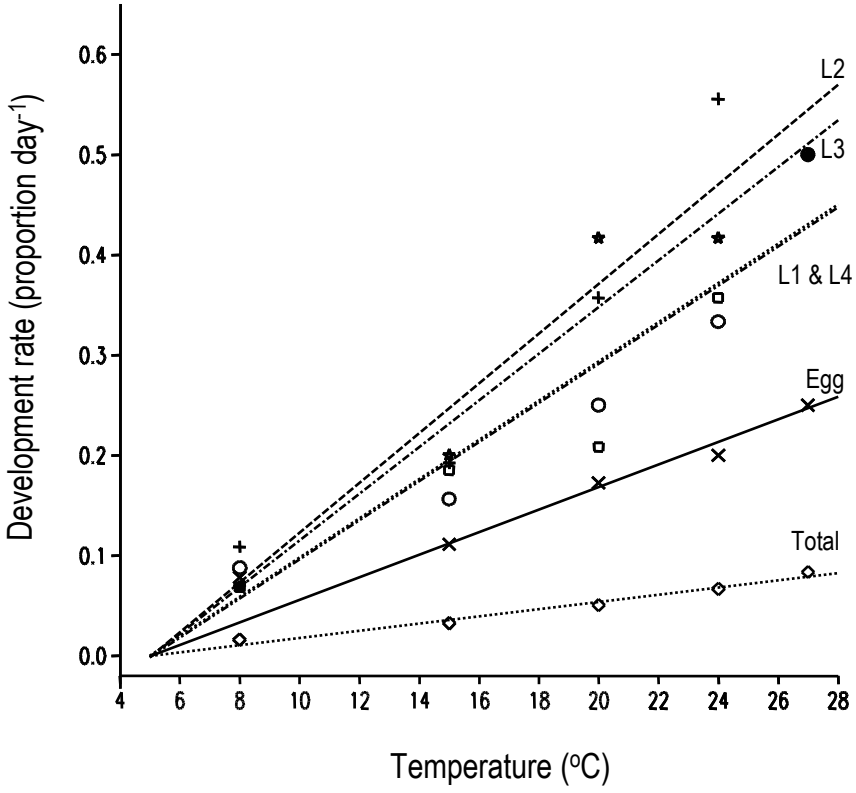

Figure 6.1 Linear development rate models (6.1) for each of stages: (**x**) egg, instars (○) L1, (**+**) L2, (*****) L3, and (□) L4 with common response parameter estimate. The models for development rate for total development time from oviposition to completion of L4 stage (◊) were fitted using the prior estimate for the response parameter.

The parameter estimate for θ_2 and the stage-specific estimates of θ_1 and their standard errors for model (6.2a) are given in Table 6.2. The corresponding estimated development time in physiological units given by

$$\hat{\theta}_1^{-1} = l \exp\left(\hat{\theta}_2 T - \frac{\hat{\theta}_2 T^2}{2T_{opt}}\right)$$

is the nonlinear analogue of *DD* and will be denoted by *NDD*. Figure 6.2 shows the fit of this model for an extended upper temperature range.

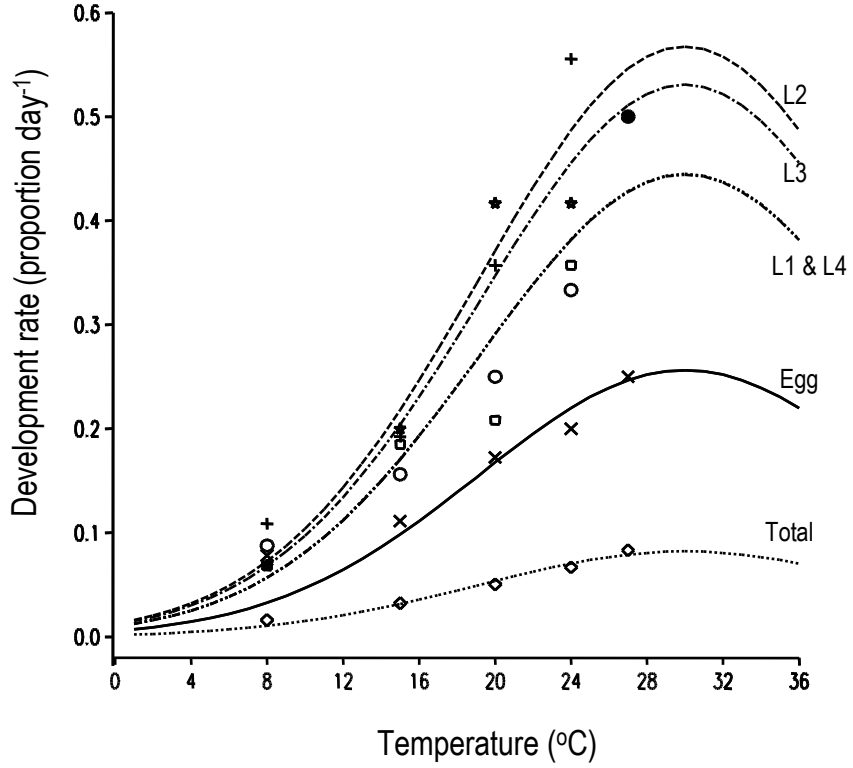

Figure 6.2 Nonlinear development rate models (6.2a) for each of stages : (**x**) egg, instars (○) L1, (**+**) L2, (*****) L3, and (□) L4 with common response parameter estimate. The models for development rate for total development time from oviposition to completion of L4 stage (◊) were fitted using the prior estimate for the response parameter.

6.3 MODELS OF DEVELOPMENT RATE AS A FUNCTION OF TEMPERATURE : AMBIENT FIELD TEMPERATURES

6.3.1 Linear and nonlinear thermal sums

For fluctuating temperatures, such as ambient temperatures in the field or those produced artificially in the laboratory, θ_1 can be defined so that the integral over time, *t*, of the development rate function is given by

$$1 = \theta_1 \int_0^l F^* \{T(t), \boldsymbol{\theta}^*\} dt \qquad (6.4)$$

where $\boldsymbol{\theta}^*$ is the vector of temperature response parameters (i.e. excluding θ_1),

$$F^*\{T(t),\boldsymbol{\theta}^*\}=\theta_1^{-1}\,F\{T(t),\boldsymbol{\theta}\},$$

and l can be interpreted as the time taken to complete development under temperatures $T(t)$ from a given starting time, $t_0 = 0$, for the hypothetical individual with mean development rate response to temperature.

For the linear model (6.1) the relation (6.4) is given by

$$1=\theta_1\int_0^l F_D^*\{T(t),\boldsymbol{\theta}^*\}\,\delta(t)dt$$

where $\delta(t)$ is unity if $T(t)>\theta_2$ and zero otherwise. This gives θ_1^{-1} as the mean day-degrees required to complete development. Similarly, for (6.2) the relation (6.4) is

$$1=\theta_1\int_0^l F_N^*\{T(t),\boldsymbol{\theta}^*\}dt$$

where θ_1^{-1} in this case gives the nonlinear thermal sum to mean development time. Note that for the following, the subscript denoting the particular model will be dropped if it is unnecessary to distinguish between rate models.

The above is fairly obvious but a subtle difference in interpretation can be made if the limit to the integral is generalised to the random variable *L*. The general form of (6.4) with general parameter vector $\boldsymbol{\theta}=(\theta_1,\boldsymbol{\theta}^*)$ then becomes, for model (6.1),

$$p_D(L,\boldsymbol{\theta})=\theta_1\int_0^L F_D^*\{T(t),\boldsymbol{\theta}^*\}\;\delta(t)dt$$

and for model (6.2)

$$p_N(L,\boldsymbol{\theta})=\theta_1\int_0^L F_N^*\{T(t),\boldsymbol{\theta}^*\}dt$$

so that if $L < l$ then $p(L,\boldsymbol{\theta}) < 1$, corresponding to a random individual's development rate response to temperature that is greater than average while the converse is true if $L > l$ and thus $p(L,\boldsymbol{\theta}) > 1$. If the following scaling is imposed, $p_D^*(L,\boldsymbol{\theta}^*) = \theta_1^{-1}\, p_D(L,\boldsymbol{\theta})$ and $p_N^*(L,\boldsymbol{\theta}^*) = \theta_1^{-1}\, p_N(L,\boldsymbol{\theta})$, then these give the linear and nonlinear thermal sums corresponding to *DD* and *NDD* respectively required for an individual with development time of *L* Julian days from time $t_0 = 0$. In addition, for the case $L < l$ then $p(L,\boldsymbol{\theta})$ can be defined as the expected cumulative proportion of development up to time *L* for the 'individual' with average development rate response to temperature. Stinner *et al*. (1974) used this approach to predict the proportion of development given Julian time *L*, where $L < l$, and a 3-parameter nonlinear rate model similar to (6.2) with model parameters estimated from constant temperature/development data. Their parameter *C* takes the place of θ_1 here. They also suggested this procedure can be reversed by setting $p(L,\boldsymbol{\theta})$ to a constant less than or equal to 1 and solving the above integral for *L* using a numerical approximation such as that based on the trapezoidal rule.

6.3.2 Distribution theory

Sharpe *et al*. (1977) model the distribution of development times under a constant temperature regime based on a Gaussian (i.e. normal) distribution model for the *rates*. Here this approach is extended to development under fluctuating (ambient) temperatures in the field using an assumed Gaussian distribution for an *unobserved* random variable which is the analogue of the *observed* rates obtained in constant temperature studies. Estimation procedures are then developed based on the assumed distribution of this unobserved random variable and data on development times collected in the field.

First, consider the hypothetical, unobserved random variable $P = p(L,\boldsymbol{\theta})$ which is the proportion of development to time *L* where *L* is the observed random variable (i.e. across individuals) giving the time to completion of development. The expected value of P is given by $p(l,\boldsymbol{\theta})$. Also define an unobserved random variable, *Y*, as the reciprocal of *P*. For the following it will be convenient if *Y* is scaled by θ_1 and *P* is scaled by θ_1^{-1} to give

$$Y^* = \theta_1 Y$$

$$P^* = \theta_1^{-1} P.$$

It is assumed here that Y^* is distributed as NIID(θ_1, σ^2) which is a generalisation to fluctuating temperatures of the distributional assumption of Sharpe *et al*. (1977) for the random variable $R = L^{-1}$, where L is the random development time of individuals in a cohort reared under constant temperature. This can be seen if a constant temperature is assumed and Y^* is expressed as simply a scaling of R given, for example, for model (6.1), by $Y^* = \theta_1 \left[p_D(L, \boldsymbol{\theta})\right]^{-1} = (T - \theta_2)^{-1} R$.

Statistical distributions for either R or L estimated from constant temperature experiments when 'imputed' as the distribution of Y or P, respectively, have been used for stochastic simulation of development times in the field (Sharpe *et al*., 1977; Cunningham *et al*., 1981; Logan, 1988). This involves applying the same distribution and its shape parameter(s) as estimated from R or L but allowing the mean to be determined from thermal summation of the mean rate model given here by $p_D^*(l, \boldsymbol{\theta}^*)$ or $p_N^*(l, \boldsymbol{\theta}^*)$. Cunningham *et al*. (1981) modelled adult emergence times for *Heliothis armigera* (Lepidoptera : Noctuidae) using an exponential distribution which was parameterised simply by a mean and minimum value. Borrowing results from survival time analysis they assumed that the hazard function of this distribution (i.e the instantaneous probability of emergence) takes the same value, given temperature, for field development as that estimated from constant temperature experiments.

Strictly, if Y^* is assumed normally distributed then the expected value of its reciprocal, $P^* = 1/Y^*$ does not exist since the domain of Y^* theoretically includes zero. However, given the variance σ^2 is small relative to θ_1 then the lower tail of the distributions of both Y^* and P^* include zero with negligible probability. Therefore in practice, a good approximation to the expected value of P^* (and therefore P) can be obtained using a Taylor series expansion of $P^* = 1/Y^*$ about $Y^* = \theta_1$ so that

$$E(P) = E(\theta_1 P^*) = 1 + (\sigma/\theta_1)^2 + O$$

where *O* is a remainder which is a function of θ_1 and higher order central moments of Y^*. The terms *O* and $(\sigma/\theta_1)^2$ are generally very small relative to one. From results given later the term $(\sigma/\theta_1)^2$ was estimated as 0.0013 for model (6.1) and 0.0011 for model (6.2a).

The reason for taking this approach is that under field conditions the random variable *L* (and therefore *R*) does not have a single expected value under the model. This follows since *L* will be dependent not only the individual's development rate/temperature relationship but also on the particular temperatures to which it is exposed. The temperature profile for each individual will have some sections in common with other individuals, corresponding to their concurrent development, but overall will differ between individuals due to different times completion of development (i.e. starting times are assumed the same for individuals from the same cohort).

Development time over a number of successive stages

As each individual develops through the successive stages, the total development time from oviposition to the end of the pupal stage should logically be equivalent to the sum of the time taken in each stage. In modelling the development of single cohorts and multiple cohorts in the field described below, it was necessary to assume the parameters in $\boldsymbol{\theta}^*$ are independent of stage in order to satisfy the above logical constraint. This allows a common physiological time scale up to Julian time *t* to be used as either of the linear or nonlinear thermal sums given by $p_D^*(t,\boldsymbol{\theta}^*)$ and $p_N^*(t,\boldsymbol{\theta}^*)$, respectively, as shown below.

For $j=1,...,s$ stages with expected development times $l_1,...,l_j,...,l_s$, given t_0 and temperatures $T(t)$, then if $\boldsymbol{\theta}^*$ takes a common value across stages we have the consistent property that

$$p^*(l,\boldsymbol{\theta}^*)=\sum_{j=1}^{s} p^*(l_j,\boldsymbol{\theta}^*)$$

where $l = \sum_{j=1}^{s} l_j$.

This satisfies the above logical constraint and allows the total development time for a random individual, $\sum_{j=1}^{s} L_j$, to be used to estimate $\boldsymbol{\theta}^*$ without knowledge of its individual stage occupancy times (i.e. the L_j 's). Given an estimate of $\boldsymbol{\theta}^*$ then an estimate of θ_1 is obtained simply as $1/\, p^*\left(l, \hat{\boldsymbol{\theta}}^*\right)$.

If $\boldsymbol{\theta}^*$ does not have common values across stages then at *s*-1 points in Julian time a transition has to be made from the previous stage to the next stage's physiological time scale. Manel and Debouzie (1997) accomplished this by making the change at the median development time for each stage. Although, this is a practical solution it suffers from the logical inconsistency that a discontinuity is introduced to the development process within each stage for those individuals in the population which have development times longer than the median for the particular stage. Simplification of model fitting and application as well as logical consistency is obtained if the elements of $\boldsymbol{\theta}^*$ can realistically be assumed to have common values across stages. Fortunately, the hypothesis of stage-independent $\boldsymbol{\theta}^*$ was accepted for the constant temperature data.

6.3.3 Estimation

Without loss of generality define $t_0 = 0$ so that if emergence times could be observed exactly for each of *N* individuals they would be the t_i for *i*=1,…,*N*, *m*=*N*, and $n_i = 1$ for all *i* (Section 6.2.2). Thus the t_i would be the sample realisations of the random variable *L*. The nonlinear least squares fit used by computer program DEVAR (Dallwitz and Higgins, 1992) assumes the t_i are *observed* development times by estimating the model parameters, $\boldsymbol{\theta}$, as the values which minimise

$$S(\boldsymbol{\theta}) = \sum_{i=1}^{N} \left[1 - \int_0^{t_i} F\{T(t), \boldsymbol{\theta}\} dt \right]^2 .$$

If there are multiple values of each t_i, which is the usual case, then the above function corresponds to the weighted minimisation using the *m* (<*N*) unique values of

t_i and multiplying the squared term by n_i. This minimisation does not correspond to maximisation of the likelihood of the observed response, t_i. More rigorously, estimation by the method of maximum likelihood based on the distribution of the unobserved random Y^* gives the log-likelihood for the observed response t_i as

$$\ell(\boldsymbol{\theta}, \sigma^2) = -\frac{N \ln(2\pi\sigma^2)}{2} - \frac{1}{2\sigma^2}\sum_{i=1}^{N}\left(y_i^* - \theta_1\right)^2 + \sum_{i=1}^{N}\ln\left[F^*\left\{T(t_i), \boldsymbol{\theta}^*\right\} y_i^{*2}\right]$$

where the last term is the logarithm of the Jacobian, $\left|\frac{dy^*}{dt}\right|$, for the transformation of Y^* to L (=t) evaluated at $y^* = y_i^*$, and $T(t_i)$ is the temperature at the moment of emergence for the i^{th} individual. The MLEs of θ_1 and σ^2 are easily obtained as the usual mean and variance of y^* for a given value of $\boldsymbol{\theta}^*$, that is

$$\hat{\theta}_1 = N^{-1}\sum_{i=1}^{N} y_i^*$$

$$\hat{\sigma}^2 = N^{-1}\sum_{i=1}^{N}\left(y_i^* - \hat{\theta}_1\right)^2.$$

DEVAR on the other hand gives a slightly biased estimate of θ_1. This can be seen by solving $dS(\boldsymbol{\theta})/\, d\theta_1 = 0$ giving $\tilde{\theta}_1 = \left\{1 - (\sigma/\theta_1)^2\right\}\hat{\theta}_1$. From the earlier discussion of the magnitude of $(\sigma/\theta_1)^2$, the term $\left\{1 - (\sigma/\theta_1)^2\right\}$ is generally only slightly less than unity.

Concentrating σ^2 out of log-likelihood $\ell(\boldsymbol{\theta}, \sigma^2)$ and dropping unimportant terms gives

$$\ell(\boldsymbol{\theta}) = -N \ln\left\{\sum_{i=1}^{N}\left(y_i^* - \theta_1\right)^2\right\} + \sum_{i=1}^{N}\ln\left[F^*\left\{T(t_i), \boldsymbol{\theta}^*\right\} y_i^{*2}\right]$$

which can be maximised to obtain MLEs of θ_1 and $\boldsymbol{\theta}^*$ remembering that y^* depends on $\boldsymbol{\theta}^*$. The last term in $\ell(\boldsymbol{\theta})$, derived from the Jacobian, may contribute significantly to the log-likelihood and thus to more efficient estimation if the individual development times were truly observed. For example if, under fluctuation

temperatures, emergence could be observed over periods that are short compared to the 24 h diurnal cycle, say at hourly intervals, then recording the average temperature over the hour when emergence was observed to occur could be used as $T(t_i)$ in the above likelihood.

This is of only theoretical interest here since in this study the time between observations was longer than a day. However, a small simulation study with known $T(t_i)$ was used to compare the DEVAR least squares approach with the full maximum likelihood estimation procedure (Appendix A7). Appendix A7 shows that when the $T(t_i)$ are known, maximum likelihood estimation using log-likelihood, $\ell(\boldsymbol{\theta})$, was much more successful than estimation using DEVAR's least squares, $S(\boldsymbol{\theta})$, in terms of the percentage of simulations for which convergence was achieved and the accuracy of parameter estimates.

Nevertheless, the appropriate estimation procedure in most practical situations, as here, is based on modelling the n_i as an observed, multinomial response variable as follows.

Maximum likelihood estimation using grouped, interval censored data

The data in this case consists of the n_i individuals observed to complete development between observation times t_{i-1} and t_i, i=1,...,m. To account for differences in the starting time for the development process it will be assumed that there are a number of cohorts with different starting times and the n_i are recorded separately for each cohort. The log-likelihood is the sum of the log-likelihoods for each cohort, so only a single cohort is considered for the moment for simplicity. Let the total number of individuals for a cohort be N, and as described above let Y^* be distributed as NIID(θ_1, σ^2). The log-likelihood for the observed n_i is obtained from the multinomial distribution as

$$\ell(\boldsymbol{\theta}) = \sum_{i=1}^{m} n_i \ln(\pi_i) \qquad (6.5)$$

where

$$\pi_j = \Phi\left[\{1/p^*\left(t_i, \boldsymbol{\theta}^*\right) - \theta_1\}/\sigma\right] - \Phi\left[\{1/p^*\left(t_{i-1}, \boldsymbol{\theta}^*\right) - \theta_1\}/\sigma\right]$$

and $\Phi[.]$ is the cumulative normal density function. Note that the temperature at completion of development no longer enters into the likelihood.

6.3.4 Sampling methods and data

As part of an experiment that was a preliminary trial to test the experimental methods used in Chapter 4, egg batches were attached to a leaf within a shoot over which a cage had been placed (Fig. 6.3a) where these cages were similar to those described in Section 4.1.1. This experiment was located in a 6-year old plantation in central Tasmania at an altitude of 600 m (Site 4, Appendix A5). *Eucalyptus nitens* was planted as a few dispersed rows within the predominantly *E. regnans* plantation.

Each egg batch consisted of an egg raft reduced to 15 eggs. Development times were recorded for an egg batch (cohort) attached to a caged shoot for each of four *E. nitens* and four *E. regnans* trees. For all eight egg batches the time of oviposition was known from direct observation to an accuracy of 0.5 h (i.e. it takes approximately 30 minutes for an egg batch to be oviposited). Completion of development was taken to be the time when the final (L4) instar larva finishes feeding. This was determined by collecting pre-pupae from the bottom of each cage periodically (i.e. at six sampling occasions) from the start of the third week after oviposition until the last pre-pupae were collected on day 47 (Fig. 6.3b). Thus only the total development time from egg to the end of the final larval instar stage was observed corresponding to the total development time for the constant temperature data. Air temperature was logged minutely over the entire period using a STARLOG® datalogger and a temperature thermistor attached in a shaded position at a height of approximately 2m to a nearby tree. Of the initial number of 120 eggs, 55 individuals survived (28 on *E. nitens* and 27 on *E. nitens*) and were recovered as pre-pupae over a period ranging from 25 to 47 days after oviposition. The mean temperature for the period of the field trial was $13.6\,^{\circ}\mathrm{C}$. Figure 6.4 shows the temperature at 10 minute-intervals for the period from day 1 to day 47 after oviposition as well as the observation times and the number of pre-pupae collected for each of the host species.

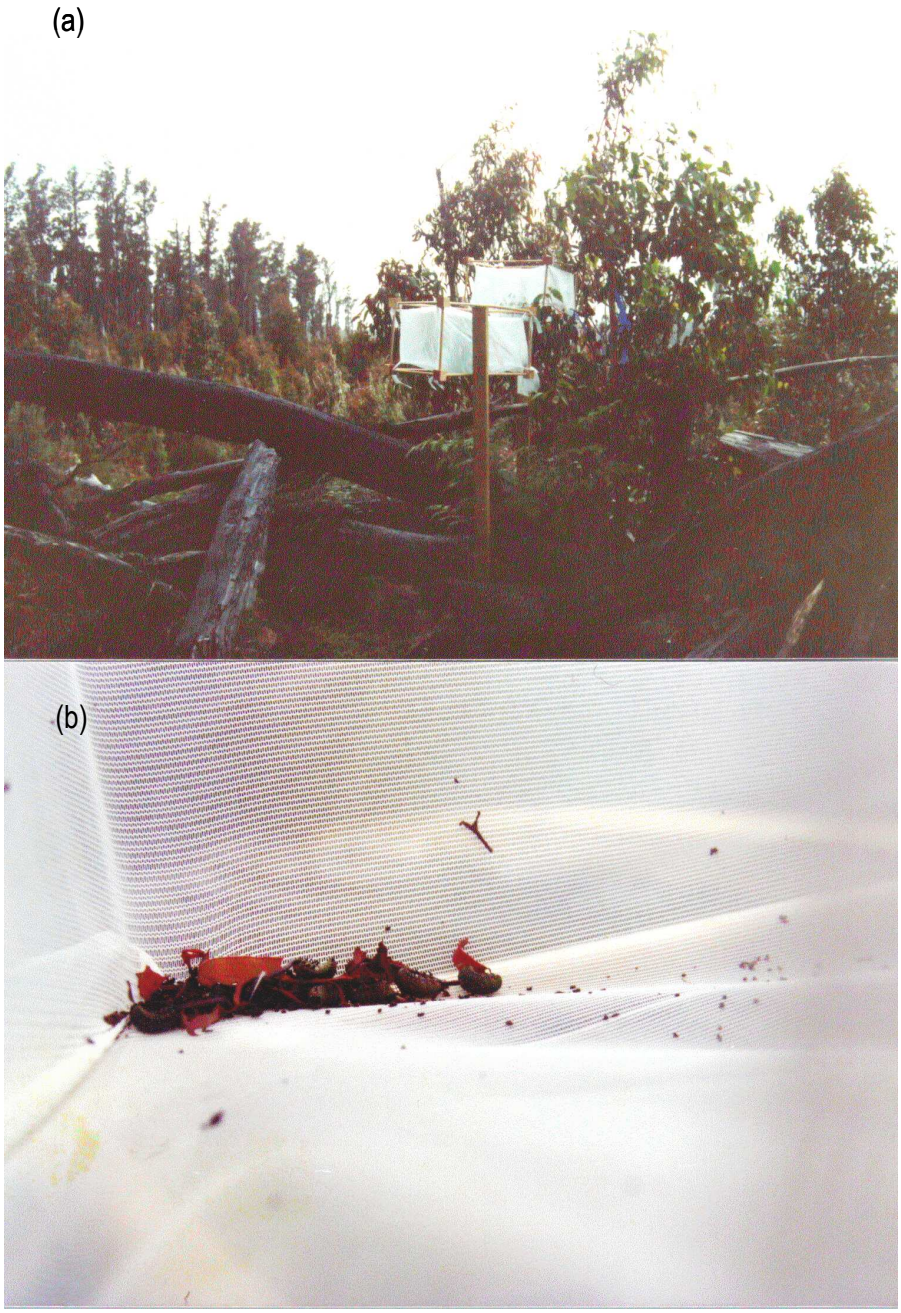

Figure 6.3 Sampling total development time at Brady's Plantation, central Tasmania : (a) site showing cages attached to an *E. regnans* tree with an *E. nitens* tree in the centre background and (b) pre-pupae collecting in the bottom of the cage.

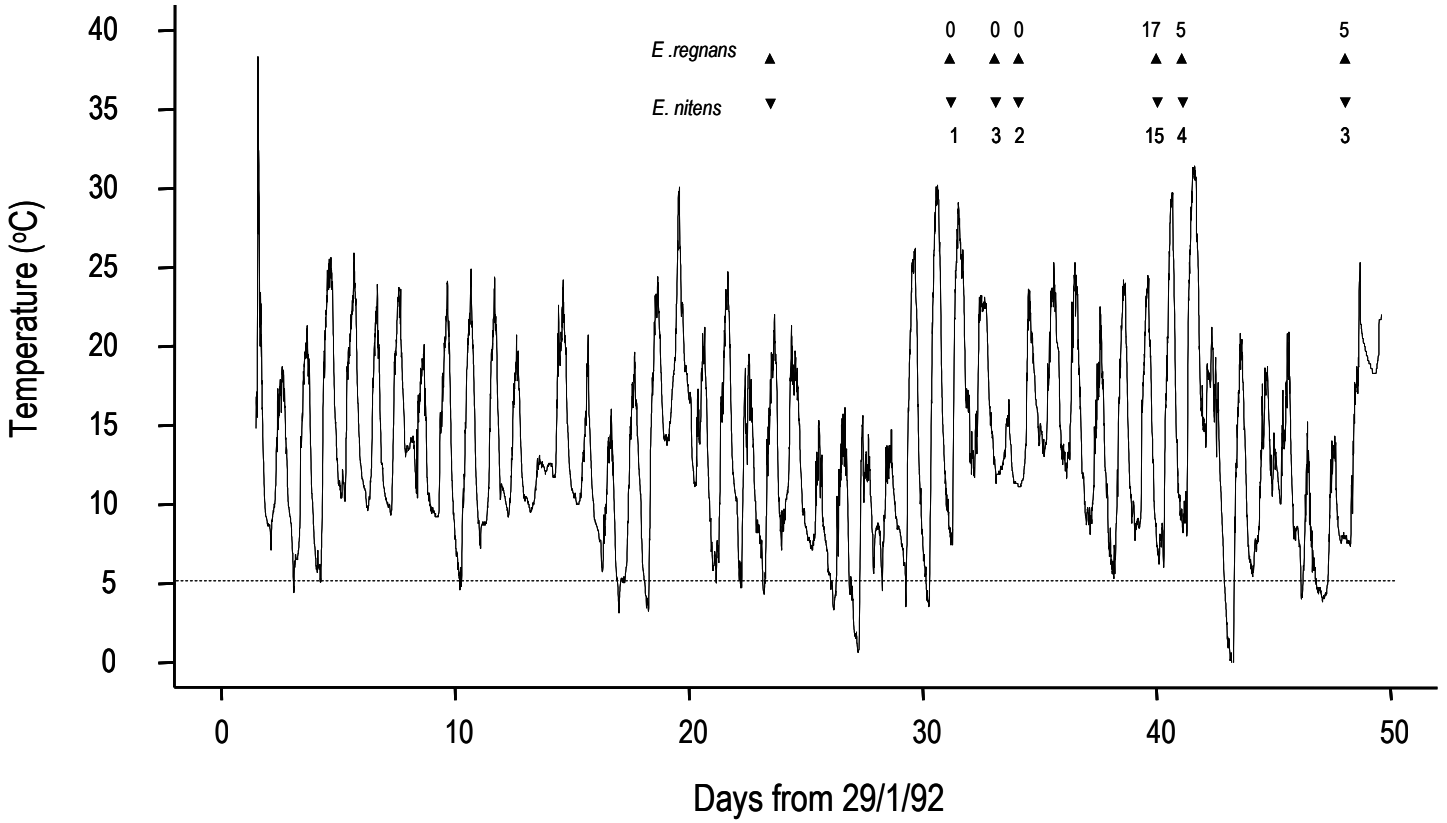

Figure 6.4 Temperature recorded at 10 minute intervals at Brady's Plantation showing number of pre-pupae recovered for each host species and sampling occasion. The dotted line shows the lower developmental threshold estimated from constant temperature experiments.

6.3.5 RESULTS

The data used for modelling were the number of individuals completing development in each of the six periods, for each of the two host species (Fig. 6.4). Models (6.1) and (6.2a) were fitted by maximising the likelihood (6.5) using a GENSTAT program employing the FITNONLINEAR directive (see Appendix A7). The estimate of $\boldsymbol{\theta}^* = \theta_2$ for each model given in Table 6.2 was used as an initial estimate for maximum likelihood estimation of $(\theta_1, \theta_2, \sigma)$. Initial estimates of θ_1 and σ were obtained by simply calculating the weighted mean and standard deviation of the Y^* using the values of $y^*(t_j) = 1/\, p^*(t_j, \hat{\boldsymbol{\theta}}^*)$. This involved using the initial estimate of θ_2 to calculate $y^*(t_j)$ and the period mid-point value, $0.5\{y^*(t_j) + y^*(t_{j-1})\}$ as the value of Y^*. The weighted mean and variance of Y^* were calculated with weights the number of individuals completing development for the particular cohort and period. In fact, it was found necessary to use this method to maximise the log-likelihood in two steps:

(1) maximise the log-likelihood with respect to θ_2 using moment estimators of θ_1 and σ obtained as the weighted mean and standard deviation described above.

(2) using the estimate of θ_2 in step (1), maximise the profile log-likelihood with respect to θ_1 and σ.

This two step procedure was required since jointly maximising the log-likelihood for all 3-parameters simultaneously failed to converge for this data set for both models (6.1) and (6.2a). Models (6.1) and (6.2a) were fitted separately for each host species.

For model (6.1) it was found that these data were not adequate to give a realistic estimate θ_2 for either host species even when it was the only parameter estimated by maximum likelihood (i.e. step 1). The only alternative was to use the estimate of θ_2 of $5.08\,^{\circ}\mathrm{C}$ obtained from the constant temperature data, and estimate of θ_1 and σ using one of two methods. Conditional on $\theta_2 = 5.08$, these two methods were : (A) moment estimation given in step (1) and (B) maximum likelihood estimation in step (1). Table 6.3 gives the parameter estimates, -2 x (log-likelihood), and estimated day-degrees for completion of development. Method (B) gave a slight improvement in fit as judged by the decrease in the deviance compared to method (A).

Table 6.3 Fit of development rate models (6.1) and (6.2) to total development time (egg to L4) from field emergence data reared for *E. nitens* and *E. regnans*.

Host species	Model	Method [a]	Parameter (s.e.)				-2Ln [b]	deviance [c]
			θ_2	θ_1	σ	θ_1^{-1}=*DD* or *NDD*		
E. nitens	Linear (6.1)	A	5.08 [d]	0.003315	0.0004108	301.6	82.1	21.7
		B	5.08 [d]	0.003299 (0.000075)	0.0003665 (0.0000525)	303.1 (6.9)	81.5	21.1
	Nonlinear (6.2a)	A	0.2549 [d]	0.001734	0.0002155	576.7	82.2	21.8
		B	0.2549 [d]	0.0017254 (0.0000393)	0.0001919 (0.0000275)	579.6 (13.2)	81.6	21.2
E. regnans	Linear (6.1)	A	5.08 [d]	0.002999	0.0002613	333.5	54.4	10.5
		B	5.08 [d]	0.003001 (0.000042)	0.0001363 (0.0000514)	333.2 (4.6)	49.4	5.5
	Nonlinear (6.2a)	A	0.2549 [d]	0.001569	0.0001375	637.5	54.4	10.5
		B	0.2549 [d]	0.0015694 (0.0000222)	0.0000720 (0.0000273)	637.2 (9.0)	49.4	5.5

[a] Method A - weighted mean and standard deviation, B – maximum likelihood
[b] -2 log (likelihood)
[c] $2\ln(L_0) - 2\ln(L)$, where L_0 is the likelihood with $\hat{m} = m$.
[d] Estimates obtained from constant temperature data

In estimating θ_2 for the nonlinear model (6.2a) using the above two-step optimisation technique, the maximum likelihood algorithm converged but again gave unrealistic values for both host species. As with model (6.1) when θ_2 was taken as the value estimated from the constant temperature data in Table 6.2, method (B) gave a slight improvement in fit over method (A) but no improvement over the linear model was achieved for either host species.

6.4 MODELLING POPULATION PHENOLOGY USING STAGE-FREQUENCY DATA

The development rate models described in the previous section allowed physiological time scales *DD* and *NDD* to be constructed for use in continuation ratio models (Candy, 1991; Manel and Debouzie, 1997) of the phenology of *C. bimaculata* calibrated using stage-frequency data (Manly 1990). These models predict the proportion of the population in each stage given time from initiation of the new generation. Stage-frequency data is obtained by collecting relatively large samples, say 200 or more individuals, at each of a number of sampling occasions over the total development period for the stages that can be easily observed. Ideally, the stages that are of interest for pest management are those which are easily observed. This is the case for *C. bimaculata* with egg to final instar easily observed on leaves sampled from the crowns of a sample of trees. The individuals once sampled are classified into each of the development stages of interest.

Stage-frequency data therefore simply consists of the number, n_{ij} in stage *j* at time t_i for each of stage 1 to *s*. Here, there are five stages to consider; egg, L1, L2, L3, and L4. The pupal and adult stages cannot be collected in the field as easily as these other stages in sufficient numbers to allow estimation of a model that includes pupal and teneral adult stages. Prediction of the proportion in these last two stages is not as important in the IPM as predictions for the four larval instar stages for the reasons given in the Introduction.

Given a reasonably accurate estimate of the start of a population that is initiated within a relatively short period (i.e. within a week) then a thermal sum of either *DD* or *NDD*, accumulated from the estimated initiation time, is used as the main driving variable in the model.

Chrysophtharta bimaculata is generally considered a univoltine species (de Little, 1983) but multiple oviposition events can occur in the same area of forest. For the following, synchrony of oviposition will be assumed, but the implications of multiple, major oviposition events will be discussed later.

There is obviously less information on development time in stage-frequency data compared to the field emergence data described in the previous section, since starting times for individual cohorts are unknown in the former case. However, much larger sample sizes can be obtained quickly and cheaply using stage-frequency sampling. In addition, observation of development at the population level rather than the individual cohort level more realistically reflects the information available to forest managers as model inputs. This is discussed in more detail in the discussion.

Manly (1990) summarised the large number of modelling approaches that have been applied to stage-frequency data. If a known sampling intensity is used (i.e. by recording the number of shoots and trees sampled) then absolute numbers in each stage can be modelled by combining an estimate of initial population size, N_0, with an age-specific model of mortality and a model for stage-duration times. Distributions that have been used to model stage duration times include the gamma (Kempton, 1979), logistic (Manly, 1989), and inverse Gaussian (Munholland and Kalbfleisch, 1991). However, it appears that the information in stage-frequency data alone is insufficient to estimate a model which simultaneously incorporates component models for *stage*-specific mortality and stage duration times (Munholland and Dennis, 1992).

An alternative, simpler, modelling approach that does not require a model of mortality can be used if interest is only in estimating the time of peak occurrence of each stage relative to other stages. This requires incorporation of the constraint that the predicted values of n_{ij} sum to the total number of individuals sampled, N_i, at each sampling time t_i. The distribution of the n_{ij} conditional on the N_i can then be considered as multinomial (Candy 1991) or a mixture of multinomials (Stedinger *et al*., 1985) rather than a Poisson or over-dispersed Poisson where the N_i are treated as random variables (i.e. the unconditional distribution of the n_{ij}) (Manly, 1990, p.34).

Since only the proportion in each stage, rather than absolute numbers, is modelled then sampling does not need to relate to a standard unit such as insects per shoot and sampling intensity does not have to be constant over time. The only requirement of sampling is that the probability of selecting individual insects of a given life-stage is representative of that stage's relative proportion in the population.

Models which predict the proportion of the population in each stage assuming an underlying unobserved development level, say $X(t)$ at time *t*, that is randomly distributed across the population with a specific probability distribution, were used by Stedinger *et al*. (1985), Dennis *et al*. (1986), Dennis and Kemp (1988), Candy (1991), and Candy and McQuillan (1998). Typically, physiological time from the start of the population, defined for example by day-degrees (*DD*) is used as the variable that determines the mean of the distribution of $X(t)$. These models are called ordinal regression models in the statistical literature (McCullagh 1980; Agresti 1984), and model the statistical properties of the population as a whole, rather than an individual's progression though life-stages (Munholland and Dennis, 1992).

Candy (1991) also introduced a new class of models based on continuation ratios (CR) (Fienberg, 1980) which have greater flexibility than the ordinal regression models in that they allow for a stage-specific response to the physiological time scale. Candy (1991) found that the CR models gave large improvements in fit to stage-frequency data for the mountain pinhole borer, *Platypus subgranosus* Schedl, and the western spruce budworm, *Choristoneura occidentalis* Freeman, compared to the ordinal regression models. Manel and Debouzie (1997) also used continuation ratios to study the phenology of three of the larval stages of the chestnut curculio *Curculio elephas*.

Models of age-specific mortality/stage-duration time have the disadvantage compared to ordinal regression and CR models that predictor variables other than time cannot be easily incorporated (Candy 1991) and estimation can be cumbersome and unstable (Munholland and Dennis, 1992). For these reasons and because of their greater flexibility attention was restricted to the continuation ratio class of models which are described below and fitted to stage-frequency data on *C. bimaculata.* However, the assertion of Munholland and Dennis (1992) that their *microscopic*

model has advantages over macroscopic models, such as CR models, is discussed in Section 6.5 in the context of the application here.

Manel and Debouzie (1997) introduced a refinement to the CR models of Candy (1991) by incorporating estimation of stage-specific, lower development thresholds for the day-degree model, [i.e. θ_2 in model (6.1)] simultaneously with other parameters. This refinement was not pursued here because (a) the hypothesis of a common θ_2 was accepted from the fit of (6.1) or (6.2a) to the constant temperature data and (b) estimation of stage-specific θ_2 within the CR model can be unreliable due to multi-collinearity. This multi-colinearity can result in there being virtually no information on the θ_2 in stage-frequency data. This is discussed in more detail in Section 6.5.

Alternative time scales used were Julian date, day-degrees (*DD*) from model (6.1) and cumulative nonlinear development rate from model (6.2a) (*NDD*) using their respective estimates of θ_2 obtained from the constant temperature data (Section 6.2).

The continuation ratio models were calibrated using stage-frequency data collected at two nearby sites, at each of 350 m and 550 m altitude, in *E. regnans* natural regeneration in southwestern Tasmania. Since similar data for *E. nitens* were not available a simple adjustment to the models based on the laboratory trial of Baker *et al*. (1999) was used to allow the models to be used to predict the phenology of *C. bimaculata* feeding on *E. nitens*.

6.4.1 CONTINUATION RATIO MODELS

Model description

Taking each stage in turn, from egg to final larval instar, the probability of an individual being in stage *j*, *j*=1...*s*-1, conditional on being in stage *j* or later is given by

$$\begin{aligned}\mu_{ij} &= \Pr(\text{in stage } j \text{ at time } t_i \mid \text{in stage } j \text{ or later}) \\ &= h^{-1}\left(\beta_{0j}+\beta_{1j}t_i\right)\end{aligned} \qquad (6.6)$$

where t_i is time measured in either Julian days or physiological units such as *DD* or *NDD*, $h(.)$ is a link function (McCullagh and Nelder, 1983), and (β_{0j}, β_{1j}) are the regression parameters for the j^{th} stage. No model is required for the final stage, *s*, as explained later. Following Candy (1991), the n_{ij} are modelled as binomially distributed conditional on N_{ij}^* with expected value $N_{ij}^* \mu_{ij}$ where

$$\begin{aligned} N_{ij}^* &= N_i , && j = 1 \\ &= N_i - \sum_{k=1}^{j-1} n_{ik} , && j = 2,...,s-1 \end{aligned} ,$$

and $N_i = \sum_{j=1}^{s} n_{ij}$ is simply the sum of all individuals sampled at time t_i.

A commonly used link function is the logit, $h(\mu_{ij}) = ln\left(\frac{\mu_{ij}}{1-\mu_{ij}}\right)$, with the expected probability of being in stage *j* conditional on being in stage *j* or later given by $\mu_{ij} = h^{-1}(\eta_{ij})$ where $h^{-1}(\eta_{ij}) = \frac{exp(\eta_{ij})}{1+exp(\eta_{ij})}$ and $\eta_{ij} = \beta_{0j} + \beta_{1j} t_i$ is the linear predictor.

The continuation ratios[2], c_{ij}, (Fienberg, 1980) are the odds $c_{ij} = \mu_{ij}(1-\mu_{ij})^{-1}$ with sample values $n_{ij}\left(\sum_{k>j}^{s} n_{ik}\right)^{-1}$ so that the logarithm of the continuation ratio is equivalent to the logit of the conditional probability, μ_{ij}. Alternative link functions can be used for the conditional probabilities such as the probit, $h(\mu_{ij}) = \Phi^{-1}(\mu_{ij})$ where $\Phi(.)$ is the normal probability integral, and the complementary log-log link (CLOG), $h(\mu_{ij}) = ln\{-ln(1-\mu_{ij})\}$.

---

[2] There is a discrepancy in the definition of continuation ratios in the literature. In the discussion to McCullagh (1980), Fienberg describes alternatives to ordinal regression models, such as the cumulative logit, as the logit of the continuation ratios which implies the continuation ratios are the μ_{ij} rather than the c_{ij}. That definition was also used by Cox (1988). Candy (1991) also used this definition but subsequently published a correction (*Environmental Entomology*, 1991, vol. 20) defining the continuation ratios as the c_{ij} corresponding to Fienberg (1980) and this is the definition used here though either definition if applied consistently is appropriate.

An estimate of the unconditional probability of being in stage *j* at time t_i, q_{ij}, can be recovered from the fitted model (6.6) (Candy 1991) as

$$\begin{aligned} \hat{q}_{ij} &= h^{-1}\left(\hat{\beta}_{01} + \hat{\beta}_{11} t_i\right) && j = 1 \\ &= \left(1 - \sum_{k=1}^{j-1} \hat{q}_{ik}\right) h^{-1}\left(\hat{\beta}_{0j} + \hat{\beta}_{1j} t_i\right) && j = 2,\ldots,s-1 \\ &= \left(1 - \sum_{k=1}^{s-1} \hat{q}_{ik}\right) && j = s \end{aligned} \qquad (6.7).$$

So although the (*s*-1) models are fitted to the observed conditional probabilities, n_{ij} / N_{ij}^{*}, it is the predicted unconditional probabilities, $\hat{q}_{ij}$, that are the required proportions of the population in each stage at time t_i. No model is required for the final stage since the unconditional probability for this stage is obtained by difference as seen in equation (6.7).

Incorporating site as an extra predictor variable

Interpretation of the unconditional probabilities is straightforward, but this is not the case for the conditional probabilities or continuation ratios particularly when extra predictor variables besides time are included. For example, in this study the effect of site is of interest. Hopefully, use of temperature-mediated time scales ,such as day-degrees, will account for temperature differences between the sites. However, site differences apart from temperature may still occur. In this context, the linear predictor is

$$\eta_{ijk} = \beta_{0j} + \tau_j + (\beta_{1j} + \kappa_j)\, t_{ik}$$

where k=1,2 refers to site 1 and 2 respectively, τ_j is an effect on the regression intercept due to site 2, additional to site 1 for the j^{th} stage, and κ_j is an effect on the regression slope due to site 2, additional to site 1 for the j^{th} stage. The hypothesis of parallel regressions is given by $\tau_j \neq 0, \kappa_j = 0$ and the hypothesis of coincident regressions by $\tau_j = 0, \kappa_j = 0$. These hypothesis tests can be carried out easily, from the fit of (6.6), but their interpretation requires a re-parameterisation. For example,

for the logistic link function the linear predictor can be re-parameterised as $\eta_{ij} = -(t_i - \alpha_j)/\rho_j$ where $\rho_j = -\beta_{1j}^{-1}$ and $\alpha_j = -\beta_{0j}\beta_{1j}^{-1}$.

If we consider $1-\mu_{ij}$ as the probability of being in stage *j*+1 or later conditional on being in at least stage *j*, then this probability is, from equation (6.6), $1-h^{-1}(\eta_{ij})$. In the case of the logit link function this probability is given by $\{1+\exp(-\eta_{ij})\}^{-1}$ which is the cumulative probability density function of the logistic distribution with mean α_j and variance $\pi^2\rho_j^2/3$. Borrowing terminology from bioassay analysis (Finney, 1971, p.9), the probability of an individual being in stage *j*+1 or greater conditional on being in at least stage *j* is dependent on an underlying logistic tolerance distribution, and the current time (or 'dose'). This follows given that a random individual's 'tolerance-time', *T*, is distributed as the above logistic so that at a specified time (i.e. 'dose'), *t*, the individual is predicted to be in stage *j*+1 or greater if *t* > *T* but in stage *j* if $t \le T$. For the model given by $\mu_{ij} = h^{-1}(\eta_{ij})$, $\rho_j = -\beta_{1j}^{-1}$ and $\alpha_j = -\beta_{0j}\beta_{1j}^{-1}$, parallelism of regressions can therefore be interpreted as constant logistic variance but site-specific mean 'tolerance-times', while coincident regression implies constant variance and means across sites.

6.4.2 Estimation methods

Fitting the CR models as generalised linear models

Model (6.6) can be fitted as a generalised linear model (GLM) (Candy, 1991) in a number of widely available statistical packages using a binomial error distribution for n_{ij} with binomial denominator N_{ij}^*, linear predictor η and the required link function (e.g. logit). Observations where the binomial denominator N_{ij}^* is zero should be given a prior weight of zero in the fit.

Accounting for overdispersion using the methods of Williams (1982)

The standard errors of parameter estimates obtained in the fit of equation (6.6) using the binomial likelihood need to be scaled upwards if overdispersion is apparent (Finney, 1971, p.33; Williams, 1982; McCullagh and Nelder, 1989, p.126). Williams (1982) gives three methods of accounting for overdispersion. Williams method I

(Williams 1982) assumes that the N_{ij}^{*} are the same within a stage and the variance of the observed counts n_{ij} conditional on N_{ij}^{*} is given by

$$Var\left(n_{ij} \mid N_{ij}^{*}, t_i\right) = \phi N_{ij}^{*} \mu_{ij}\left(1-\mu_{ij}\right)$$

where ϕ is the overdispersion parameter or heterogeneity factor (Finney, 1971, p.33). William's method II assumes that the μ_{ij} have themselves a sampling distribution with expected value γ_{ij} and variance $\phi\gamma_{ij}(1-\gamma_{ij})$. This gives

$$Var\left(n_{ij} \mid N_{ij}^{*}, t_i\right) = N_{ij}^{*}\gamma_{ij}\left(1-\gamma_{ij}\right)\left\{1+\phi\left(N_{ij}^{*}-1\right)\right\}.$$

Williams method III, described in detail in Chapter 2 for the case of the complementary log-log link, assumes that the linear predictors have constant variance, σ^2, so that for the logit link function

$$Var\left(n_{ij} \mid N_{ij}^{*}, t_i\right) \cong N_{ij}^{*}\mu_{ij}\left(1-\mu_{ij}\right)\left\{1+\sigma^2\left(N_{ij}^{*}-1\right)\mu_{ij}\left(1-\mu_{ij}\right)\right\}.$$

The modification to GLM fitting algorithm to fit method III was described in Section 2.3. Method II involves a similar modification (Williams, 1982).

Incorporating sites as random effects

Williams methods of modelling overdispersion are appropriate when there is a simple, single-level error structure. However, if sampling is multi-level or nested then this should be reflected in a multi-level error structure (e.g. Section 2.2). In modelling stage-frequency data the stages are a common, fixed set of population attributes of intrinsic interest whereas sites and seasons can be considered sample units that are nested within stages (i.e. random effects). The inclusion of SITE as a 'fixed effect' in the above models is useful in indicating if the physiological time scales can account for the difference between sites in *C. bimaculata* phenology. The inference is that this difference is attributable to the difference in altitude between the sites and the effect of altitude on temperature via the lapse rate (Munn, 1966, p.43). However, in applying model (6.6) (Section 7.9) parameter estimates cannot be site-

specific since this would require collection of stage-frequency data for each site for which predictions are required over a number of seasons in order to obtain such estimates. Such data is not routinely available but is restricted to research programs such as that described here. Therefore, sites and seasons need to be considered as random effects within the coincident regression model (i.e. the τ_j become random intercepts and the κ_j random slopes).

A relatively straightforward way to do this is to fit a Generalised Linear Mixed Model (GLMM) such as that described in Section 2.2 for Poisson and negative binomial conditional error structures. Here the error structure for each CR model, conditional on the random site effects, is assumed binomial. Fitting the CR models as a binomial GLMM was carried out using GENSTAT's GLMM Procedure (Payne *et al*., 1997) using the marginal-form of the model given by Breslow and Clayton (1993). The coincident GLM regression model is therefore of the same form as the GLMM but parameter estimation for the GLMM takes into account the random site (and season) effects in the error structure.

More realistic models could be considered such as the hierarchical GLMs (HGLMs) of Lee and Nelder (1996). In HGLMs the random effects are not restricted to be Gausssian, as in the GLMMs, and can for example incorporate a beta (error) distribution for the random intercepts. However, with data from only two sites and a single season available in this study the ability to discriminate between competing random effects distributions using data analytic techniques, such as residual plots, is severely limited. Since HGLMs are subject-specific models (Section 2.3) obtaining the marginal means given the predictor variables is more difficult so the extra effort required was not considered justified.

Assessing goodness of fit of the GLM

The goodness of fit of the model, combining all stages can be compared assessed using the deviance statistic (McCullagh and Nelder, 1989) calculated for a multinomial distribution as $-2\ln(L_C / L_0)$ where L_0 is the likelihood with $\hat{q}_{ij}$ calculated using (6.7), and L_0 is the likelihood calculated for the saturated model (i.e. $\hat{q}_{ij} = n_{ij} / N_i$). This deviance statistic is given by

$$D_C = 2\sum_{i=1}^{m}\sum_{j=1}^{s} n_{ij} \ln\left\{ \frac{n_{ij}}{N_i \hat{q}_{ij}} \right\}$$

where $\hat{q}_{ij}$ is given by (6.7) and *m* is the total number of sampling times. The deviance is approximately distributed as a chi square with {*ms* - *m* - 2(*s*-1)} degrees of freedom. An analagous statistic to the coefficient of determination for multiple linear regression was defined by Candy (1991) as the percentage of deviance explained by (6.7) which is given by

$$P_C = 100\frac{D_N - D_C}{D_N}$$

where D_N, the null deviance, is calculated in the same way as D_C except that $\hat{q}_{ij}$ is calculated as $\sum_i n_{ij} / \sum_i N_i$, the common-across-times proportion in stage *j*.

6.4.4 Sampling methods and data

Stage-frequency data was collected at two sites in the Florentine Valley in south-western Tasmania. Ambient temperature recorded at one minute intervals at each site using a STARLOG® datalogger and a temperature thermistor attached to a tree in well-shaded position approximately 2m above ground. The more elevated site, Snake Rd (Appendix 5), had a northerly aspect at 550m altitude in seven year-old *E. regnans* regeneration (Fig. 6.5a). The other site, Tiger Rd (Appendix 5), was located on the valley floor at an altitude of 350m in 10 year-old *E. regnans* regeneration (Fig. 6.5b).

Occupied shoots were randomly selected at 2-day to weekly intervals between November 1991 and March 1992 from sampling stations within five transects. At the Snake Rd site the transects were approximately 10m apart running perpendicular to the road while at the Tiger Rd site, snig tracks from previous logging were used as ‘transects’ because of the high density of regeneration at that site. No attempt was made to estimate total population numbers. Shoots were sampled without regard to

(a)

(b)

Figure 6.5 Sites in *E. regnans* regeneration in the Florentine Valley, southwestern Tasmania where *C.bimaculata* stage-frequency data were collected : (a) Snake Rd (b) Tiger Rd.

the stages present but sample intensity was varied in an ad hoc manner to obtain sufficient total numbers at each sampling occasion. The probability of selecting an individual in a given stage should therefore correspond to the proportion in the population that the stage represents at the particular sample occasion. Figure 6.6 shows part of a typical sample shoot with a leaf occupied by L3 and L4 larvae.

The start times of the major peaks in oviposition were estimated by noting the first sample occasion when large numbers of eggs were present and then determining from temperature records the previous day, or days when maximum temperature exceeded $25\,^{o}\mathrm{C}$. The start was taken to be 12 h on the most recent day on which temperature exceeded this level. This approach is based on the observation of de Little (1979) that major oviposition events do not occur until temperature is above this level. Time scales were calculated by integrating the development rate functions (6.1) and (6.2a), with parameter estimate for response parameter θ_2 in each case given in Table 6.2, using the trapezoidal rule. Figure 6.7 shows the temperature trace at each site from the starting date of each population along with upper and lower quartiles for ambient shaded air temperatures.

Figure 6.6 *Eucalyptus regnans* leaf with L3 and L4 larvae at the Tiger Rd site, Florentine Valley, southwestern Tasmania.

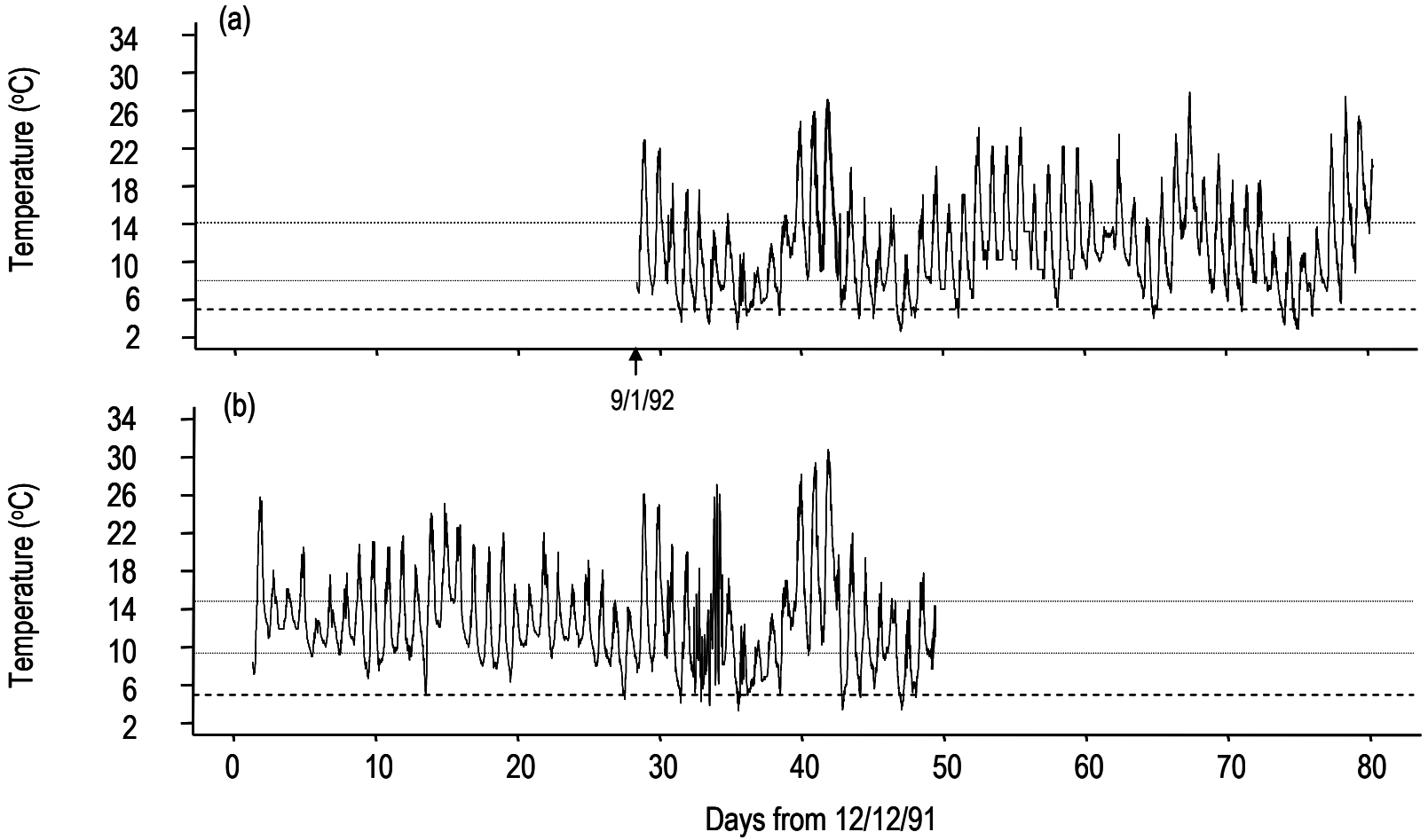

Figure 6.7 Shade temperatures recorded in 10 min intervals at two sites in the Florentine Valley, southwest Tasmania (a) Snake Rd (550 m asl) (b) Tiger Rd (350 m asl). The dotted lines represent upper and lower quartiles at each site. The dashed line shows the lower threshold temperature for *C.bimaculata* development.

6.4.5 Results

The start of oviposition at the Tiger Rd site was estimated to have occurred on the 24/11/91 with no evidence of *C. bimaculata* oviposition activity on the sample occasion on 22/11/91 while a moderate size population of eggs was found on the 26/11/91. Almost all this population was eaten by predators so that by the second, much more massive oviposition event, estimated to have occurred on the 13/12/91, only a few L2 and L3 larval instars from the earlier population were found at the sample occasion on the 17/12/91. For the purposes of model building only stage-frequency data from this second population is used. There were no further major oviposition events at this site and the population was sampled until almost all individuals were L4 larvae on the 23/1/92, 41 days after the estimated start of oviposition. A small amount of intermittent oviposition occurred after this date but samples from those populations have not been used here. At the Snake Rd site one large oviposition event was estimated to have occurred on the 9/1/92. This population was observed until the 2/3/92, 53 days later, when the majority of larvae were 4th instar. The stage-frequency data consisted of a total of 14336, 5384, 2865, 1528, 831 individual eggs, L1, L2, L3, and L4 larvae, respectively, across the sites and sampling occasions. Appendix A9 gives the complete data set.

Fitting the GLM using William's methods I, II and III and fitting the GLMM

William's method II and III were fitted using EXTRABINOMIAL, with logit link function and SITE (the 2-level factor representing the two sites) as a fixed effect. Convergence of the estimate of the respective overdispersion parameter (i.e. ϕ or σ^2) was usually acceptable. However, it was found necessary to revert to the William's method I due to problems of divergence of the parameter estimates and wild oscillations in the overdispersion parameter estimate when the logit model was fitted to the data for L3 larvae. In addition, for all time scales and stages, predictions of μ_{ij} using methods II and III were unrealistic since they gave extremely long right-tails to the unconditional probability plots.

For the fit of the GLMM, again with logit link function, SITE was included as a random intercept. A random slope effect was not included because acceptance of the hypothesis for parallel regressions (described below) indicated that there was little scope to model this source of variation. The fitting algorithm for the marginal

GLMM converged for each stage and time scale but, as expected for a sample of only two sites, the variance of the random site intercepts was very imprecisely estimated with the standard error exceeding the estimate in each case. Therefore, it was concluded that fitting the GLM with these more complex error models was not justified given the limitations of the data. The simple, single error-level GLM combined with William's method I was then used exclusively.

Fitting the models as GLMs with William's model I for overdispersion

Alternative models tried were the logit link with each of the time scales transformed to a logarithmic scale, and the complementary log-log link using each of the untransformed and log-transformed time scales. The best class of model was found to be the logit link with the untransformed time scale. The fit of the probit was similar but the logit is more convenient to use since the logistic CDF is an explicit function of time and the regression parameters. Candy (1991) found the complementary log-log link superior to the logit for CR models fitted to the stage-frequency data given by Dennis *et al*. (1986) for the western spruce budworm, *Choristoneura occidentalis* (Freeman). However, here there were numerical problems in fitting the complementary log-log link for all time scales for the L3 data, in particular, divergence of the residual deviance. The data for this instar is the least adequate for fitting these models, and the fact that the inverse link function in this case involves double exponentiation makes it more sensitive to inadequacies in the data than the logit link function. The logit link function combined with the untransformed time scale was therefore used for all subsequent modelling.

Common regression intercepts (β_{0j}), and slopes (β_{1j}) across sites (coincident regressions) were compared to the model with site-specific intercepts and common slope (parallel regressions) and the model with separate intercepts and slopes (separate regressions). The results of the fit of these models are given for egg, and L1 to L3 larval stages in Tables 6.4 to 6.7 respectively.

Table 6.8 compares the different time scales in terms of the fit for each stage separately using the residual mean deviance. Table 6.8 also gives the deviance combined across all four stages and the percent deviance explained, P_C, calculated using unconditional probabilities and the multinomial deviance. For all stages and

Table 6.4 Test of parallel and coincident logistic regressions for eggs

Time scale	Site	Parameter estimate (s.e.) β_0	Parameter estimate (s.e.) β_1	F_p[1]	F_c[2]
Days	Snake Rd	9.900 (2.754)	-0.388 (0.107)	0.8^{ns}	49.0^{**}
	Tiger Rd	7.732 (1.376)	-0.526 (0.102)		
	Pooled[3]	4.273 (0.944)	-0.220 (0.049)		
DD[5]	Snake Rd	7.428 (1.927)	-0.054 (0.014)	0.3^{ns}	6.5^{*}
	Tiger Rd	7.255 (1.250)	-0.065 (0.012)		
	Pooled[3]	6.077 (0.902)	-0.049 (0.008)		
DDN	Snake Rd	7.741 (2.000)	-0.029 (0.008)	0.6^{ns}	32.9^{**}
	Tiger Rd	7.182 (1.221)	-0.036 (0.007)		
	Pooled[3]	5.614 (0.897)	-0.024 (0.004)		

Table 6.5 Test of parallel and coincident logistic regressions for L1 larvae

Time scale	Site	Parameter estimate (s.e.) β_0	Parameter estimate (s.e.) β_1	F_p[1]	F_c[2]
Days	Snake Rd	11.713 (3.383)	-0.337 (0.100)	0.1^{ns}	40.5^{**}
	Tiger Rd	7.021 (1.539)	-0.316 (0.066)		
	Pooled	4.412 (1.638)	-0.163 (0.060)		
DD[5]	Snake Rd	9.303 (2.437)	-0.044 (0.012)	0.1^{ns}	10.6^{**}
	Tiger Rd	7.286 (1.507)	-0.042 (0.008)		
	Pooled	7.647 (1.515)	-0.041 (0.008)		
DDN	Snake Rd	9.662 (2.520)	-0.024 (0.006)	0.0^{ns}	30.8^{**}
	Tiger Rd	7.371 (1.522)	-0.024 (0.005)		
		7.268 (1.640)	-0.021 (0.005)		

[1] $F_{1,16}$ statistic for test of parallelism of regressions on logit scale.

[2] $F_{1,16}$ statistic for test of coincident regressions on logit scale.

[3] Fitted coincident regressions on logit scale.

^{ns} $P>0.05$, * $P<0.05$, ** $P<0.01$

Table 6.6 Test of parallel and coincident logistic regressions for L2 larvae

Time scale	Site	Parameter estimate (s.e.) β_0	Parameter estimate (s.e.) β_1	F_p[1]	F_c[2]
Days	Snake Rd	9.767 (2.412)	-0.231 (0.057)	2.1^{ns}	39.1**
	Tiger Rd	10.605 (1.889)	-0.362 (0.065)		
	Pooled	4.620 (1.619)	-0.137 (0.049)		
DD[5]	Snake Rd	9.037 (2.120)	-0.035 (0.008)	4.2^{ns}	23.7**
	Tiger Rd	11.387 (1.849)	-0.051 (0.008)		
	Pooled	8.750 (1.602)	-0.037 (0.007)		
DDN	Snake Rd	9.102 (2.121)	-0.018 (0.004)	3.3^{ns}	41.3**
	Tiger Rd	11.059 (1.781)	-0.027 (0.004)		
	Pooled	7.696 (1.600)	-0.018 (0.004)		

Table 6.7 Test of parallel and coincident logistic regressions for L3 larvae

Time Scale	Site	Parameter estimate (s.e.) β_0	Parameter estimate (s.e.) β_1	F_p[1]	F_c[2]
Days	Snake Rd	11.034 (3.007)	-0.230 (0.061)	6.6$^{*?}$	34.4**
	Tiger Rd	18.225 (3.355)	-0.511 (0.098)		
	Pooled	6.066 (1.878)	-0.142 (0.048)		
DD[5]	Snake Rd	8.689 (2.892)	-0.029 (0.010)	3.7^{ns}	6.1**
	Tiger Rd	16.780 (3.642)	-0.063 (0.014)		
	Pooled	10.231 (1.909)	-0.036 (0.007)		
DDN	Snake Rd	8.694 (2.847)	-0.015 (0.005)	4.4^{ns}	14.8**
	Tiger Rd	16.129 (3.459)	-0.033 (0.007)		
	Pooled	8.976 (1.763)	-0.017 (0.004)		

[1] $F_{1,16}$ statistic for test of parallelism of regressions on logit scale.

[2] $F_{1,16}$ statistic for test of coincident regressions on logit scale.

[3] Fitted coincident regressions on logit scale.

^{ns} $P>0.05$, * $P<0.05$, ** $P<0.01$

Table 6.8 Residual (binomial) deviance for each time scale and stage for the logistic regression and multinomial deviances over all stages

Time scale	Residual mean deviance				Parallel regressions		Coincident Regressions	
	Egg	L1	L2	L3	D_C	P_C	D_C	P_C
Days	99.5	29.8	11.7	86.7	3313	96.6	13510	86.2
DD[5]	95.3	24.5	16.4	75.0	3133	96.8	5290	94.6
DDN	93.4	24.4	16.0	73.3	3073	96.9	6596	93.3

Table 6.9 Predicted logistic means for parallel and coincident (i.e. pooled) regressions for each time scale

Time Scale	Site	Stage means (s.e.)			
		$\hat{\alpha}_1$ (Egg)	$\hat{\alpha}_2$ (L1)	$\hat{\alpha}_3$ (L2)	$\hat{\alpha}_4$ (L3)
Days	Snake Rd	25.5 (7.9)	34.8 (11.4)	42.0 (13.1)	48.5 (19.2)
	Tiger Rd	14.9 (4.4)	22.2 (7.5)	29.5 (9.1)	36.2 (13.8)
	Pooled	19.4 (8.4)	27.1 (19.8)	33.8 (24.0)	42.6 (27.2)
DD[5]	Snake Rd	137.2 (40.4)	209.5 (63.9)	258.5 (72.2)	297.7 (119.4)
	Tiger Rd	111.8 (31.3)	171.6 (54.2)	224.7 (62.5)	273.5 (105.0)
	Pooled	123.3 (37.1)	185.3 (72.5)	234.6 (86.5)	283.9 (108.0)
DDN	Snake Rd	267.6 (78.1)	400.7 (121.9)	492.6 (137.4)	567.7 (225.1)
	Tiger Rd	202.4 (56.1)	311.6 (98.2)	408.6 (113.5)	501.2 (190.0)
	Pooled	232.4 (74.7)	343.7 (153.4)	434.3 (182.0)	531.4 (213.0)

time scales, with the exception of L3 and Julian days, the hypothesis of parallelism was accepted (P>0.05). In all cases the hypothesis of coincident regressions was rejected(P<0.05). However, to allow general application of the models (as discussed earlier) the coincident (i.e. pooled) regression model was fitted in each case with results for egg to L3 stage given in Tables 6.4 to 6.7.

Table 6.9 gives the estimates of logistic mean, α_j and variance, $\pi^2\rho_j^2/3$, for egg to L3 stages (i.e. α_1 to α_4) based on each of the fit of the parallel and coincident (i.e. pooled) logistic regressions for each time scale. The estimates of the α_j give the time from oviposition to the time when 50% of the population, defined as all individuals in stage *j* or later, are in stage *j* and 50% are in stage *j*+1 or later. Note that for direct comparison with development time from oviposition to the end of the L4 stage given in Tables 6.2 and 6.3 it would have be necessary to include the pupal stage (i.e. including the pre-pupal stage) in the stage-frequency data with α_5 giving the corresponding total development time. To allow comparison with the results from the constant temperature experiments, the estimated thermal sums to the end of the L3 stage were (from Table 6.2) 223 *DD* and 447.6 *NDD*. Therefore, the estimates of α_4 for the *DD* and *NDD* time scales of 283.9 and 531.4 respectively given in Table 6.9 confirm the results given in Table 6.3. That result is that the development times on *E. regnans* obtained in Greave's constant temperature experiments are substantially shorter than those obtained in field sampling at Brady's Plantation, the two Florentine Valley sites, and those obtained in the laboratory by Baker *et al*. (1999) (see Discussion).

Figures 6.8 to 6.10 plot the observed and predicted proportions (i.e. unconditional probabilities) for the parallel-regression logit model for each stage, site and time scale.

6.5 PREDICTING TIME OF PEAK OCCURRENCE

6.5.1 Peak relative occurrence

The method of estimating time of peak relative occurrence for L1, L2, and L3 larvae for the CR models is similar to that described by Dennis and Kemp (1988) for their phenology model which can be classified as an ordinal regression model

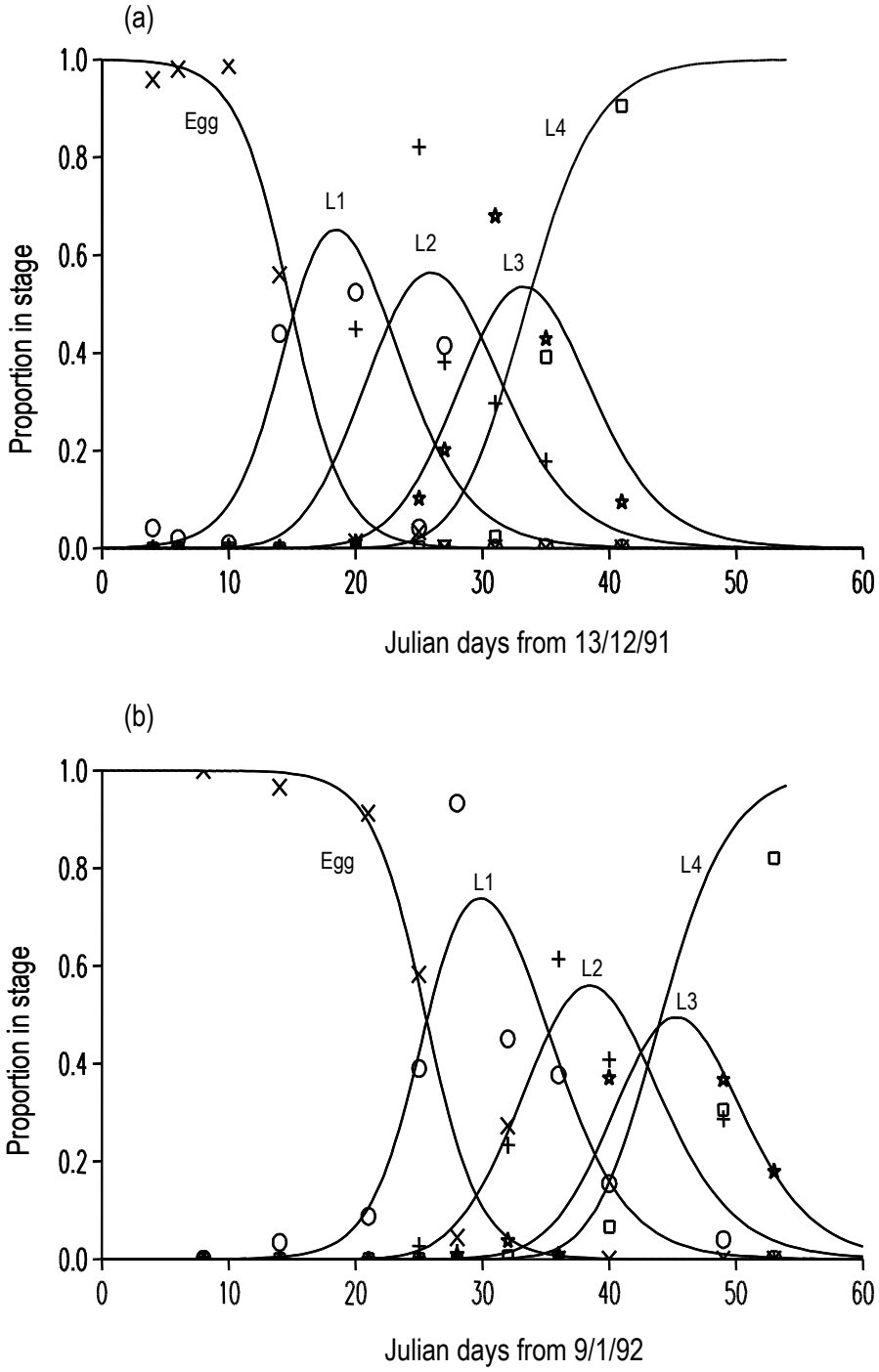

Figure 6.8 Observed and predicted proportion in each life-stage versus Julian days from oviposition at two sites in the Florentine Valley, southwestern Tasmania, (a) Tiger Rd (b) Snake Rd. Predictions from parallel regression model. Observed proportions : (x) egg, instars (○) L1, (+) L2, (*) L3, and (□) L4.

310

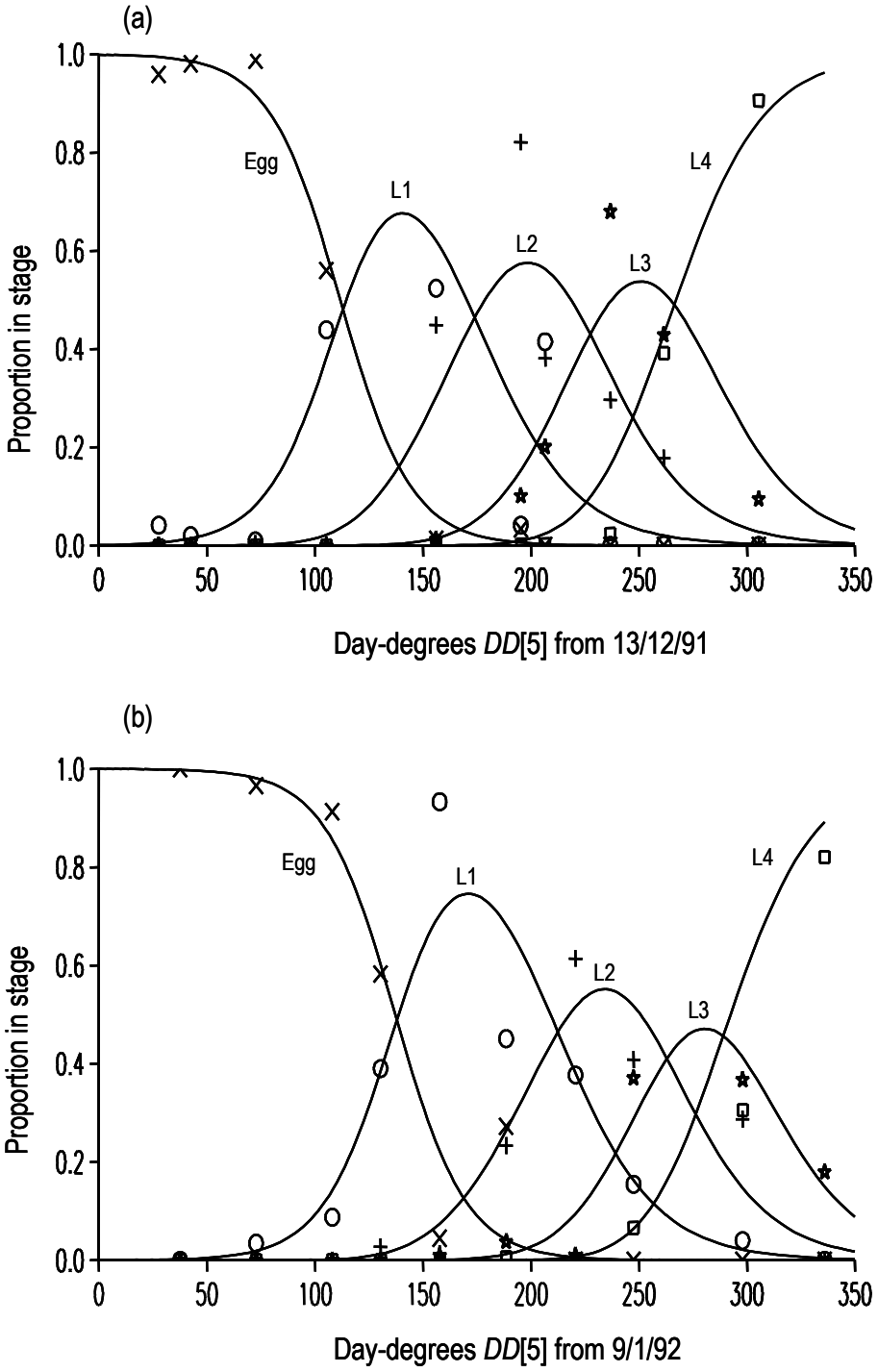

Figure 6.9 Observed and predicted proportion in each life-stage versus day-degrees from oviposition at two sites in the Florentine Valley, southwestern Tasmania, (a) Tiger Rd (b) Snake Rd. Predictions from parallel regression model. Observed proportions : (x) egg, instars (○) L1, (+) L2, (*) L3, and (□) L4.

311

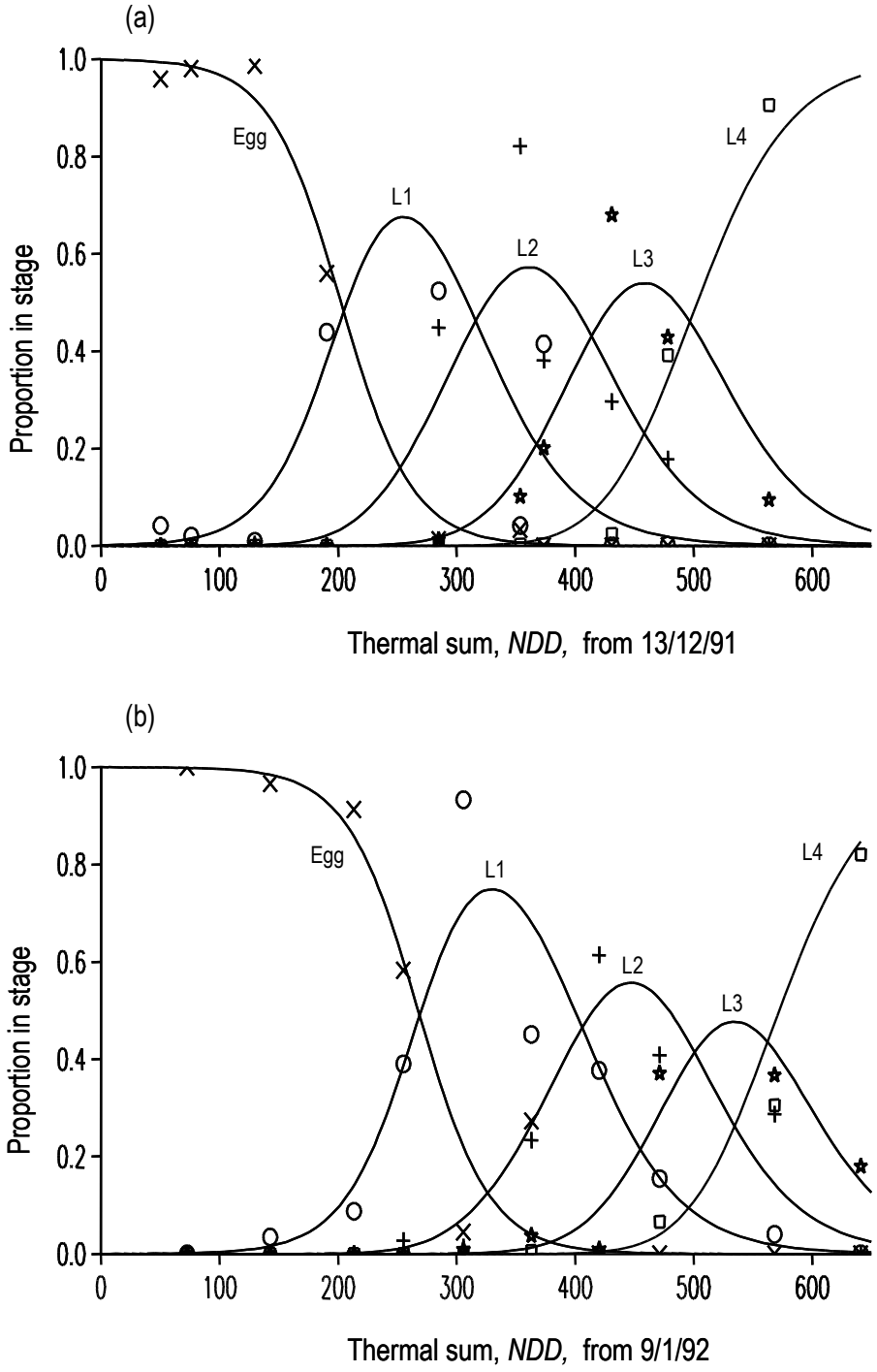

Figure 6.10 Observed and predicted proportion in each life-stage versus thermal sum, *NDD*, from oviposition at two sites in the Florentine Valley, southwestern Tasmania, (a) Tiger Rd (b) Snake Rd. Predictions from parallel regression model. Observed proportions : (x) egg, instars (○) L1, (+) L2, (*) L3, and (□) L4.

(Candy, 1991). Generalising to stage *j* and time *t*, the peak time, t_j^*, is obtained as the solution, in terms of *t*, of

$$\frac{dq_j(t)}{dt} = 0 \qquad ; \; j = 2,...,s-1 \tag{6.8}$$

where q_j is given by (6.7) with the subscript *i* suppressed since *t* is general time and not specific sampling times. Considering t_j^* as a variable with values in the region of its maximum likelihood estimate, the general form of (6.8) can be expressed as the function

$$f\left(t_j^*, \beta_j\right) = 0 \tag{6.9}$$

where $\boldsymbol{\beta}_j = \left(\beta_{01}, \beta_{11}, ..., \beta_{0j}, \beta_{1j}\right)^T$.

Since there is no algebraic solution to (6.9) then, implicitly,

$$t_j^* = g\left(\beta_j\right) \tag{6.10}.$$

The form of $f(.)$, using the logit link function for $h(.)$, is given from (6.7) by

$$f\left(\eta_1^*, ..., \eta_j^*\right) = \frac{exp\left(\eta_j^*\right)}{\prod_{r=1}^{j} 1 + exp\left(\eta_r^*\right)} \left[\frac{\beta_{1j}}{1 + exp\left(\eta_j^*\right)} - \left\{ \sum_{r=1}^{j-1} \frac{\beta_{1j}\, exp\left(\eta_r^*\right)}{1 + exp\left(\eta_r^*\right)} \right\} \right] \tag{6.11}$$

where $\eta_j^* = \beta_{0j} + \beta_{1j}\, t_j^*$. Using (6.9), if $\hat{\boldsymbol{\beta}}_j$ is the conditional maximum likelihood estimate (CMLE) of $\boldsymbol{\beta}_j$ obtained from the fit of the GLM (6.6), then the CMLE of t_j^*, $\hat{t}_j^* = g\left(\hat{\boldsymbol{\beta}}_j\right)$, is obtained by numerically solving (6.9). An approximate standard error of the estimate of $\hat{t}_j^*$ can be obtained using the δ-method which uses a first-order Taylor series expansion of (6.10) about $\hat{\boldsymbol{\beta}}_j$ (Bard, 1974, p.205). The standard error is given as the square root of the variance

$$var(\hat{t}_j^*) = g'(\hat{\boldsymbol{\beta}}_j)^T \hat{\Sigma}_{\hat{\boldsymbol{\beta}}_j} g'(\hat{\boldsymbol{\beta}}_j)$$

where $\hat{\Sigma}_{\hat{\boldsymbol{\beta}}_j}$ is the estimated, 2*j* x 2*j*, block-diagonal covariance matrix for the pairs of estimated regression parameters (i.e. intercept and slope) obtained from the fit of the CR models for stage 1 to *j*, and

$$g'(\hat{\boldsymbol{\beta}}_j) = \frac{dt_j^*}{d\hat{\boldsymbol{\beta}}_j} = \frac{\partial f}{\partial \hat{\boldsymbol{\beta}}_j}\left(\frac{\partial f}{\partial t_j^*}\right)^{-1}.$$

To obtain the derivatives, $g'(\hat{\beta}_j)$, numerical solutions for the partial derivatives

$$\frac{\partial h}{\partial \boldsymbol{\beta}_j}, \frac{\partial f}{\partial t_j^*}$$

at $\hat{\boldsymbol{\beta}}_j$ and $\hat{t}_j^*$ are required.

6.5.2 Peak (absolute) occurrence

Following Munholland and Dennis (1992), the number in each stage *j* at time *t*, $N_j(t)$ (expressed in standard units such as insects per shoot or per tree), can be modelled by

$$N_j(t) = N(t)q_j(t) \quad ; \quad j = 1,...,s \tag{6.12}$$

where $q_j(t)$ is the proportion of the population in stage *j*, given by model (6.7), and the total surviving population at time *t* is given by

$$N(t) = N(0)\exp(-\psi\, t) \tag{6.13}$$

where $N(0)$ is initial population size at time zero, and ψ is the instantaneous mortality rate parameter (i.e. the proportion of deaths per unit time). This can be seen by expressing cumulative mortality to time *t*, $D(t)$, as $D(t) = N(0)\{1 - \exp(-\psi\, t)\}$ so that ψ, the mortality rate parameter, can be expressed as the relative mortality rate

$$\psi = \frac{1}{N(t)}\frac{dD(t)}{dt}.$$

The above model assumes that the mortality rate does not vary with stage. Using stage-frequency data alone (i.e. mortality is not observed directly) more complex mortality/survival models than constant-rate model cannot be successfully fitted simultaneously with the model for q_j (Munholland and Dennis, 1992). Since the great majority of the mortality in *C. bimaculata* populations occurs in the egg stage (de Little *et al*., 1990), model (6.13) is unrealistic. Therefore, to account for the higher egg mortality rate the following model was employed

$$N(t) = N(0)\left\{Q\exp\left(-\psi_e t^{\lambda}\right) + (1-Q)\exp(-\psi t)\right\} \quad ; \quad Q, \psi_e, \psi > 0,\ \lambda > 1 \qquad (6.14)$$

where Q is the proportion of the population removed by predation at the egg stage, parameters ψ_e and λ determine the rate at which this occurs, and ψ is an average mortality rate parameter for all stages excluding that due to egg predation. Mortality in the egg stage due to predation is given by $D_e(t) = N(0)Q\left\{1-\exp\left(-\psi_e t^{\lambda}\right)\right\}$ where this corresponds to an 'accelerated failure time' model based on Weibull-distributed survival times (Cox and Oakes, 1984, p.19,69). The greater the value of λ the greater the rate of decline in the egg population. This model therefore allows a much more rapid decline in the egg population due to predation than that for general mortality in the 'all-stage, constant mortality rate' model. Total cumulative mortality at time *t* is therefore $D(t) + D_e(t)$ where $D(t) = N(0)(1-Q)\left\{1-\exp(-\psi t)\right\}$.

An estimate of ψ can be obtained from the final population size of L4 larvae at time t', $N(t')$, and $D(t')$ assuming t' is the time when mortality has effectively ceased. This estimate is given by

$$\hat{\psi} = -ln\left\{\frac{N(t')}{N(0)(1-Q)}\right\}\frac{1}{t'} \qquad (6.15).$$

The peak in numbers of stage *j* for $j = 2,..,s-1$ (i.e. L1 to L3) is obtained by solving

$$\frac{dN_j(t)}{dt} = N(t)\frac{dq_j(t)}{dt} + q_j(t)\frac{dN(t)}{dt} = 0 \qquad ; \quad j = 2,...,s-1 \qquad (6.16).$$

Assuming the term in (6.14) given by $Q\exp(-\psi_e t^{\lambda})$ is negligible relative to the term $(1-Q)\exp(-\psi t)$ for the range of *t* covering the peaks in L1 to L3 numbers, so that $N(t) = N(0)(1-Q)\exp(-\psi t)$, then (6.16) can be approximated by

$$\frac{1}{q_j(t)}\frac{dq_j(t)}{dt} \cong \hat{\psi} \qquad ; \quad j = 2,...,s-1 \qquad (6.17).$$

Therefore, the solution to (6.17) gives the approximate time to peak absolute occurrence, t_j'', for stage *j*. The same equation is obtained if model (6.13) is assumed for $N(t)$ but the estimate of ψ, obtained by setting *Q*=0 in (6.15), would be inflated by the failure to account for stage-specific mortality rates. Given an estimate of ψ from (6.15), with *Q* estimated as the total proportion of eggs removed by predation, then (6.17) can be solved using the method described above for determining t_j^*. Note that since the functions $q_j(t)$, for $j = 2,...,s-1$, are concave down then for $t \le t_j^*$ their derivatives, with respect to time, are positive but declining to zero at time t_j^*. Therefore, since $q_j(t)$ and ψ can only take positive values then comparison of (6.8) with (6.17) proves that $t_j'' < t_j^*$.

6.5.3 RESULTS

The estimated times of peak relative occurrence, $\hat{t}_j^*$, for L1, L2, and L3 larvae were calculated using the pooled (coincident) regression parameter estimates for the *DD*[5] time scale (Tables 6.4 to 6.7) combined with (6.7) and (6.10). Standard errors for $\hat{t}_j^*$ were estimated using the δ-method. These peak times are given in Table 6.10.

The estimates of times of peak absolute occurrence, $\hat{t}_j''$, require an estimate of mortality rate parameter, ψ, in model (6.14). The only data on mortality available were those given by de Little *et al*. (1990). They found that total mortality from egg

to L4 stages ranged from 95 to 97% for two sites. Of this total the range for mortality from egg to 'mid-first instar' larvae was 66 to 84%. To obtain a corresponding range for the estimate of ψ in model (6.14) the values of *Q* were taken as 0.34 and 0.16 corresponding to the 66 to 84% 'egg' mortality (i.e. this will include some L1 larval mortality). The corresponding estimates of ψ were obtained from (6.15) as $\hat{\psi} = -\ln(0.05/0.34)/262.6 = 0.0073$ and $\hat{\psi} = -\ln(0.03/0.16)/262.6 = 0.0064$ where the divisor of $t' = 262.6$ *DD*[5] is taken to be the estimate of t_4^* from Table 6.10. Table 6.10 gives the corresponding estimates of the t_j'''s. For comparison Table 6.10 also gives $\hat{t}_2''$ calculated using (6.15) with *Q*=0 and $\hat{\psi} = \hat{\psi}_e = -\ln(0.34)/154 = 0.007$ and $\hat{\psi}_e = -\ln(0.20)/154 = 0.0105$ corresponding to 34% and 20% egg survival rates respectively where the divisor 154 *DD*[5] corresponds to $t' = \hat{t}_2^*$. All the above estimates of ψ are based on approximations which assume mortality in the egg stage decays to zero by $\hat{t}_2^*$ and the 'all-stage' constant mortality rate only applies up to t_4^* (i.e. the time of peak in L3 larvae) after which time mortality is negligible. Numerical problems were encountered in solving (6.17) when survival was below 20% [e.g. the 84% egg mortality of de Little *et al*. (1990)].

Table 6.10 Time of peak relative and absolute occurrence of L1 to L3 larvae in day-degrees from population initiation

Parameter	Time of Peak (s.e.) (units=*DD*[5])		
DD[5]	L1 (*j*=2)	L2 (*j*=3)	L3 (*j*=4)
t_j^*	154.0 (4.7)	211.5 (9.8)	262.6 (14.3)
t_j'', ψ=0.0073	138.2	191.6	240.0
t_j'', ψ=0.0064	140.6	195.1	244.0
t_j'', ψ_e=0.0070	138.9		
t_j'', ψ_e=0.0105	124.8		

6.5 DISCUSSION

Development rate models : comparison of hosts

The estimated development time, measured either in units of *DD* or *NDD* (Table 6.3), for feeding on *E. regnans* is significantly (*P*<0.01) greater than that for

total development given in Table 6.2 for Greave's constant temperature data. De Little (1989) reared *C. bimaculata* larvae on adult leaves of *E. nitens*, *E. globulus*, and F1 *E. nitens* x *E. globulus* hybrids for a single, constant temperature regime of 23^{o}C and a 16:8 h light:dark photophase and observed mean larval development time (i.e. from L1 to L4) for the three hosts of 11.6, 15.8, and 13.5 days respectively. This corresponds to 208.8, 284.4, and 243.0 *DD*[5]. Baker *et al*. (1999) observed development times of L1 to L4 larvae fed on *E. regnans* and *E. nitens* foliage for a single temperature regime of 18^{o}C:12^{o}C corresponding to a 16:8 h light:dark photophase. This gives an average temperature of 16^{o}C so that the average time taken from L1 to L4 was 262.7 *DD*[5] for *E. regnans* and 216.7 *DD*[5] for *E. nitens*. This last value is similar to that obtained by de Little (1989).

If the development time for eggs is taken as approximately 88.7 *DD*[5] (Table 6.2), the development times obtained by Baker *et al*. (1999) after including the egg stage give approximately 351.4 for *E. regnans* and 305.4 *DD*[5] for *E. nitens*. These values are similar to the values obtained from the field emergence data of 333.2 and 303.1 respectively (Table 6.3). For *E. regnans*, these development times are considerably longer that that obtained from the constant temperature study of Greaves where the corresponding value is 277.5 (Table 6.2). The reason for this difference is uncertain but it could be related to the different cohorts or source of foliage used in the different experiments. The method of recording development time was similar in each study. Greaves (1966) recorded total larval development time in days from the time when 50% of eggs had hatched to that when 50% of L4s had entered the pre-pupal stage. In Baker *et al*. (1999) time between moults was taken as the time when 40% of larvae had moulted to the next instar.

Clarke (1998) used the same constant temperature data of Greaves to obtain stage-specific thresholds, ranging from a minimum of 0.55^{o}C for eggs to a maximum of 5.4^{o}C for L1 larvae, and calculated corresponding *DD*s for each stage. The *DD*s which were substantially different to those in Table 6.2 were those for eggs (112 *DD*[0.55]), L3 (46 *DD*[3.77]), and L4 (64 *DD*[3.78]) larvae. However, since the day-degree calculations given in Tables 6.2 and 6.3 use a common threshold, the difference thermal sums between these two tables cannot be due to differences in stage-specific thresholds.

Despite these unexplained differences in development time on *E. regnans*, since representative stage-frequency data have been used to predict time of peak relative occurrence of each of L1 to L3 larvae, then reasonable confidence can be placed in the accuracy of these estimates. The one parameter not estimated from this data is the common, lower development threshold, θ_2, since its estimate of 5.08^{o}C was used to calculate day-degrees (Table 6.2). However, since θ_2 is purely a temperature-response parameter, its estimate should be more robust than that for development time, θ_1^{-1}, since the slope of the regressions, given by the $\hat{\theta}_1$ in Table 6.2 (Fig. 6.1), will be determined by host type and foliage quality as well as temperature.

To obtain similar predictions for *E. nitens* it is clear that model (6.6), calibrated using stage-frequency data from *E. regnans* regeneration, needs to be adjusted for the shorter development times on *E. nitens* as indicated by Baker *et al*. (1999) and Table 6.3. The simplest correction for the day-degree models is to multiply either each of the $\hat{\beta}_{1j}$'s from Tables 6.4 to 6.7 or *DD*[5] by the ratio 262.7/216.7 obtained from Baker *et al*. (1999) as described above. A similar correction can be made for the *NDD* time scale.

Estimation of development rate models using field emergence data

Section 6.3 gives a formal statistical basis, lacking in the literature, for estimation of rate models from development or emergence times observed in the field under ambient temperatures. For the usual case of interval-censored times, where these intervals are long relative to the scale over which diurnal temperature fluctuations occur the response variable was modelled as multinomially distributed. Appendix A7 demonstrates that when observation periods are short (e.g. 2 hourly) then temperature at time of emergence can be used to improve estimation.

The difficulty of fitting rate models and, in particular, estimating temperature response parameters, such as a lower threshold, from field data was demonstrated using both real and simulated data. Although the real data was very limited the simulated data in Appendix A7 demonstrated that DEVAR's least squares approach can be unreliable. In addition, DEVAR's approach of attributing all the development

times observed for a given sampling period (i.e. the period between observation times) to the mid-point of the period will result in a tendency to over-estimate goodness of fit and under-estimate the standard error of parameter estimates.

Other distributions to the normal could be used for Y^*, the fluctuating temperature analogue to empirical rates obtained from constant temperature studies. However, given the coarseness of interval-censored development times it is doubtful whether adequate discrimination between distribution models could be achieved in terms of goodness of fit.

Continuation ratio models

The best time scale over all stages for the parallel logistic regression were *NDD* since it gave the lowest deviance. However, *NDD* gives only a slight improvement over *DD* while for the coincident regression model the *DD* model gave a substantially better fit than *NDD* (Table 6.8). In practice, as discussed earlier, it is only the coincident regression model that can be applied since site-specific regression intercepts will not be available. Therefore, the *DD*[5] time scale is recommended for predicting *C. bimaculata* field phenology. The inaccuracy of predictions for each site using the coincident regressions is only of the order of between 24 and 38 *DD*[5] (i.e. the differences between the two sites in Table 6.9). Given an average daily temperature of around 15^{o}C, this corresponds to between 2.4 and 3.8 days. A difference between the two sites of this magnitude could easily be due to errors in specifying the date of oviposition.

Changing the assumed starting or initiation time for the population does not affect the fit of the CR model because this model is conditioned on the population being in at least the first stage. However, a known event that starts the development process must be used as the starting time so that the fitted model is relevant from place to place and year to year (Candy, 1991). In this case the starting date is taken to be time of the start of a major oviposition event. Estimating this starting date when carrying out routine population monitoring is dealt with in Chapter 7.

As seen in Figs. 6.8 to 6.10, the CR models fitted to the stage-frequency data have produced predicted (unconditional) probability trajectories which show clear peaks

for instars L1, L2, and L3 with the exception of the L3 larvae at Snake Rd. In this last case, the peak relative occurrence is only just distinguishable before the proportion of L3 larvae is overtaken by that of the final instar. This problem could be overcome in future stage-frequency sampling by timing sampling to coincide more closely with the predicted peak occurrence of this instar.

Estimating stage-specific development thresholds from stage-frequency data

The CR model requires a common physiological time scale, such as $DD[\theta_2]$ or $NDD[\theta_2]$, and therefore a common θ_2 across stages. Even though a common time scale is used, unlike the microscopic models and ordinal regression models, the CR model quantifies the response of stage proportions to this time scale as stage-specific (Candy, 1991). This is effectively achieved by estimating the stage-specific values $\hat{\beta}_{1j}$. However, Manel and Debouzie (1997) generalised the CR model of Candy (1991) by incorporated maximum profile likelihood (MPL) estimation of stage-specific θ_2 parameters for the linear model (6.1). This extra sophistication may be unnecessary if the hypothesis of a common θ_2 is accepted from the fit of (6.1) or (6.2a) to constant temperature data. This hypothesis was accepted for both models (P>0.05) in this study but it can be argued that this simply means that a significant difference could not be detected from the available data. More useful than the hypothesis test itself is the estimate of the standard error of the common estimate of θ_2 for the linear model given in Table 6.2 as approximately $1\,^{o}\mathrm{C}$. Given a corresponding approximate 95% confidence interval of 3 to $7\,^{o}\mathrm{C}$, this implicit extra variation in θ_2 may reflect, to a degree, true differences in stage-specific values. However, the evidence is that these differences are minor since the amount of variation explained by stage-specific θ_2's, from Table 6.1, is only 5% for model (6.1) and 14% for (6.2a).

Any benefit of incorporating stage-specific thresholds in the CR models follows from the improvement it gains in the accuracy of the predictions of $\hat{q}$. This clearly depends on the ability of the method of Manel and Debouzie (1997) to successfully estimate stage-specific values of θ_2 from stage-frequency data. It is argued here that

this estimation is unlikely to be successful and this is supported by the results given by Manel and Debouzie (1997).

Firstly, it is probably unreasonable to expect simultaneously estimation of both the $\beta's$ and θ_2 from stage-frequency data to be successful for similar reasons to the failure of simultaneous estimation of model parameters for both stage-specific mortality and stage duration times from such data as mentioned earlier. In Manel and Debouzie (1997) this appears to be the case since they report the stage-specific MPL estimates of θ_2 as $0\,^{o}\mathrm{C}$ for all larval instars. Although these identical estimates could reflect a common θ_2 which is $0\,^{o}\mathrm{C}$, it is surprising if realistic estimates of θ_2 can be obtained using MPL that there is no difference in the reported point estimates. It is also surprising that these estimates are as low as $0\,^{o}\mathrm{C}$ when Manel and Debouzie (1997) report the estimate of θ_2 as $6.5\,^{o}\mathrm{C}$ for the eggs. Their model is likely to suffer from a high degree of multi-collinearity. This can be seen in the case of $t_i = DD\lceil\theta_2\rceil$ in the linear predictor $\eta_{ij} = \beta_{0j} + \beta_{1j} t_i$ of model (6.6) if the temperature does not fall, or rarely falls, below θ_2 over the sampling period. In this case it can be seen that $\eta_{ij} = \beta_{0j} + \beta_{1j}\overline{T}_i d_i + \beta^*_{1j} d_i$ where $\beta^*_{1i} = -\theta_2\beta_{1j}$, and $\overline{T}_i$ is the average daily temperature up to time d_i where d_i is in Julian day units. If $\overline{T}_i$ does not vary much, then $\overline{T}_i d_i$ will be highly collinear with d_i resulting in poor simultaneous estimation of β^*_{1i} and β_{1j} and thus β_{1j} and θ_2.

From Fig 6.7 it can be seen that the above conditions are a reasonable approximation to the observed temperatures remembering that the range of d_i for any one of the $s-1$, CR models is a subset of that for the total sampling period. For the coincident regression model, the difference in average temperatures between the two sites should reduce the multi-collinearity and with a larger number of sites covering a wide range of average temperatures then application of the method of Manel and Debouzie (1997) might be worthwhile. Such a dataset incorporating a range of average temperatures is the field-equivalent of a set of constant temperature experiments.

Clearly, obtaining stage-specific estimates of θ_2 using development times observed under constant temperature regimes is much more likely to be successful. Even with

good stage-specific estimates of θ_2 the method of Manel and Debouzie (1997) requires a shift to a new the physiological time scale at the median development time for each stage. This suffers from the logical inconsistency mentioned earlier and is considerably more difficult to implement than the CR model with a single, common physiological time scale. Given the above problems, unless there is good evidence for large differences in stage-specific θ_2's, it is doubtful if the method of Manel and Debouzie (1997) is a worthwhile improvement to the fitted CR models so it was not pursued here.

Time of peak relative versus peak absolute occurrence

The estimates of time of peak relative and peak absolute occurrence for each of L1, L2, and L3 larvae feeding on *E. regnans* (Table 6.10) indicate that, except for the most extreme mortality rate of 80%, the absolute peak is about 20 *DD*[5] earlier. For an average daily temperature of $15^{\circ}C$ with few daily minimums below $5^{\circ}C$ (i.e. the usual case) this corresponds to approximately 2 days. Therefore, for egg mortality rates that are low enough to result in a population density above the action threshold, this difference will be considerably smaller.

Adjustment of these times for feeding on *E. nitens*, based on Baker *et al*. (1999), required multiplying these estimates by the ratio 216.7/262.7. For example, the times to peak proportions of L1 and L2 larvae using this scaling are 127.0 and 174.5 *DD*[5], respectively, corresponding to Table 6.10 values of 154.0 and 211.5 *DD*[5]. Therefore, the 'control window' between these times is approximately 48 *DD*[5] or 5 days given the average temperature conditions above.

Multi-cohort stage frequencies

A difficulty arises when a second, major oviposition event occurs before the population derived from the first has not developed to pre-pupal stage. In this case the proportions in each stage will be a mixture of individuals resulting from each oviposition event. To some degree there will always be different cohorts combining to produce temporal variation in proportions in each stage because all eggs are not oviposited at exactly the same time. Manly (1990, p.42) describes the data in this case as multi-cohort stage-frequency data where recruitment of new individuals to the

population (i.e. eggs here) occurs over a substantial part of the total sampling period. The greater the length of time over which recruitment of eggs occurs, the greater the range in time over which subsequent stages occur resulting in the flattening of the probability curves, such as those in Figs. 6.8 to 6.10, making the peaks less discernible.

If one major oviposition event occurs followed by minor events (i.e. low levels of egg recruitment) then fitting and applying the models described here will give reasonable results in terms of predicting peak occurrence of intermediate stages. The CR model allows recruitment of eggs to the population after the nominated starting date for the population as long as this recruitment does not exceed recruitment to the L1 larval stage after L1 recruitment begins. This is because the CR model for the proportion of eggs in the population simply describes a sigmoidal decay in the observed proportion of eggs (Figs. 6.8 to 6.10). However, if after recruitment to the L1 stage begins, there is still substantial egg recruitment then the CR models (and the other macroscopic or microscopic models) cannot predict any subsequent increase in the observed proportion of eggs and corresponding decrease in the proportion of L1 larvae. Therefore, if a number of major oviposition events occur over a period of a few weeks resulting in multiple 'population-level' cohorts then fitting or applying phenology models of the type described here will not be successful. If these 'population-level' cohorts are spatially separated then the CR models could possibly be applied to each population separately.

Despite this, the problems that 'population-level' cohorts introduce into scheduling the application of insecticidal control are minimised by the nature of oviposition at the population level. This is because, in general, oviposition at this level is similar to that observed at the two sites sampled in this study in the 1991/92 summer. This corresponds to the general observation of *C. bimaculata* population dynamics that co-occurrence of population-level cohorts at the same location is uncommon (D. Bashford FT, *pers. comm.*) since mass oviposition will not occur when there are few suitable oviposition sites due to feeding by an existing population of larvae. Therefore, if the early Tiger Rd population had survived in large numbers then it is unlikely that the second, larger, oviposition event would have occurred.

The effect of thermoregulation on predictions of development rate in the field

Insects are poikilothermic so their body temperature is closely coupled to the ambient temperature of their micro-environment. However, they can control their body temperature to some extent using behavioural adaptions such as basking to increase body temperature relative to air temperature by absorbing solar radiation (May, 1979; Kemp, 1986; Casey, 1988; Carruthers *et al*., 1992; Maddox, 1996). For the fourth instar larvae of the chrysomelid beetle *Paropsisterna tigrina* feeding on tea tree (*Melaleuca alternifolia*) Maddox (1996) found that body temperature, T_b, could be up to $7^{o}\mathrm{C}$ above ambient air temperature, T_a, for larvae exposed to the sun. Larvae kept in shade had body temperatures very close to ambient air temperatures.

In calibrating or applying models of field phenology which employ thermal sums based on air temperatures, errors in predictions can result from thermoregulation effects such as basking (Higley *et al*., 1986). Modelling thermoregulation is very complex since it involves a combination of insect behaviour and the physiology of heat exchange between the insect and the air (May, 1979; Casey, 1988). In addition, the availability of solar radiation needs to be measured during the collection of stage-frequency or development time data and, in model application, predicted in terms of daily sunshine hours (Bryant *et al*., 1998).

It was beyond the resources of this study to directly study thermoregulation in *C. bimaculata* and its influence on field phenology. However, Maddox (1996) found that that the increase in T_b above T_a can be approximated by a linear relationship with T_a. Bryant *et al*. (1998) also report that such a linear relationship is common though Kemp (1986) reports this relationship as nonlinear for rangeland grasshoppers. It is reasonable to assume that at sufficiently low values of T_a the increase in T_b due to basking will be offset by losses due to the extra exposure of the adaxial leaf surface. Following this line of reasoning, if it is assumed that this 'break-even' temperature occurs at the lower threshold for the linear model (6.1), so that

$$\begin{aligned} T_b &= T_a + \kappa(T_a - \theta_2) \quad ; \kappa > 0 \; ; T_a > \theta_2 \\ &= T_a \qquad\qquad\qquad\qquad\quad ; T_a \le \theta_2 \end{aligned} \tag{6.18}$$

where κ is a proportionality constant, then the CR phenology model calibrated from field data implicitly incorporates average thermoregulation effects in terms of both average availability of solar radiation and average daily periods of basking for the sampling period. This is because only development rate parameters [i.e β_{1i} in model (6.6)] are in effect modified by basking and these were calibrated using field data. This can be seen by re-arranging (6.18) to give $T_b - \theta_2 = (\kappa + 1)(T_a - \theta_2)$ so that *DD* is increased proportionally by the constant $(\kappa + 1)$ which can be subsumed into the β_{1i} in model (6.6).

Modelling phenology using continuation ratios versus other modelling approaches

As mentioned earlier, Munholland and Dennis (1992) give estimates of life-history parameters obtained from their *microscopic* model. This model incorporated inverse Gaussian-distributed stage-duration times and a constant mortality rate function. These life-history parameters, such as expected recruitment rates for each stage per area sampled, stage-specific mortality, and mean sojourn time for each stage, cannot be estimated from macroscopic models, such as CR models. However, the usefulness of some of these quantities is questionable when a model assuming constant mortality rate is applied to populations in which the mortality rate varies substantially between stages, as is the case here. For example the stage-specific mortality rate that Munholland and Dennis (1992) estimate from their model is defined as the probability, m_j, that an individual in stage *j* will die before entering stage *j*+1. So in this sense it is stage-specific but it is not based on a stage-specific mortality rate function within their overall model [i.e. their equation (3)]. Therefore, the estimates of m_j could be misleading when estimated purely from stage-frequency data. A similar problem was noted by Manly (1990, p.83) when the advantage of incorporating stage-specific mortality rates in the model of Bellows and Bailey (1981) was not realised because estimation failed for stage-frequency data on the grasshopper *Chorthippus parallelus*. Manly found it necessary to constrain mortality to a constant rate across stages for estimation to be successful.

In contrast, predictions of the quantities of most interest to forest managers, that is the stage proportions over time and time of peak relative occurrence, can be obtained from both the macroscopic and microscopic models. For stage proportions (and by

inference times of peak relative occurrence) Munholland and Dennis (1992) concede that the estimates from their model are very similar to those obtained from the macroscopic models of Stedinger *et al*. (1985), Dennis *et al*. (1986), and Kemp *et al*. (1989). Note that Kemp *et al*. (1989) combined a constant mortality rate function with the stage proportion model of Dennis *et al*. (1986) as was done here by combining models (6.7) and (6.13). Since the CR models were shown by Candy (1991) to be substantially better than these other macroscopic models, in terms of goodness of fit, the conclusion is that the CR models will give a superior fit to observed stage proportions that those obtained from the model of Munholland and Dennis (1992). This is because stage-specific development rates cannot be incorporated in their model. However, this is not a limitation for the CR model since stage-specific rates correspond to the stage-specific β_{1j}'s in model (6.6). This results in the improved predictive ability of this class of model.

In addition, the microscopic models are restricted to a single time-dependent predictor variable while this is not the case for the macroscopic models (Candy, 1991). Further, the CR models were combined here with a more realistic mortality rate model, (6.14), than that estimable in microscopic models, albeit using the ancillary stage-specific mortality data of de Little *et al*. (1990). This allowed prediction of times of peak absolute numbers in each stage (i.e. peak occurrence). Finally, the CR models also have the practical advantages over these other models that (a) initial parameter values are not required before estimation can proceed (Candy, 1991), and (b) inverse estimation to initialise the model is straightforward, as shown later in Section 7.9.

Another common approach to prediction of the distribution of development time in the field is that based on simulation using models of both the mean and distribution of development times or rates observed in constant temperature experiments (see Wagner *et al*. 1984 for a review). This approach was generalised to predict development times for each of a number of life-stages by Logan (1988) using a 'cohort' method with cohorts corresponding to stage (see also Bentz *et al*., 1991). The simulation approach assumes that the distribution of times or rates, after normalisation (i.e. adjustment for the dependence of the mean on temperature), is independent of temperature (i.e. same shape distributions). A distribution model is

typically fitted to the normalised development times or rates obtained in constant temperature experiments and rate-summation (i.e. thermal summation) under ambient field temperatures (Stinner *et al*., 1975) used to predict the distribution of times to emergence (Cunningham *et al*., 1981) or entry to a stage (Logan, 1988). Distributions that have been used include the normal and quadratic for rates, (Sharpe *et al*., 1977) and the exponential (Cunningham *et al*., 1981), Weibull (Wagner *et al*., 1984), and logistic (Regnière, 1984) for times. Note that predictions can be compared to field observations, such as stage-frequency data, but such field data were not used in the above studies for model calibration.

An advantage of this simulation approach is that stage-specific development rate models estimated from constant temperature experiments can be incorporated in the simulation algorithm (Bentz *et al*., 1991). The disadvantage is that all model parameters, including rate and distribution models, are estimated from constant temperature experiments. For the macroscopic and microscopic models described above, the only parameter not estimated from field data is the temperature response parameter(s) (e.g. θ_2 in the linear day-degree model). Therefore in this last case the average effects of factors affecting the mean and other distribution parameters for development rate which operate in the field (e.g. thermoregulation) are incorporated in model predictions. This is not the case for the simulation approach. However, this could be overcome by fitting rate models using the field emergence data and the maximum likelihood estimation described in Section 6.3 or DEVAR's least squares estimation. Even in this case, natural variability occurring in stage-frequency data due to the distribution of starting times for (egg) cohorts, is not incorporated in predictions.

Manly (1990, p.97) dismissed the macroscopic class of models as of questionable value on the basis that they only provide an empirical 'smoothing' of the data. However, given the ability of the CR models, possibly in combination with mortality rate models, to better predict the quantities of interest to forest managers than the alternative models discussed above, this claim is unjustified.

6.6 CONCLUSION AND SUMMARY

Continuation ratio (CR) models are presented which allow prediction of the proportion of the population of Tasmanian leaf beetles, *Chrysophtharta bimaculata*, in each of egg, and L1 to L4 larval stages at a given time from a known or estimated date of initiation of the population. Parameter estimates were obtained from stage-frequency data collected from two sites in the Florentine Valley, in southwestern Tasmania in *E. regnans* regeneration. Alternative time scales used were based on (a) Julian date and (b) integrated development rate, including day-degrees, determined from logged ambient air temperatures and development rate models.

The best phenology model was obtained by regressing the logarithm of the continuation ratios on a linear function of time measured in day-degrees calculated with a $5^{o}C$ lower threshold. This lower threshold was estimated from published development times from constant temperature experiments. The hypothesis of a common threshold across egg to L4 stages was accepted which considerably simplified prediction of phenology using the CR model.

The times of peak relative occurrence for each of L1 to L3 stages were predicted from the CR model. To obtain time of peak (absolute) occurrence the CR model was combined with a stage-specific mortality model. Given moderate egg mortality rates which result in populations worth controlling, the difference between the time of peak absolute and peak relative occurrence is likely to be unimportant in practice. Adjustments were made for the shorter development time for feeding on *E. nitens* foliage based on the laboratory trial of Baker *et al*. (1999). The time to peak occurrence of L2 larvae was estimated at approximately 175 *DD*[5].

Development of new modelling/statistical methodology is described to (a) estimate development rate models using interval-censored development time data, and (b) predict time of peak occurrence of intermediate stages using continuation ratio models. The use of predictions from these models to assist in scheduling pre-control population monitoring and insecticidal control operations (Fig. 1.4) is described in Chapter 7.

CHAPTER 7

A DECISION SUPPORT SYSTEM FOR THE LEAF BEETLE IPM PROGRAM

7.1 INTRODUCTION

The primary motivation behind the research trials, sampling studies, statistical analyses and modelling described in the preceding chapters was to provide predictive models for the Decision Support System (DSS) for the Leaf Beetle IPM program outlined earlier in Fig. 1.4.

To place this DSS in the larger context of forest pest management, Fig. 7.1 outlines the processes involved for the two general types or levels of decision-making required by forest managers. These are strategic decisions that are applied to the overall forest resource and operational decisions that are applied at the individual compartment level.

At the strategic level it may be decided that the use of an insecticide to control the pest is unacceptable due to either economic or environmental costs, or due to the lack of an effective insecticide. In that case, assuming that any viable alternative methods of control such as silvicultural treatments (e.g. improvement of general forest hygiene and health) and biological control programs have been implemented, the main issue facing the forest manager is how to predict the effect of long-term average pest population densities on sustainable harvest volumes.

If insecticidal control is acceptable, given firstly government regulation and secondly forest management policy, a strategic-level decision is whether or not operational (or routine) population monitoring should be carried out. Without population monitoring the control program, if attempted, must rely on set calendar dates for insecticide application or application at regular intervals over the period of pest activity to ensure crop protection at all times (prophylactic control).

When operational population monitoring is carried out this information can used to make a decision, for each sampled compartment, on the need to control the pest

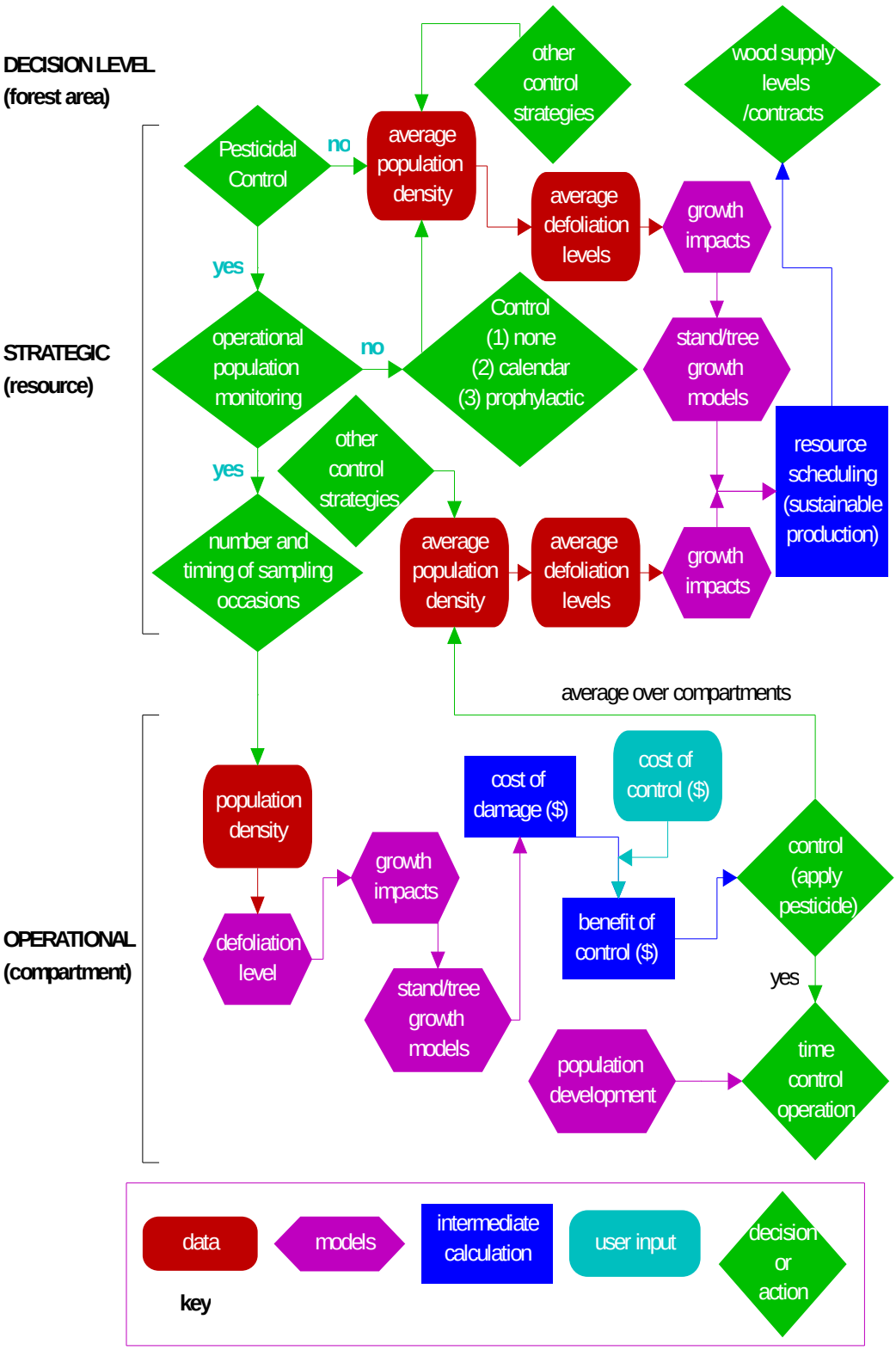

Figure 7.1 Strategic and operational decision making for forest pest management.

using insecticide. This decision can be made by comparing the sample estimate of the population density to a generic ‘action threshold’ or by carrying out a cost-benefit analysis. A cost-benefit analysis has the advantage of using inputs that are specific to the particular compartment rather than average or typical values used to determine action thresholds.

The decision support systems for forest pest management are most often of the strategic type and typically provide hazard or risk ratings for damage of each individual stand over a large area of forest (Hedden *et al*., 1981; Shore and MacLean, 1996). For insect pest control programs which operate by attempting, over a number of years, to suppress or eradicate the pest population from a particular location these hazard rating systems allow prioritisation of stands for treatment using applications of insecticide and/or silvicultural treatments. However, DSSs which use detailed economic cost-benefit analyses or generic action thresholds for decisions on treatment by insecticide for a given individual forest compartment, monitored population, and season are much less common in forestry (Fox *et al*., 1997) than is the case in agriculture. (Mumford and Norton, 1984; Deen *et al*., 1993). This is partly due to the much longer production cycle in forestry. Fox *et al*. (1997) described a framework for decision support for pest control for individual forest management units (=compartments here) using economic thresholds (=action thresholds here, see below). The objective in this study was the development of such an operational DSS for the *E. nitens*/*C. bimaculata* crop/pest system along the lines of that described by Fox *et al*. (1997).

Figure 7.2 gives a flowchart outlining the DSS that is based primarily on a cost-benefit analysis. This flowchart shows how the predictive models described in this study are incorporated as components of the DSS. In what follows the DSS components in Fig. 7.2 are described and the implementation of the cost-benefit analysis using *The Farm Forestry Toolbox* (TOOLBOX) DSS software program (Private Forestry Tasmania, 1999) is given.

The same process as that described by Figure 7.2 was also used to derive a number of generic action thresholds for a range of site qualities, early versus late season populations, and realistic fixed values for other inputs. These generic action

Figure 7.2 Flow chart of the operational Decision Support System for the Leaf Beetle IPM program showing model components. Steps (1) to (3) refer to the method of calculating yield loss due to browsing.

thresholds were then combined with a probability density function, describing the long-term distribution of population densities across compartments and seasons, in order to estimate the economic value of each of the three sampling schemes described in Chapter 2.

Figure 7.2 also outlines a decision support process or sub-system for providing the forest manager with predictions of population development through key life stages that can be used to assist in scheduling both pre-control population monitoring (Fig. 1.4) and insecticide application. The application of the predictive models given in Chapter 6 in this process is described. Finally, the conclusions from this study and recommendations for future research are given.

Before describing the details of the DSS, the economic theory for determining action thresholds is given followed by a description of the decision theory for calculating the economic value of population monitoring and the associated control decision.

7.2 ECONOMIC AND ACTION THRESHOLDS

The model of the profit, *B*, obtained from the control of a pest of primary production can be expressed using a simple Net Present Value (NPV) calculation as

$$B = pY(\mu_C)\left(\frac{1}{1+R/100}\right)^{T_H-T_C} - C_P D - C_A \qquad (7.1)$$

where

p is the unit price of the output or yield (e.g. timber volume)

$Y(\mu_C)$ is the expected yield in the single harvest year T_H

μ_C is the population density after treatment in the year of the pest infestation given by the function $\mu_C = f(\mu, D)$

μ is the pre-treatment population density

D is the dosage of insecticide applied

T_H is the harvest year

T_C is the year of infestation and control decision

C_P is the unit cost of the insecticide

C_A is the application cost of the insecticide

R is the cash discount rate (%).

The only costs considered in (7.1) are those incurred by insecticide application. The economic threshold (ET) as defined by economists (Moffit, 1986) is the residual population size, μ_C^*, resulting from the application of the particular insecticide dosage, $D = D^*$, that maximises the profit, *B*. That solution can be expressed using (7.1) as

$$Maximum\ B = pY\left[f\left(\mu, D^*\right)\right]\left(\frac{1}{1+R/100}\right)^{T_H - T_C} - C_P D^* - C_A$$

from which $\mu_C^* = f\left(\mu, D^*\right)$ is obtained.

This is also called the marginal optimisation problem (Mumford and Norton, 1986) since it balances the cost of the extra damage caused by a marginal increase in the population density with the extra cost of eliminating that increase. Note also that model (7.1) is a generalisation of that given by Moffitt (1986) who assumed that the infestation year and harvest years are the same (i.e. annual harvests).

In contrast the 'action threshold' (AT) is the smallest pre-treatment population size, μ_0, for which a standard dosage of insecticide, D_S, gives a profit greater than the zero dose (i.e. no application of insecticide). The action threshold therefore solves the discrete choice decision problem for which *D* can take one of two values, zero (i.e. no control) or D_S. Given that only the standard dose of insecticide is considered, the cost of control can be expressed as a single fixed cost, $C_C = C_P D_S + C_A$. The action threshold is therefore the value of μ, μ_0, which satisfies the relation

$$p[Y(\mu_C) - Y(\mu)]\left(\frac{1}{1+R/100}\right)^{T_H - T_C} = C_C \quad ; \quad T_H \geq T_C \qquad (7.2).$$

If $\mu_C = 0$ then the term $[Y(\mu_C) - Y(\mu)]$ is simply the expected yield in the absence of the pest minus the yield when the population is uncontrolled with mean density, μ.

The term 'action threshold' is preferred here for μ_0 since the term 'economic threshold' is ambiguous as entomologists have used it to refer to μ_0 while economists to refer to μ_C^* (Mumford and Norton, 1984; Moffitt, 1986). Fox *et al*. (1997) use the terminology : 'fixed treatment threshold' for μ_0 and 'optimal treatment threshold' for μ_C^* where, in this last case, they generalise insecticide dosage, *D*, in (7.1) to 'effort' expended on pest control.

Economic thresholds, economic injury levels, and generic action thresholds

Even within the entomological literature there has been confusion over the calculation of ETs stemming from simplifications for specific cases which were assumed to apply more generally (Onstad, 1987). The term 'economic threshold' was first used by Stern *et al*. (1959) as an adjustment to the 'economic injury level' (EIL) to account for an increasing population density and the time it takes for a control operation to be carried out. The EIL was defined by Stern *et al*. (1959) as the lowest population density that will cause economic damage where economic damage is the amount of injury which will justify the cost of artificial control measures. Given a sample estimate of population density is taken on a given date, then if the population is expected to increase after this date the ET should be less than the EIL. However, this assumes that (a) the population density is increasing, and (b) that the ability of an individual insect to cause damage does not change with time. Onstad (1987) generalised the ET by defining it as "a current pest density that represents a future population the control of which will prevent economic loss equal to the cost of implementing the control tactic". Onstad's approach allows for a range of sampling and control times, and the interaction of these with pest population dynamics and corresponding injury levels.

The particular case Onstad (1987) considers that is relevant to the Leaf Beetle IPM is the case where sampling and implementation of control occur in the non-injurious

life stage of the population therefore preventing damage above the EIL caused by subsequent injurious stages. In the Leaf Beetle IPM the non-injurious stages are the egg, L1 and (to a lesser degree) L2 stages while L3 and L4 larval stages are considered the 'injurious-stages' (Elliott *et al*., 1992). This is based on the results of Greaves (1966) who found that L3 and L4 larvae together accounted for 90% of the leaf area of *E.regnans* foliage consumed by an individual insect over the total larval development period. More recently Baker *et al*. (1999) found the corresponding percentage of green weight consumed to be 87% for feeding on *E. nitens* and 86% for *E. regnans*.

A simplification of the relationship between the ET and EIL can be obtained if it is assumed that population density does not change from the time of sampling of the non-injurious stage until feeding by the L4 population ceases. In this case the ET and EIL must take the same value since they are defined as an overall density and not a stage-specific density. Therefore, the ET and EIL can be replaced by a single action threshold (AT), without increasing the economic loss, as long as control is carried out before the population enters the L3 and L4 stages. Given the sample population density to be compared with the AT is obtained after predation has effectively ceased (i.e. at the end of the L1 stage=date#1 or date#2 in Fig. 7.2) then it can be realistically assumed for the Leaf Beetle IPM that negligible damage has occurred prior to, and negligible mortality will occur after, this sampling time. Therefore, decision making based on the complex dynamic ETs of Onstad (1987) can be replaced by that based on a single ET (=AT) combined with a prediction of the *control window* between the sampling date (date#1 or date#2 Fig. 7.2) and the time of the peak in L2 population density (date#3).

However, it should be noted that a single AT, or one of a limited number of generic ATs, is a relatively crude approximation to the true AT since many factors influence the cost of control to cost of damage relationship and therefore the EIL for a specific compartment (or farm) (Stern *et al*., 1959). A cost-benefit analysis for each specific situation is the best approach in terms of maximising profit. Nevertheless, generic ATs are useful in some situations as described in Section 7.3.

Models (7.1) and (7.2) assume a fixed harvest year and calculate the benefit of pest control as a function of the additional volume produced at harvest. This is the method demonstrated by Fox *et al*. (1997) in their framework for the use of 'economic' (=action) thresholds in forest pest management. They also describe an alternative approach that measures the benefit from pest control as a function of the reduction in the rotation length to obtain a given, fixed, harvest volume. In addition, model (7.1) assumes a single product of unit price is produced at harvest but this can be generalised to *s* products simply by replacing $pY(\mu_C)$ by $\sum_{i=1}^{s} p_i Y_i(\mu_C)$. However, to limit the number of generic action thresholds used in overall comparisons of the economic value of population monitoring, model (7.1) was used assuming a fixed rotation age of 15 years and a single product at harvest of pulpwood.

Determination of action thresholds given the standard operational control method of aerial spraying of the broad-spectrum insecticide, cypermethrin (Dominex® 100, Agchem, South Australia) (D. Bashford, FT *pers. comm*.) is one of the key objectives of this study. This control method can be assumed to be completely effective since it has been shown to cause 100% mortality of larvae and adults within 24 h (Elliott *et al*. 1992; Greener and Candy, 1994). Therefore it was assumed that the post-treatment pest density is given by $\mu_C = f(\mu, D_S) = 0$. Also, for the following, the LHS of (7.2) will be denoted the 'cost of damage' function $C_D(\mu)$ where this cost has been discounted to the year of infestation. Expressed in words, the cost of damage as a function of the mean population density is the expected loss in revenue in the year when saleable products are produced (i.e. at harvest) due to the impact of larval feeding in the season of the infestation of the pest.

In forestry, the time lag between the year (season) of infestation and year of harvest can be substantial. Therefore the yield loss, $[Y(\mu_C) - Y(\mu)]$, is based on predictive models rather than direct measurement of the population density/yield loss relationship as is possible for crops which are harvested annually. A number of growth impact models for insect pests of North American conifers such as the Douglas-fir tussock moth (*Orgyia pseudotsugata* McD.) (Colbert and Campbell, 1978), the western spruce budworm (*Choristoneura occidentalis* Freeman) (Sheehan *et al*. 1989; Crookston, 1991) and the Douglas-fir beetle (*Dendroctonus*

pseudotsugae Hopk.) (Marsden *et al*., 1993) use the stand growth model called the 'Stand Prognosis Model' (Stage, 1973; Wykoff *et al*., 1982) to calculate yield loss. The method of calculating yield loss for *E. nitens* /*C. bimaculata* crop/pest system uses the growth models described in Candy (1997b) as outlined in Chapter 3.

7.3 ECONOMIC VALUE OF POPULATION MONITORING/CONTROL DECISIONS

Binns and Nyrop (1992) outline a method of calculating the value of the population monitoring/control decision component of an IPM system based on the expected economic loss for a given sampling scheme and its associated decision rule and action threshold. This approach, described in general as decision theory, calculates the expected loss using: (a) a likelihood function for possible values of the sample estimate given the unknown true density for any given compartment, (b) the cost incurred for each possible decision outcome given the true density, and (c) prior knowledge of pest population densities expressed as a probability density function (Nyrop *et al*., 1986).

The economic loss when population monitoring is carried out and used for making control decisions, for a given true mean population μ and action threshold μ_0, is given by

$$L(\mu,\mu_0)=Pr(\hat{\mu} \geq \mu_0 \mid \mu)C_C + [1 - Pr(\hat{\mu} \geq \mu_0 \mid \mu)]C_D(\mu) + C_S(n,\mu) \qquad (7.3)$$

where $\hat{\mu}$ is the sample estimate of the population density for a given compartment, $\Pr(\hat{\mu} \geq \mu_0 | \mu)$ is the probability of a positive control decision (i.e. carry out the standard application of insecticide) that was used to define the operating characteristic (OC) function given by (2.14) for OLC sampling (Section 2.2.4), and $C_S(n,\mu)$ is the cost of sampling function where *n* represents sampling intensity. For binomial sampling the OC function is that derived from (2.24) and $\Pr(\hat{\mu} \geq \mu_0 | \mu)$ is replaced by $\Pr(m \geq n^* q_0 | \mu)$ [where *m* is the number of occupied trees in the sample, see equation (2.21)] in (7.3). Therefore, the cost of sampling depends on the sampling method used and the number of sample units taken and may also depend on

μ as in the case of the double sampling scheme described in Section 2.4. The sampling method and estimate of $\hat{\mu}$ in (7.3) can be $\tilde{\mu}$ for an OLC sample (Section 2.2), $\hat{\mu}'_{BA}$ for a binomial sample (Section 2.3), or $\breve{\mu}^*$ for a double sample (Section 2.4).

Note that $Pr(\hat{\mu} \geq \mu_0 | \mu) = \int_{\mu_0}^{\infty} f_{\hat{\mu}}(u|\mu) du$ where $f_{\hat{\mu}}(u \mid \mu)$ is the likelihood function (i.e. the probability of observing $\hat{\mu} = u$ given μ) so that (7.3) incorporates decision theory components (a) and (b).

The economic loss function in the absence of population monitoring, assuming that without information on the population density for the particular compartment no control is carried out (i.e. excluding the option of calendar or prophylactic insecticide application), can be obtained from (7.3) by setting the threshold to an extreme value thus making sampling of no economic value (i.e. equivalent to setting *n* to zero) so that

$$L(\mu, \infty) = C_D(\mu) + C_S(0, \mu) = C_D(\mu).$$

Given the cost functions in (7.3) are known, as described later, the expected loss over the long term can be calculated, using the assumed long-term probability density function (PDF) for μ, $f_{\mu}(.)$, (i.e. over compartments and seasons), by

$$EL(\mu_0) = \int_u L(u, \mu_0) f_{\mu}(u) du \qquad (7.4).$$

The long-term average (i.e. expected) profit or economic value of the population monitoring/control decision component of the IPM system is therefore

$$EB(\mu_0) = \int_u C_D(u) f_{\mu}(u) du - EL(\mu_0) \qquad (7.5).$$

The economic value of sampling is implicitly expressed in (7.5) via the expected loss function (7.4) and its dependence on the sampling method and sample size where

these determine the cost of sampling and OC functions in (7.3). The overall economic value or profit of a given sampling scheme can therefore be obtained as the expected profit (7.5) using the scheme's OC function/decision rule and cost function. Thus the final component (c) of the decision theory approach, given by $f_{\mu}(.)$, is incorporated in (7.4) and (7.5).

Since the sample size used in a scheme affects both its cost and reliability the expected economic value of the sampling scheme can be optimised as a function of its sample size. In addition, different sampling schemes can be directly compared, assuming inputs other than cost of sampling and OC function are held constant, using their optimised value of $EB(\mu_0)$.

The average cost of control for a sampling scheme given an action threshold and the scheme's decision rule and corresponding OC function is given by

$$EC_C(\mu_0) = C_C \int_u \Pr(\hat{\mu} \geq \mu_0 \mid u) f_{\mu}(u) du \qquad (7.6)$$

for OLC sampling and similarly for binomial sampling using its particular OC function. Similarly the average loss of yield is given by

$$ELY(\mu_0) = \int_u [1 - \Pr(\hat{\mu} \geq \mu_0 \mid u)][Y(0) - Y(u)]\, f_{\mu}(u) du \qquad (7.7).$$

7.4 PREDICTING LOSS OF HARVEST YIELD FROM LARVAL BROWSING IN A SINGLE SEASON

Given an estimate of population density obtained from population monitoring for a given season, for stands ranging in age from 2 to 6 years, the process of calculating the yield loss are described in the three steps given below. Figure 7.2 refers to these steps as part of the IPM decision support system. Note that the ages are restricted to be between 2 and 6 (inclusive) since below age 2 adult foliage is absent or an insignificant component of the crown while above age 6 the height of crowns and degree of crown closure generally precludes both OLC and binomial sampling (Chapter 2). These steps are :

1. The ‘occupied leaf count per shoot’ (OLPS) is converted to the number of eggs per monitored shoot. Based on a regression of number of egg batches per shoot, *y*, as a function of OLPS, *x*, given by $y = -0.0205 + 1.1848x$ (R^2=0.964) for a sample of shoots from 158 branches across 6 trees (N.Beveridge, FT *unpublished data*) and estimated average number of eggs per egg batch from a sample of 360 shoots from field monitoring of 20.5 (s.e. 0.5) (N.Beveridge, FT *unpublished data*), the number of eggs per shoot, N_{eggs} is calculated as 20.5*y*.

2. The percent defoliation, *P*, at the shoot level is predicted using the regression given in Table 4.7. This prediction requires the number of eggs per shoot as the predictor variable so the value of N_{eggs} obtained in Step (1) is used, after scaling that value to account for the larger average total shoot leaf area in the calibration data set used to estimate the defoliation/population density relationship than that of monitored shoots. For an ‘early season’ (Nov-Dec-Jan) population/infestation the number of eggs given by step (1) is multiplied by 956.3/232 where the numerator is the average total shoot leaf area for the early treatment given in Table 4.3 while the denominator of 232 cm^2 (s.e. 13) is the average total leaf area of a sample of 120 monitored shoots obtained for a single compartment in early December (D. Bashford, FT *unpublished data*). For a ‘late season’ (Feb,Mar) population this factor is 563.7/232 (Table 4.3).

3. Given data on initial stand conditions at age T_C , which at a minimum involves an estimate of the mean dominant height (MDH) and stocking of the stand (stems per hectare, SPH), the stand is projected to a selected harvest year under each management option of ‘control’ and ‘no control’.

   3.1. For the ‘control’ option it is assumed that the mortality in the pest population of larvae due to the application of insecticide (combined with any natural mortality) is 100%. The projection of the stand to harvest age, T_H , and prediction of log volumes for the ‘control’ option then simply follows the usual method described in Candy (1997b) and Candy and Gerrand (1997) (Sections 3.3, 3.4, Fig. 3.20). If only minimal information on the stand is available (i.e. MDH and SPH) the stand basal area (BA) is predicted using

models (1), (8) and (4) of Candy (1997b) in that order. If a sample of tree DBH's have been measured the actual stand basal area at age T_C can be estimated from SPH and the quadratic mean DBH [QMDBH = $100\sqrt{4.\text{BA}/(\pi\text{SPH})}$]. The basal area projection model (4) of Candy (1997b) can then be used to predict the basal area at harvest. Using the single tree volume equation (Section 3.3), incorporating the predicted average tree height for DBH set equal to QMDBH obtained using models (15) and (16) of Candy (1997b), the (average) tree volume from ground to tip is obtained. The standing pulpwood volume can be calculated by multiplying stocking by the (average) tree merchantable volume which is the tree volume above minus the volume between an upper stem diameter of 10 cm (ub) and the tree tip. For multiple-product regimes which include sawlog products (Candy and Gerrand, 1997) the projected stand basal area at age T_H can be disaggregated to the individual trees corresponding to the list of DBH's measured at age T_C and log product volumes calculated using the tree taper model outlined in Section 3.3 (Fig. 3.20). The effect of silvicultural treatments such as thinning and pruning on growth and log product out-turn also need to be incorporated for multi-product regimes (Candy and Gerrand, 1997).

3.2. For the 'no control' option using the percentage defoliation, *P*, predicted in Step (2) above, the growth projection for the stand is carried out as described in Step (3.1) with a modification to incorporate the impact of browsing. This involves : (a) projecting the stand BA and MDH to age $T_C + 3$ for an early and $T_C + 4$ (see below) for a late population using the method described in Step (3.1), (b) using percent defoliation, *P*, the projected QMDBH (obtained from BA) and the MDH are reduced using model (5.5) (Section 5.5) and the parameter estimates in Tables 5.8 and 5.9 respectively, and then (c) projecting these reduced values to the harvest age, T_H . If a sample of tree DBH's have been taken, the reduction in growth can be applied to each tree individually using model (5.5). The same approach can be used for tree heights that have either been measured along with the tree's DBH or predicted from DBH using models (15) and (16) of Candy (1997b). A further refinement can be incorporated if the individual trees in the sample of DBH's

(and heights) can be related to the OLC sample trees. The percent defoliation, *P*, used in model (5.5) is then the particular value for the sample tree based on the same procedure as that used for the compartment as a whole described in steps (1) and (2).

The results in Chapter 5 on the effect of defoliation on tree DBH and height growth suggest that a period of three full growing seasons after defoliation (i.e. excluding the season in which defoliation took place) was adequate to fully express the impact on relative growth. The MDH and BA growth projection models used in Step (3.1) predict these values at the end of the growing season if integer values of age are used. Therefore an early defoliation requires model (5.5) to be applied to the projected values of MDH, and QMDBH at age $T_C + 3$ (i.e. four growing seasons including the growing season in year T_C). Using a similar argument for late populations the corresponding age is $T_C + 4$. In both cases the fraction of the growing season before the early population and the fraction after the late population are assumed sufficiently similar to the corresponding values in the calibration dataset (Section 5.2) that model (5.5) takes into account these fractional growth periods. Also, since population monitoring can be carried out only up until approximately age 6 and predictions of yield loss at harvest are only required for ages greater than 12 years in Steps (1) to (3), then the requirement of a minimum growth projection period of 4 years is easily satisfied.

7.5 THE CONTROL DECISION FOR A MONITORED COMPARTMENT

The process by which the control decision for a particular monitored compartment is carried out is outlined in the flowchart given by Fig. 7.2. This involves comparing the discounted cash flow for ‘control’ and ‘no control’ options, given the yield loss for the latter option, and choosing the option which gives the greater profit (i.e. cost-benefit analysis). The method of determining the yield loss was described above. It is convenient to calculate the benefit as the harvest revenue discounted to the year of the infestation/control decision as in (7.1) and compare this to the undiscounted cost of control. This is called the Net Present Value (NPV) method of comparing costs and revenues over time (Clutter *et al*., 1983, p.161; Fox *et al*. 1997).

For the current operational method of control, involving the application of a broad spectrum insecticide described in the introduction, complete eradication (i.e. 100% mortality) of the population of *C. bimaculata* exposed to the operational dosage can be assumed. However, the use of this insecticide (cypermethrin) has environmental costs that have not been included in model (7.1) and Fig. 7.2. An alternative biotic insecticide is Novodor FC® (Abbott, North Ryde, NSW, Australia) with the active ingredient the *Bacillus thuringiensis* subspecies *tenebrionis* toxin. Novodor FC is much less harmful to beneficial insects and other non-target invertebrates (Greener and Candy, 1994; Beveridge and Elek, 1999) but is considerably more expensive and less effective than cypermethrin (Elliott *et al.*, 1992; Elek and Beveridge, 1999). If insecticidal control is limited to the use of Novodor FC in particular situations then the cost-benefit analysis for the control decision involves applying the method described in Step (3.2) with a residual population of $\mu_C = (1 - M)\mu$, where *M* is the proportion of the population killed or rendered non-damaging (i.e. due to inhibition of feeding) (Elek and Beveridge, 1999). This becomes an extra step; Step (3.3) corresponding to a '<100% control' option. The loss of yield prevented by application of Novodor FC is then the yield obtained from Step (3.3) minus that from step (3.2).

7.6 DETERMINING GENERIC ACTION THRESHOLDS

In Section 7.5 the process of making the control decision for a *particular* monitored compartment, based on the sample estimate of population density and the procedures given in Section 7.4 and Fig. 7.2, was described. However, to calculate the average or expected benefit of the population monitoring/control decision process for the overall Leaf Beetle IPM program an action threshold, μ_0, is required as expressed in (7.3), (7.4) and (7.5). In addition, it may be convenient to specify a set of 'generic' action thresholds which can be used to make 'on-the-spot' control decisions when it is not possible to use a computer running the decision support system described by Fig. 7.2. For example, the double sampling scheme described in Section 2.4 used an action threshold of $\mu_0 = 0.5$ OLPS to determine if a follow-up sample was required before making a control decision with the 'required' reliability. Given a set of generic action thresholds, the three sampling schemes described in Chapter 2 were compared in terms of the expected profit, $EB(\mu_0)$, as described in Section 7.7.

To calculate generic action thresholds, the process of calculating the discounted cash flow described by Fig. 7.2 [and steps (1) to (3)] above was simulated for population densities, μ, ranging from 0.0 to 2.5 OLPS in 0.05 unit increments, for each of three assumed site qualities. These site qualities were defined as site indices of 20 m (low), 24 m (medium), and 28 m (high) where site index is defined as the predicted MDH at age 15 (Candy, 1997b). A single population was assumed to occur in each season. For the control option, application of cypermethrin was assumed giving *M*=1 and therefore $\mu_C = 0$.

The age at the year of infestation was assumed to be $T_C = 4$, therefore age 4 was taken to be the reference year for calculating the profit, *B*, using (7.1). For comparison with the above single, age-4 infestation, a population of the same density was assumed to also occur at age 5. The calculation of loss of yield in step (3.2) using model (5.5) was therefore modified by incorporating the 'repeat' defoliation term. An age of 4 was retained as the reference year and the cost of control was taken as the sum of the costs in years 4 and 5 after discounting this last value by one year by dividing by (1+*R*/100). The profit, *B*, obtained for control decisions in both years 4 and 5 was divided by two to give the equivalent per-annum value.

A pulpwood regime with harvest age of 15 years, stumpage value of \$30 m^{-3}, cost of control of \$35 ha^{-1} for a single application of insecticide, and discount rate, *R*, of 8% were assumed. These are realistic values based on actual costs of control with cypermethrin (D.Bashford, FT *unpublished data*) while the stumpage value falls in the middle of the range between international (Candy and Gerrand, 1997) and domestic prices (J.Dawson, FT *unpublished data*) for eucalypt pulpwood. The discount rate of 8% is used as the standard 'hurdle' rate for evaluating investment in plantations by Forestry Tasmania. The MDH at age 4 for each site index was calculated using equation (1) of Candy (1997b) and similarly for BA and QMDBH as described in Step (3.1). The stocking of the stand was assumed to be 1100 stems ha^{-1}.

7.7 RESULTS

Action thresholds

Figure 7.3 shows the loss in pulpwood volume $[Y(\mu_C) - Y(\mu)]$, for each population density. The relationship is shown for scenarios of either 'no disbudding' or 'complete disbudding' of shoots by feeding larvae. For the 'no disbudding' scenario the prediction of *P* described in Step (2) was approximated simply as $P = 100\,b.(N_{eggs} - 5)$ for $N_{eggs} > 5$ and $P = 0$ for $N_{eggs} \leq 5$ where *b* is the regression slope given in Table 4.7. For the 'complete disbudding' scenario $P = 100[a + b.(N_{eggs} - 5)]$ for $N_{eggs} > 5$ and $P = 0$ for $N_{eggs} \leq 5$ where *a* is the regression intercept given in Table 4.7. The predicted effect of disbudding on growth of tree DBH and height in Step 3.2 excluded the disbudding term, $\hat{\beta}_1 D$, in model (5.5) since this effect was already included in *P* (but see below). Approximate 95% confidence bounds for the relationship for the 'no disbudding' scenario are also shown in Fig. 7.3. These bounds were calculated using the upper and lower bounds for *b* given in Table 4.7. The volume loss reaches a maximum for a population density that gives 100% defoliation (i.e. assuming further growth losses are not incurred for populations above this level).

Figure 7.4 shows the relationship between profit *B* **(**for *B*>0) of control and population density for an early population for each of the three site qualities with approximate 95% confidence bands obtained in a similar fashion to those shown in Fig. 7.3. Figures 7.5 and 7.6 show these predicted relationships for 'late' populations.

An alternative way of including the effect of complete disbudding to that used above is to exclude the effect of disbudding on *P* but include the disbudding term $\hat{\beta}_1 D$ in predictions from model (5.5) if $N_{eggs} > 5$. Figure 7.7 shows the effect of disbudding incorporated in this way for the medium site quality.

The action threshold for each site quality and disbudding scenario is the population density at which the profit versus density relationship intercepts the zero-profit axis.

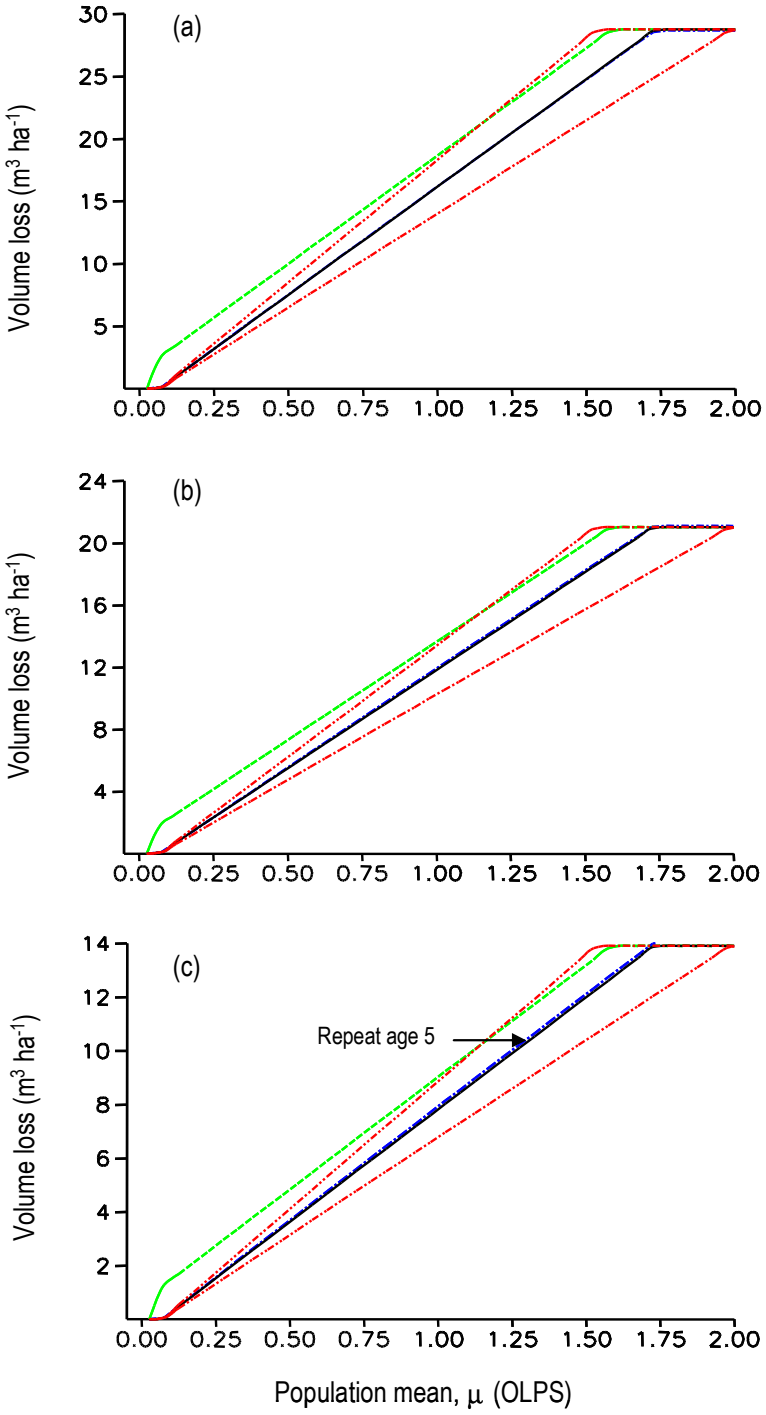

Figure 7.3 Predicted volume loss for no control of an age 4 'early' population for three site qualities (a) high (*S*=28 m) (b) medium (*S*=24 m) and (c) low (*S*=20) for each of 'no disbudding' (solid line), with repeated defoliation at age 5 (blue line), and 'complete disbudding' (green line). Approximate 95% confidence bands (red lines) shown for 'no disbudding'. Volume loss for repeated defoliation was averaged over the 2 years.

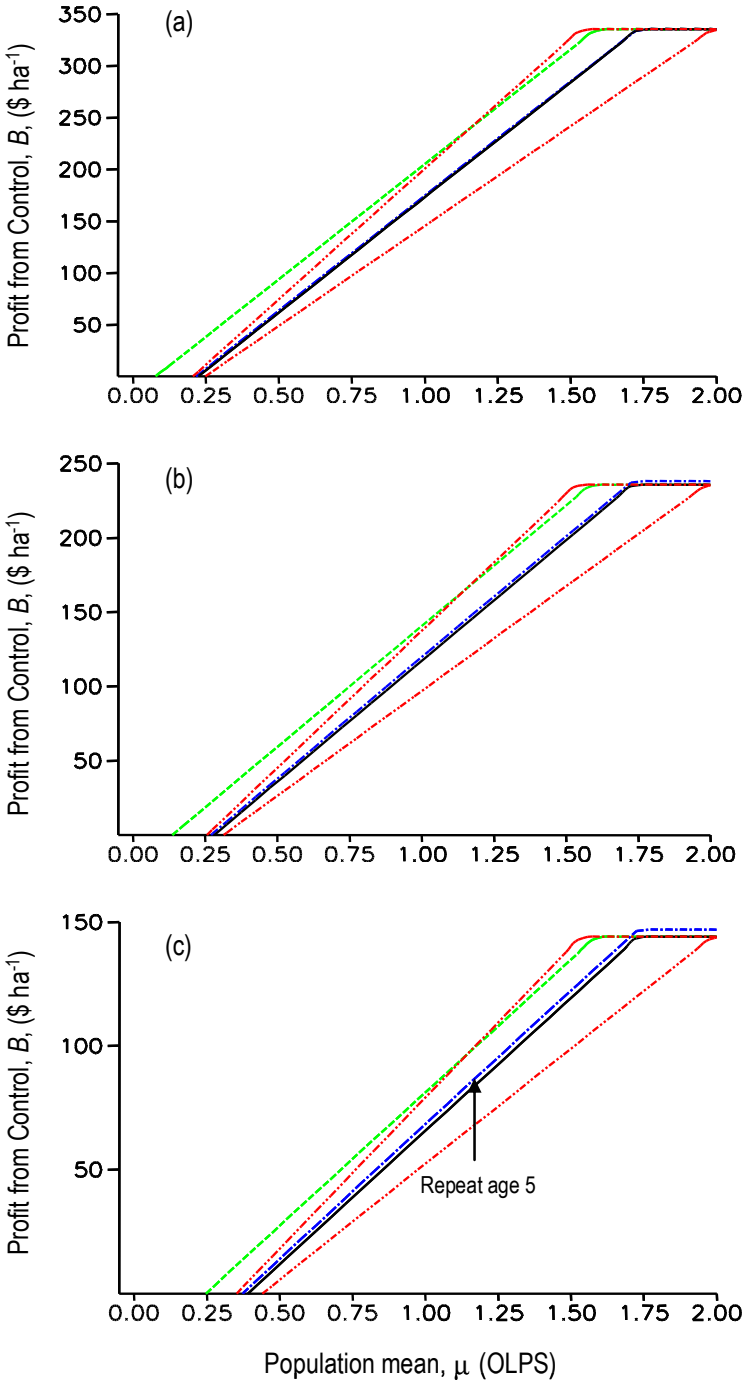

Figure 7.4 Predicted profit from control of an age 4 'early' population for three site qualities (a) high (*S*=28 m) (b) medium (*S*=24 m) and (c) low (*S*=20) for each of 'no disbudding' (solid line), with repeated defoliation at age 5 (blue line), and 'complete disbudding' (green line). Approximate 95% confidence bands (red lines) shown for 'no disbudding'. Profit of repeated control was averaged over the 2 years.

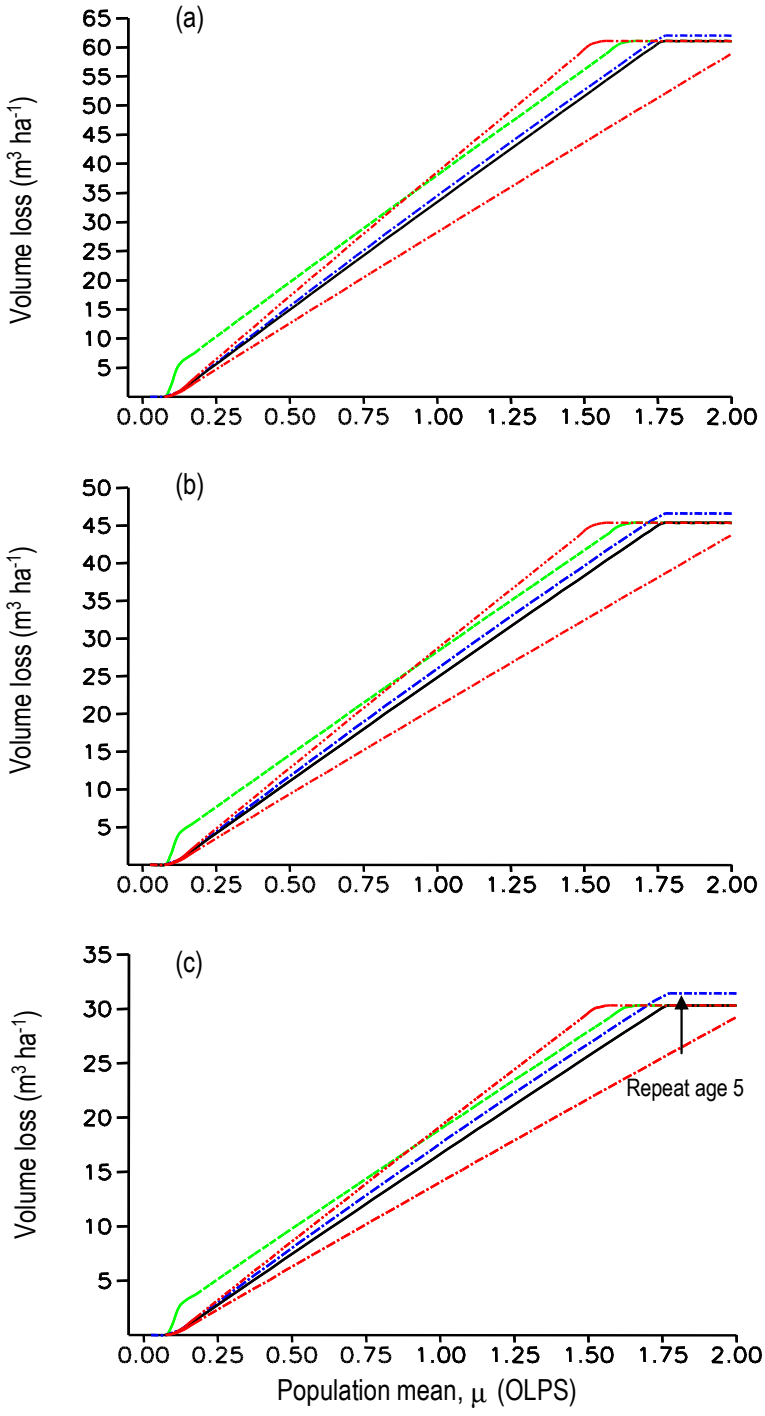

Figure 7.5 Predicted volume loss for no control of an age 4 'late' population for three site qualities (a) high (*S*=28 m) (b) medium (*S*=24 m) and (c) low (*S*=20) for each of 'no disbudding' (solid line), with repeated defoliation at age 5 (blue line), and 'complete disbudding' (green line). Approximate 95% confidence bands (red lines) shown for 'no disbudding'. Volume loss for repeated defoliation was averaged over the 2 years.

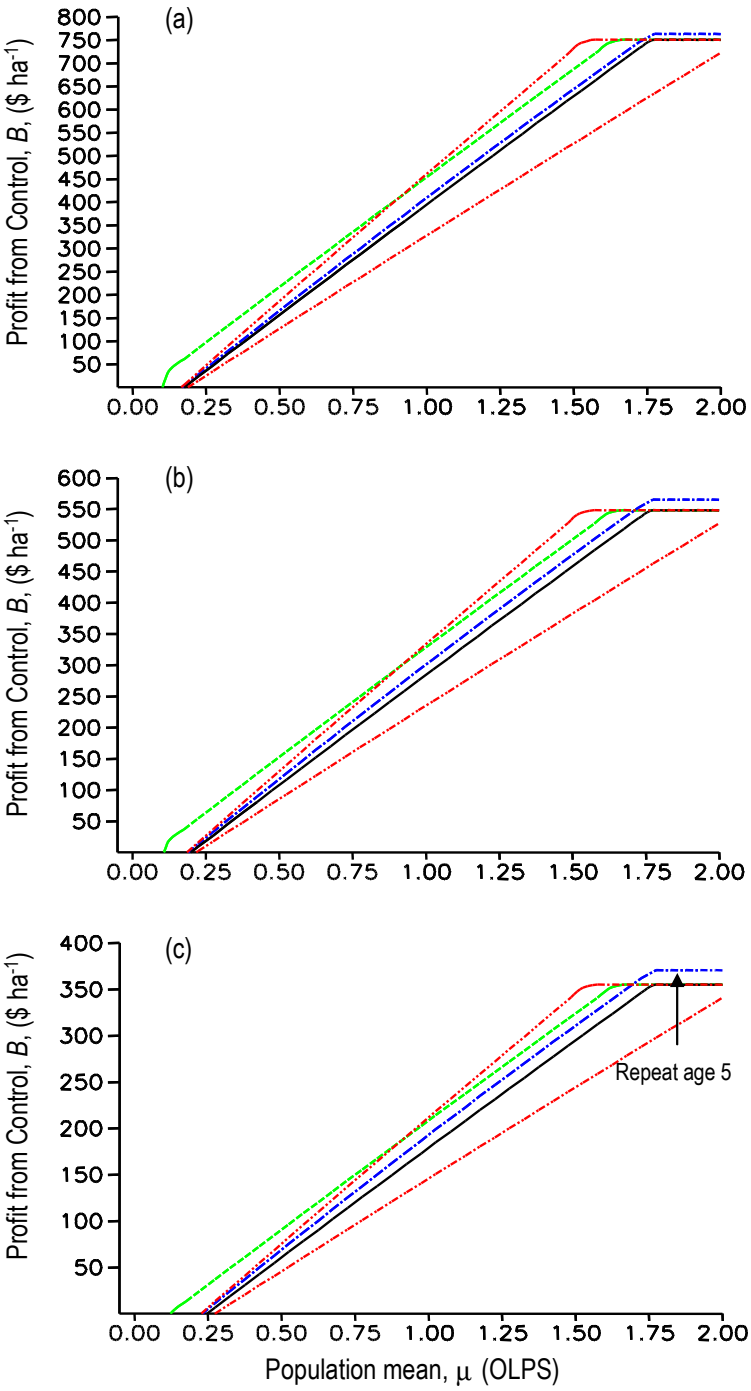

Figure 7.6 Predicted profit from control of an age 4 'late' population for three site qualities (a) high (*S*=28 m) (b) medium (*S*=24 m) and (c) low (*S*=20) for each of 'no disbudding' (solid line), with repeated defoliation at age 5 (blue line), and 'complete disbudding' (green line). Approximate 95% confidence bands (red lines) shown for 'no disbudding'. Profit of repeated control was averaged over the 2 years.

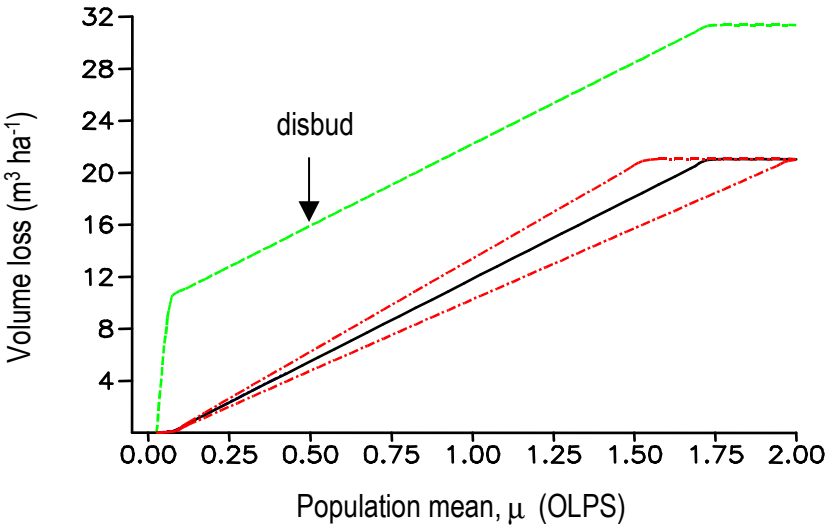

Figure 7.7 Predicted volume loss for no control of an age 4 'early' population for medium site quality (*S*=24 m) and each of 'no disbudding' (solid line), and 'complete disbudding' (green line) using the disbudding term in model (5.5). Approximate 95% confidence bands (red lines) shown for 'no disbudding'.

For simulated early populations, excluding disbudding, the action thresholds for site indices 28, 24, and 20 m were 0.2, 0.3, and 0.4 OLPS respectively (Fig. 7.4). Note that the accuracy of these values is limited to increments of 0.05 OLPS. Similarly, for late populations (Fig. 7.6) the corresponding values were 0.15, 0.2, and 0.25.

These thresholds are the theoretical optimum or 'break-even' value for the specific values of site index and other inputs. However, it may be necessary to set a minimum value for the action threshold that is larger than any of the break-even values. In Chapter 2 an action threshold of $\mu_0 = 0.5$ OLPS was used since this value is considered the minimum achievable, or 'operational', threshold due to restrictions on the number of control operations that can be carried out during periods of peak leaf beetle activity (D. Bashford, FT *pers. comm.*). Dropping the action threshold from 0.5 to 0.3 OLPS gives a large increase in the predicted number of required control operations from approximately 28% to 45% of monitored compartments (see below).

Economic value of the population monitoring/control decision component of the IPM

The economic value of each of the sampling schemes described in Chapter 2 was determined using the expected benefit, $EB(\mu_0)$, as a function of sample intensity via its affect on the OC and cost of sampling functions. To evaluate (7.3), (7.4) and (7.5) the same inputs as those described in the previous section were used. These were combined with each of the 'break-even' action thresholds corresponding to the three site indices and, in addition, the single operational threshold of 0.5 OLPS. Early populations combined with 'no disbudding' were assumed.

The long-term average probability density function, $f_\mu(.)$, for population density was assumed lognormal with mean and variance estimated from the combined sample of 56 compartment OLPS means (i.e. determined for egg batch occupancy only) described in Section 2.2 and Appendix A1. All 56 samples were taken in the 'early' (Dec-Jan) part of the season. Figure 7.8(a) shows the lognormal density function and the observed frequency histogram for the 58 mean densities. Figure 7.8(b) shows the corresponding cumulative density function and the 0.5 OLPS action threshold below which approximately 72% of the means fall. Reducing the AT to 0.3 OLPS results in 55% of means falling below this value.

Figure 7.9 shows the expected profit, $EB(\mu_0)$, or average value of the sample, for OLC sampling (Section 2.2) for tree sample sizes, n_2, ranging from 4 to 40 with the sample size of shoots per tree fixed at the optimum value of 6. The cost of sampling function is independent of population density and is given by

$$C_S(n_2) = C_F + \frac{C_L[(90+120)n_2]}{(3600)(22)} \qquad (7.8)$$

where C_F is the average fixed cost of sampling (e.g. cost of travel to the compartment, labour cost of time taken to traverse an average size compartment of 22 ha) estimated to be \$1.24 ha^{-1} (D.Bashford, FT *unpublished data*), C_L is the cost of labour taken to be \$20 h^{-1}, and the time (sec) taken to sample a tree is made up of 90 secs to obtain a sample of one or two branches and 20 secs for each of the 6

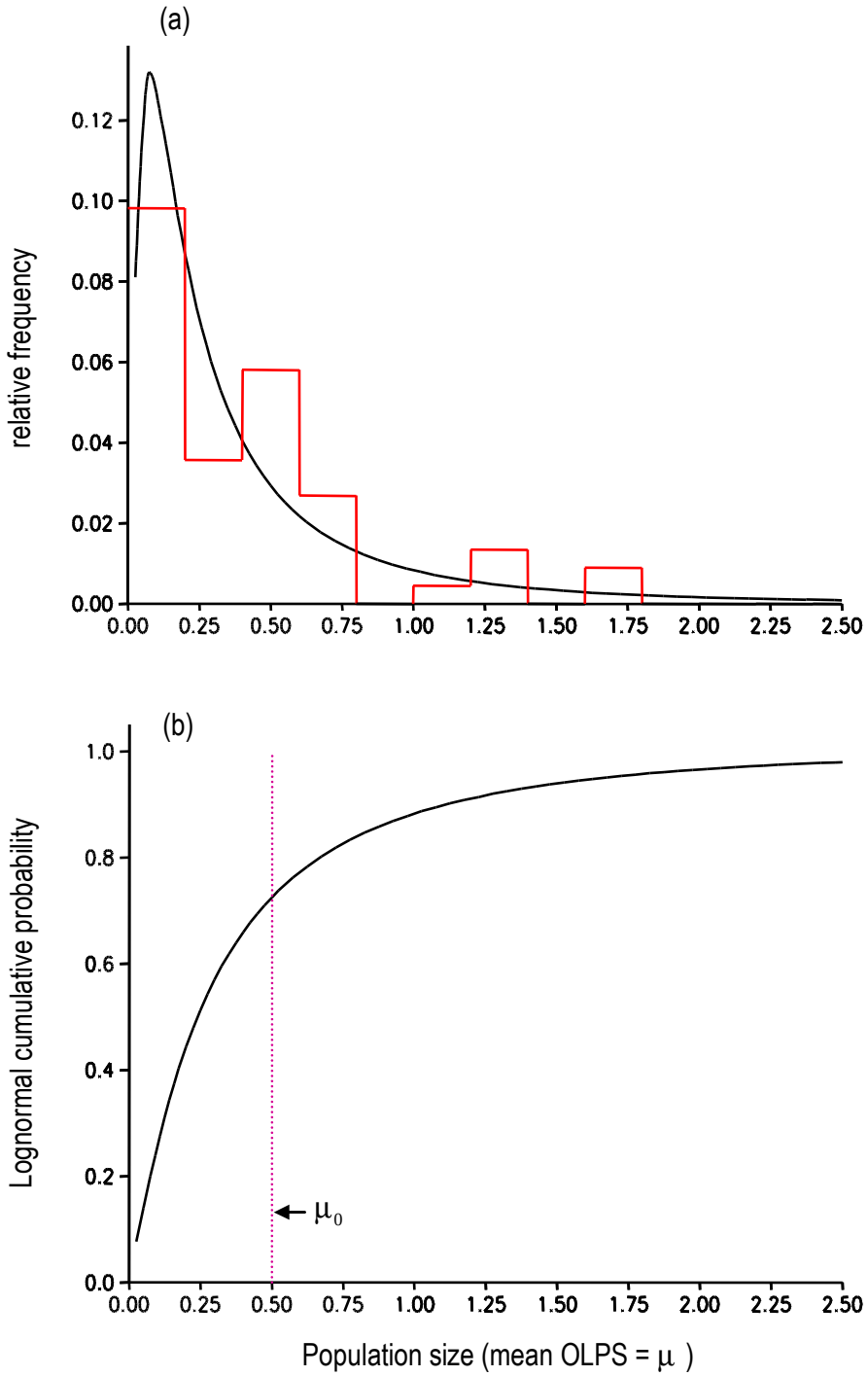

Figure 7.8 Lognormal probability functions for the distribution of population size across compartments and seasons (a) relative frequency histogram for compartment means and fitted probability density function (b) cumulative density function with 'operational' action threshold of 0.5 shown.

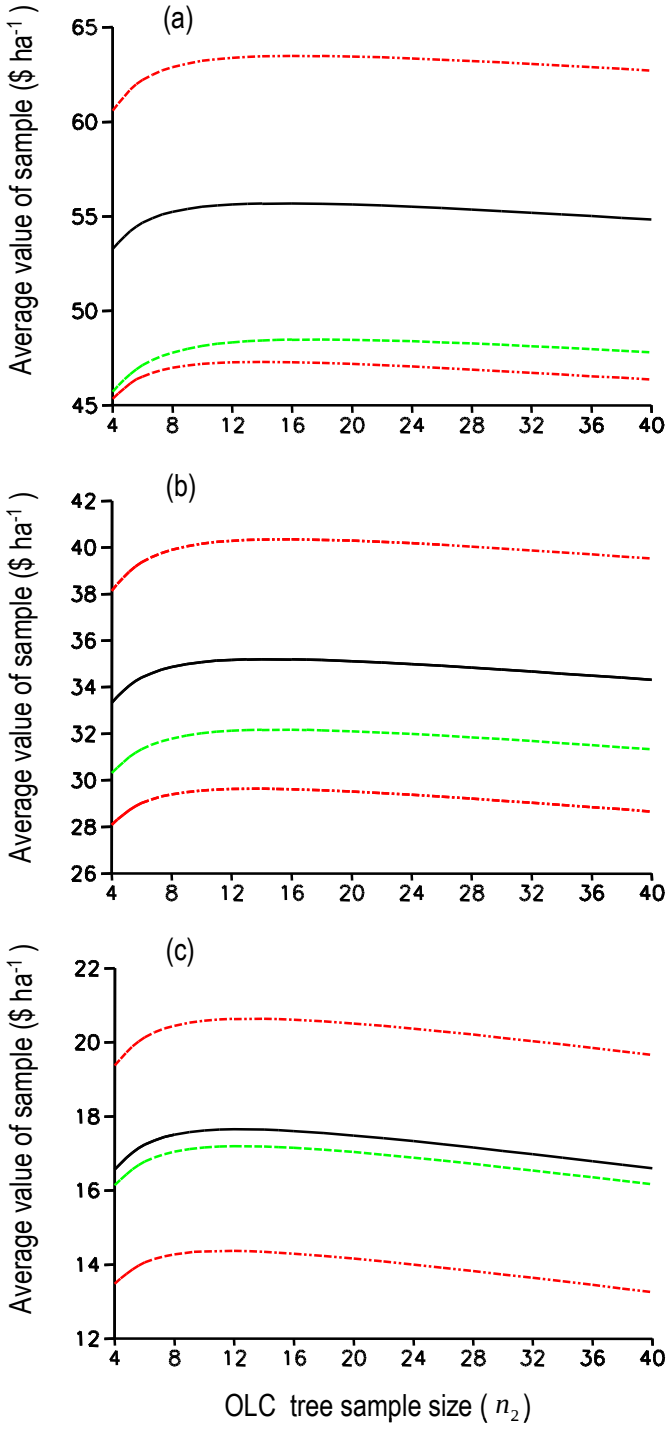

Figure 7.9 Average value of OLC sample information for the control decision for three site qualities (*S*) and corresponding action thresholds (*AT*) (a) high (*S*=28 m) *AT*=0.2 (b) medium (*S*=24 m) *AT*=0.3, and (c) low (*S*=20 m) *AT*=0.4. The average value for an 'operational' threshold *AT*=0.5 is shown (green dashed line) for each site quality. Approximate 95% confidence bands are shown. Other inputs are given in the text.

sample shoots (Table 2.4). The relationship between $EB(\mu_0)$ and n_2 is shown for both the break-even threshold for each site quality and the operational threshold of 0.5 OLPS. These values for $n_2 = 20$ are given in Table 7.1. All other inputs and cost are those that were used to obtain Figs. 7.3 and 7.4 for 'early' populations. Approximate 95% confidence bands are shown for the break-even threshold in Fig. 7.9 were these were obtained using the same method as described for Figs. 7.3 and 7.4. The expected profit foregone by using this operational threshold rather than the break-even threshold is simply the difference between their respective economic values (e.g. \$3.01 ha^{-1} for sample size of 20 for the medium site quality, Table 7.1).

Table 7.1 Cost and economic value of sampling.

Sampling scheme	Cost[1] (\$ ha^{-1})	AT[2] (μ_0)	Economic value, $EB(\mu_0)$ (\$ ha^{-1})		
			S=20 m (low)	*S*=24 m (med)	*S*=28 m (high)
OLC (n_2=20)	2.30	0.5	17.03	32.10	48.46
		BE[3]	17.48	35.11	55.62
Binomial (n^*=40)	1.44	0.5	16.90	31.63	47.62
		BE[3]	16.87	34.06	54.89
Double (n^*=40) (follow-up n_2=20)	1.84	0.5	17.15	32.31	48.78

[1] Cost of a single monitoring occasion for an average size compartment of 22 ha. For double sampling the cost is an average taking into account the proportion of monitoring occasions which require a follow-up OLC sample.

[2] Action threshold, operational (=0.5 OLPS) and break-even.

[3] Break-even thresholds of 0.2, 0.3, and 0.4 OLPS for site indices of 28, 24, and 20 m respectively. Follow-up OLC sampling based on an AT of 0.5 OLPS.

For binomial sampling (Section 2.3) a similar procedure was used whereby sample sizes of $n^* = 20$, 40, 60, and 80 were used to calculate the expected benefit. To do this the PA OC function was calculated for each sample size using (2.24) and combined with the cost of sampling function to calculate (7.3). The cost of sampling function corresponded to that for OLC sampling, (7.8), but with the sampling time per tree reduced from (90+120) to 20, corresponding to the 20 sec maximum scan

time for each binomial sample tree (Section 2.3), and n^* replacing n_2. The maximum benefit was obtained at $n^* = 40$ for each site index but the variation in the value of $EB(\mu_0)$ across the four sample sizes was very small in all cases (i.e. less than \$1) so only the values for $n^* = 40$ are given here. Table 7.1 gives these values for both the operational threshold of 0.5 OLPS and the break-even thresholds corresponding to the value of site index.

The corresponding economic values for the three site indices for the double sampling scheme (Section 2.4) using an operational threshold of 0.5 OLPS, an initial binomial sample of $n^* = 40$, and a follow-up OLC tree sample size of $n_2 = 20$, are also given in Table 7.1. The follow-up OLC sample is only taken if the predicted mean density from the binomial sample is in the range 0.34 to 1.06. The OC function used for this scheme was that for the binomial sample for mean density outside the above range and that for the OLC sample within the range. The cost of sampling is therefore a function of mean population density and is calculated as

$$C_S(n_2) = C'_F + \delta(\mu)\left\{C_T + \frac{C_L[(90+120)n_2]}{(3600)(22)}\right\} \quad ; \quad \delta(\mu) = 1 \text{ if } 0.34 \le \mu \le 1.06$$
$$= 0 \text{ otherwise}$$

where C'_F is the cost of the $n^* = 40$ binomial sample [including the fixed cost C_F in (7.8)] and C_T is the cost of traversing an average 22 ha compartment where $C_T = \$0.30$ ha^{-1} (D.Bashford, FT *unpublished data*). The effect of changing the OLC sample size n_2 between 4 and 40 was even less noticeable than that seen in Fig. 7.9. For example $EB(\mu_0 = 0.5)$ only varied by a maximum of \$1.27 ha^{-1} for *S*=24 m, corresponding to the value for $n_2 = 20$ (Table 7.1) minus the value of \$31.04 ha^{-1} for $n_2 = 4$. The approximate 95% confidence bounds for the above estimates of $EB(\mu_0)$ for binomial and double sample were very similar in size to those shown for OLC sampling in Fig. 7.9.

It may be necessary to carry out population monitoring a number of times in any single season during the period in which mass oviposition events occur. Also, as mentioned earlier, a population of eggs that is above the action threshold should not

automatically trigger a control operation. The objective of the IPM program is to minimise insecticide application so that re-sampling the compartment before the time of peak numbers of L2 larvae (see Section 7.9 below) allows the effect of natural mortality factors to operate before making the control decision. Therefore to adequately assess the benefit of sampling more than a single monitoring occasion should be considered.

For the single-pass binomial and OLC sampling schemes the extra cost of two additional monitoring occasions is \$2.88 ha^{-1} ($n^* = 40$) and \$4.60 ha^{-1} ($n_2 = 20$) respectively. Subtracting these costs slightly reduces the $EB(\mu_0)$ in each case. The average cost of control was calculated using (7.6) as \$10.45 ha^{-1} for binomial and \$10.14 ha^{-1} for OLC sampling. Allowing for three monitoring occasions and given the estimates of $EB(\mu_0)$ in Table 7.1, the rate of return (i.e. profit as a percentage of investment) on monitoring/control for a medium site quality (S=24), 0.5 OLPS operational threshold, and average cost of control is 195% [=100(31.63-2.88)/(4.32+10.45)] for binomial sampling. The corresponding figure for OLC sampling is 161% [=100(32.10-4.60)/(6.90+10.14)] while for double sampling, given an average sampling cost of \$1.84 ha^{-1} per monitoring occasion ($n_2 = 20$) and average cost of control of \$10.66 ha^{-1}, the figure is 176% [=100(32.31-3.68)/(5.52+10.66)].

To assess the impact of the IPM program on wood supply, given the inputs used above, the average loss of pulpwood volume at harvest, $ELY(\mu_0)$, for an 'early' population in year 4, a medium site quality (S=24 m), $\mu_0 = 0.5$ OLPS, and binomial sampling ($n^* = 40$) was estimated from (7.7) as 1.35 m^3 ha^{-1} with approximate 95% confidence interval of (1.17, 1.53). The corresponding average loss when there is no monitoring/control program (i.e. $\mu_0 = \infty$) was estimated as 4.35 m^3 ha^{-1} (4.22, 5.21).

The effect of the age of infestation

The results given above were based on an assumed age of infestation, T_C, of 4 years. To examine the effect of different values of T_C, the above calculations were repeated for each of ages 3 and 5 years for the medium site quality, an early population, and

'no disbudding'. All costs were incurred at, and NPVs for revenue calculated for, age T_C. Figure 7.10 shows the effect of T_C on volume loss, profit from control (and break-even threshold), and average value of OLC sampling.

7.8 COST-BENEFIT ANALYSIS USING *THE FARM FORESTRY TOOLBOX*

The Farm Forestry Toolbox (Private Forestry Tasmania, 1999) (*TOOLBOX*) 'point-and-click' software program for Windows™ 95 and 98 incorporates a number of 'tools' useful to forest managers and non-industrial forest growers. These tools range from simple 'calculators' for determining stocking from planting spacing, log volumes for a standing tree given its DBH, total height, and heights to the top and bottom of each log, to more complex 'forest inventory', and 'stand management' tools. Growth models for *Pinus radiata* (Candy, 1989a), *E. nitens* (Candy, 1997b), and *E. globulus* (Battaglia and Sands, 1997) are used in the growth prediction tool. The *E. globulus* model is a process-based site-productivity prediction model, called *PROMOD*, that requires site inputs of soil fertility class, average temperature, average rainfall, and altitude where these last three inputs can be predicted by *TOOLBOX* from the map coordinates of the site. Stand-level growth trajectories and disaggregation to individual tree diameters and heights are obtained using the models given by Candy (1989a, 1997b) and Battaglia *et al*. (1999).

Operations on the stand such as planting, fertilisation, inventory, pest control, thinning, pruning, and clearfall harvest can be defined and the associated cost or revenue assigned by the user. In the case of harvest, the revenue can be predicted by *TOOLBOX* given user-defined stumpage rates. Net present value is calculated by *TOOLBOX* at the planting year.

The only model of a growth impact, caused by natural or management events that disrupt "normal" growing conditions, that is explicitly programmed into *TOOLBOX* is the component of the stand basal area growth model expressing the impact of thinning (i.e. deliberate removal of some of the trees by the forest manager) (Candy, 1989a, 1997b). However, the 'stand management' tool allows growth-effect 'events' to be defined by the user in combination with a generic growth impact model. This impact model allows the user to input the percentage of normal growth, called the '% of current growth' value, that the defined growth- effect event produces and how

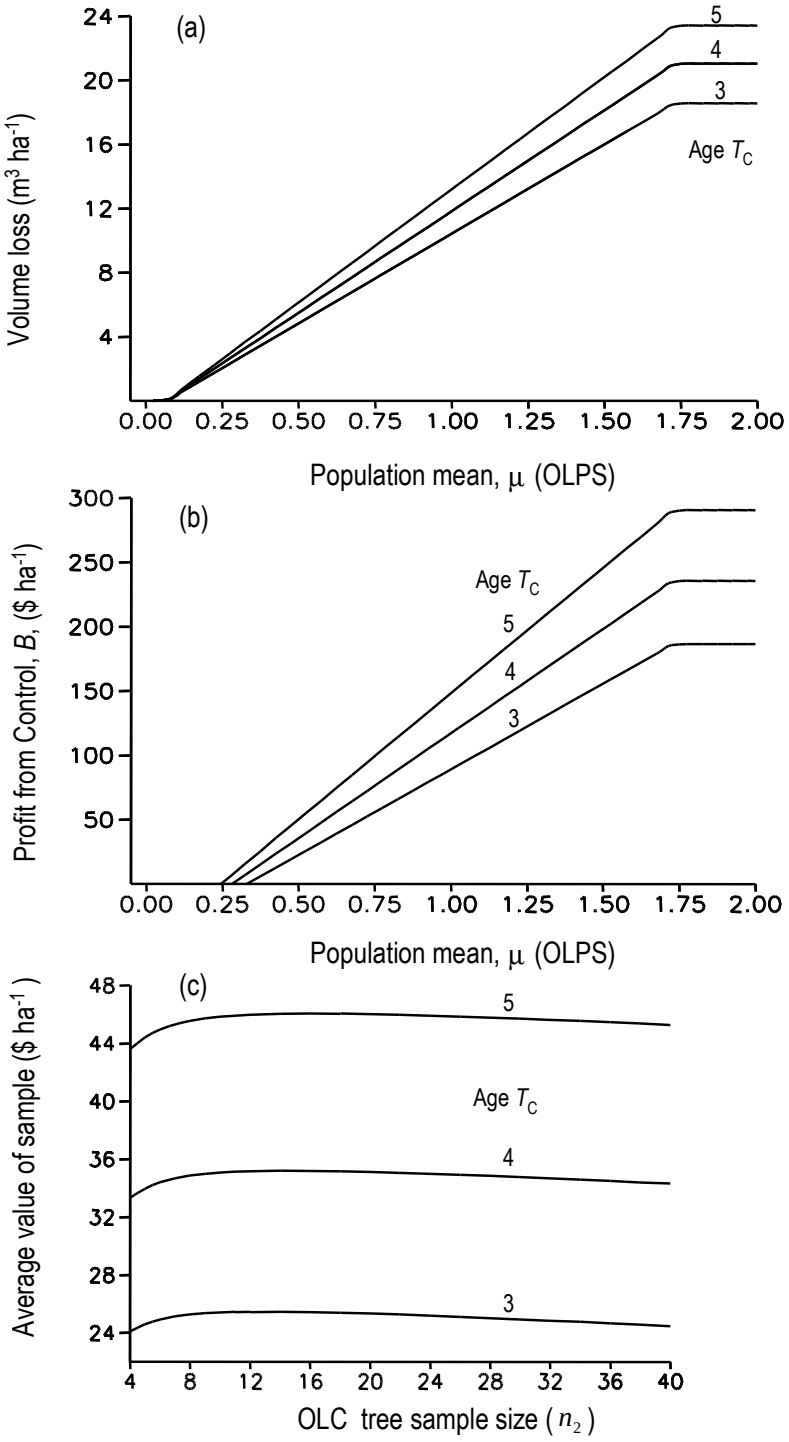

Figure 7.10 The effect of age of infestation on (a) volume loss, (b) profit from control (versus population density), and (c) average value of OLC sample information for the control decision for medium site quality (S=24), an 'early' population, no disbudding, and action thresholds of AT=0.35 (T_C =3), AT=0.3 (T_C =4), and AT=0.25 (T_C =5). Other inputs are given in the text.

many years the effect lasts for, called the ‘duration’. When the ‘decline’ option is set to ‘on’ by the user, *TOOLBOX* uses a simple linear decay function to return the stand’s growth to ‘normal’ (i.e. 100%) by the end of the period defined by ‘duration’.

Using this simple impact model, research results such as those given in this study can be simply and immediately implemented in *TOOLBOX* by providing the user with a ‘look-up table’ for a given growth-effect event (e.g. fertilisation at a given rate of fertiliser X applied at age T_C for soil type Y) that gives the appropriate value of ‘% of current growth’ and ‘duration’.

Appendix A9 describes how a growth-effect event, defined as defoliation by *C. bimaculata* larvae, can be modelled using *TOOLBOX* to modify normal growth. This is achieved by the construction of a look-up table for ‘% of current growth’ with inputs (1) the density (i.e. in terms of ‘occupied leaves per shoot’, OLPS) of a *C. bimaculata* egg population and (2) the age at the year of infestation, T_C. These tables and the instructions for their use in *TOOLBOX* are provided to users as part of the *TOOLBOX* documentation. These instructions and look-up tables are given in Appendix A10.

The inputs to these tables are the number of occupied trees from a sample of 40 trees (i.e. binomial sampling) or the mean OLPS (OLC or double sampling), the age of the infestation (i.e. ages 2, 3, 4, 5, or 6). The user then reads from the table the value of ‘% of current growth’ for the recommended duration of the growth-effect event. The tabulated values were calculated for a site index of 24 m. The effect of site index on ‘% of current growth’ was investigated but was found to be small compared to that for age of infestation, varying by less than 2% across a site index range of 20 m to 28 m. However, the formula used to generate the look-up tables is given in Appendix A9 as a function of age and site index so that values of ‘% of current growth’ can be obtained directly for any particular values of these variables.

Net present values (NPVs) for scenarios of (a) a leaf beetle defoliation growth-effect event without control and (b) normal growth resulting from a control operation, assuming 100% control, can be compared to give the required cost-benefit of the control decision. For a control operation that gives less than complete eradication, the

cost of control and the growth impact of the residual population need to be incorporated in (b).

7.9 APPLICATION OF POPULATION PHENOLOGY MODELS TO THE SCHEDULING OF PRE-CONTROL SAMPLING AND INSECTICIDE APPLICATION

The phenology models described in Chapter 6 have two primary practical applications in the Leaf Beetle IPM program. These are described below in terms of the important 'milestones' in the development of the population of immature *C. bimaculata* life-stages up to the L4 larval stage. The main difficulty in the application of these models is in obtaining a reasonably accurate estimate of the date of population initiation. A sample-based method of obtaining such an estimate is described below after the application of model predictions is outlined.

Given that a positive benefit is predicted for application of control, either from the cost-benefit analysis or by direct comparison of the sample estimate of population density with a generic action threshold, then a positive control decision may be appropriate. However, as described in the Section 6.1, if population monitoring at this time (i.e. date#1 Fig. 7.2) indicates that the population is predominantly in the egg stage then the forest manager may decide to delay the decision on control until after the population is re-assessed (the pre-control sample). At this time (date#2 Fig. 7.2) if natural mortality has been sufficient to reduce the population density below the action threshold or optimum point for the cost-benefit analysis then an unnecessary control operation can be avoided. The ideal time (date#2 Fig. 7.2) for the pre-control sample the population is when the peak in the number of L1 larvae occurs. Therefore, one application of the phenology models is the prediction of the time of the peak in densities of the larval instars (Table 6.10).

The second important application of the models is in scheduling control operations. As mentioned in Section 7.2, approximately 90% of defoliation is caused by the last two (i.e. third and fourth) larval instars so that any application of insecticide should not be delayed past the time of the peak in the number of second instar larvae. Therefore, if the decision is made to go ahead with the control operation based on population monitoring at either date#1 or date#2, then prediction of the latest date

(date#3 Fig. 7.2) at which the operation should take place would assist in scheduling spraying operations. This can be particularly important when the resources available for control operations (i.e. aircraft) are limited and, additionally, there is competition for these resources with other, possibly, more urgent tasks such as fire-fighting. This operational 'window' mentioned in Section 6.1 is the time up until date#3 which can be taken to be the predicted date when the peak in the number of L2 larvae occurs.

Table 6.10 gives estimates of the time in day-degree units (DD[5]) from the time of population initiation (i.e. mass oviposition) to the time in peak occurrence of each of L1, L2, and L3 larvae. The time to peak L1 was estimated to be of the order of 127 *DD*[5] given a moderate level of natural mortality. The corresponding time to peak in L2 numbers was a further 48 *DD*[5] (i.e. 175 *DD*[5] from population initiation). If the forest manager needs to estimate date#2 given the current time is between date#1 and date#2, or similarly prediction of date#3 is required then two problems present themselves. Firstly, it is essential that the calculation of day-degrees be based on estimates of daily minimum and maximum temperatures for the particular compartment. Secondly, the date of population initiation is required from which day-degrees can be accumulated.

Reasonably accurate estimates of compartment-specific daily minimum and maximum temperatures can be obtained by updating estimates of these extrema using daily meteorological reports for the nearest weather station and adjusting these to that expected given the altitude, aspect, and surrounding terrain (i.e. using a digital elevation model) of the compartment. These could be incorporated in a predictive system (e.g. Schaub *et al*., 1995; Régnière, 1996) and implemented in 'user-friendly' computer software such as BioSIM (Régnière and Logan, 1996). Given these values and short-term forecasts, the day-degrees can be accumulated and used to indicate likely values for date#2 or date#3.

Accurately determining the date of population initiation is more difficult. A simple, sample-based approach is described below.

Predicting the time of population initiation from population monitoring

Since it is impractical to collect stage-frequency data during routine population monitoring, a sampling method is required which uses the current method of counting occupied leaves (Section 2.2) for a sample of trees and shoots within trees. The following method of sampling to allow estimation of the date of population initiation is suggested.

A simple tally is made of the number of occupied leaves that have (a) only eggs (N_e), (b) only larvae (N_l), or (c) both eggs and larvae (N_{el}). Using these counts estimation of the elapsed time, t_1, from the time of population initiation (i.e. mass oviposition), t_0, to the sampling date (date#1 or date#2) depends on the following results from sampling. Firstly, assuming the total number of occupied leaves, $N = N_e + N_l + N_{el}$, is large (e.g. greater than $120\mu_0$, the action threshold multiplied by the total sample size of shoots) two cases are considered:

(1) Both N_l and N_{el} are zero or relatively small (e.g. less than 2% of *N*).

(2) Either N_l or N_{el} are of significant size (e.g. greater than or equal to 2% of *N*).

For case (1), t_0 is estimated heuristically as a calendar date using a combination of local knowledge and 'guestimation', for example, using an estimate of the daily maximum temperatures for the previous 4 to 7 days and de Little's observation (de Little 1979, 1989) that mass oviposition does not take place until the temperature is above $25\,^{o}\mathrm{C}$. The elapsed time, t_1, is simply the difference between the two dates in the required day-degree units.

For case (2), inverse estimation can be used. The estimate of t_1, taking $t_0 = 0$ without loss of generality, can be obtained in *DD*[5] units from model (6.6) as

$$\hat{t}_1 = \hat{\beta}_{11}^{-1} \left\{ \ln\left(\frac{1}{1-\hat{p}} \right) - \hat{\beta}_{01} \right\} \qquad (7.9)$$

where $\hat{p} = N_e / N$. For example, using the pooled parameter estimates in Table 6.4, if $\hat{p} = 0.05$ then $\hat{t}_1 \cong 63 DD[5]$. The predicted stage proportions and time of peak relative or absolute occurrence for L1 to L3 larvae can then be predicted, given observed, estimated, or projected daily minimum and maximum temperatures, described above, by accumulating *DD*[5] forward from the sampling date and adding $\hat{t}_1$.

7.10 DISCUSSION

Effect of disbudding on growth loss

Figures 7.3 and 7.5 show the effect of including the 'complete disbudding' on volume loss via its effect on apparent defoliation level, P (Section 7.4, Step 3.2) for early and late populations respectively. Figures 7.4 and 7.6 show how the extra volume loss due to disbudding affects the profit of control versus population density relationship. The simulated effect of disbudding was applied in Step 3.2 via P estimated as part of the shoot-level defoliation impact model given by the regressions in Table 4.7. Therefore, the predicted effect of disbudding on growth of tree DBH and height in Step 3.2 excluded the disbudding term, $\beta_1 D$, in model (5.5) since this effect was already included in P.

The alternative method which excluded the effect of disbudding on P but including the above disbudding term in predictions from model (5.5) was used to obtain Fig. 7.7. Comparing Figs. 7.3 and 7.7 it can be seen that the impact of disbudding is much greater using this last method. The more conservative approach of including disbudding effects only via apparent defoliation, P, is preferred. This is because the process of manually disbudding the tree may have exaggerated the effect of natural disbudding since fine branches as well as buds were removed in the top of the crown by pole pruning and, inevitably, there was some breakage of tender young branches when stripping buds by hand.

Even so, since the prevalence and degree of disbudding as a function of the population density of larvae has not been quantified, it is difficult to know if disbudding effects should be included in simulations. Here, if the population of eggs was greater than 5 eggs then a complete disbudding was assumed if the disbudding

effect was included in predictions. Observations from the caged-shoot feeding trial suggest that the larvae do occasionally disbud the shoot particularly when there is insufficient fresh (i.e. tender) expanding foliage (Section 4.3). However, more general field observations suggest that disbudding by larvae is uncommon (D. Bashford, FT *pers. comm.*). Until better information is available it is recommended that the conservative approach, adopted here, of assuming the larvae do not disbud the shoots is appropriate.

Effects of age of infestation, persistence of growth impact, and successive years of defoliation on volume loss and economic analyses

The form of the yield loss versus population density relationship shown in Figs. 7.3, 7.5, and 7.10(a), with a plateau for each of low and high densities and a linear increase in between, corresponds to the generalised yield versus number of insects (or number of injuries) given for agricultural crops by Bardner and Fletcher (1974).

For long-lived crops such as timber-tree species the considerable time lag between age of infestation and age of harvest introduces extra complexity in the relationship between yield loss and population density. For example, the effect of increasing age of infestation is to increase the volume loss caused by a given population density which has a flow-on effect on profit of control and average value of sampling (Fig. 7.10). This is due to the property of the growth impact model that it reduces the standing basal area and MDH at age $T_C + 3$ (for an early population) but does not change the site index. Therefore, since growth rates for stand basal area and MDH predicted by the projection models depend in part on site index, the growth trajectories from age $T_C + 3$ onwards tend to converge to that obtained under the 100% control option (i.e. 'normal' growth). As a result, the further $T_C + 3$ is from the harvest year, T_H, the greater the degree of convergence and the smaller the amount of predicted growth loss.

The economic analyses given were demonstrated using the case of a short-rotation pulpwood regime. However, if other regimes such as a 25-year rotation sawlog regime (Candy and Gerrand, 1997) is planned the complex regime-specific effects of the difference between ages $T_C + 3$ and T_H on growth losses and the difference in

products and their stumpage values should be taken into account. This can be done using a cost-benefit analysis specific to the each regime and age of infestation using, for example, *TOOLBOX*.

Further complications of the yield loss/population density relationship arise due to (a) the persistence of growth impacts over a number of years after a defoliation event in a single season and, combined with this, (b) the cumulative effect of defoliation over consecutive seasons. Persistence effects (a) were incorporated empirically by calibrating growth loss, using model (5.5), after three growing seasons from the year of infestation using the artificial defoliation trials. These trials indicated that this period was sufficient to account for persistence effects, even for heavy levels of defoliation. Model (5.5) also accounts for any earlier recovery of growth rates using observed tree heights and diameters at the end of measurements of the artificial defoliation trials since these were used to calibrate this model.

Cumulative effects (b) of defoliation have been incorporated in other models using a cumulative defoliation index such as the sum of the percentage foliage loss over consecutive seasons (e.g. . Abbott *et al*., 1993; Erdle and MacLean, 1999). However, this approach assumes additivity of effects (e.g. a single 80% defoliation in year one has the same long-term impact on growth as 20% defoliation in each of years 1 to 4). Model (5.5) in contrast incorporates an effect for a single repeat year of defoliation separately from the effect of the initial defoliation. Figures 7.3 and 7.4 show that the effect of a repeat defoliation on growth loss and profit resulting from two consecutive early populations of the same density at ages 4 and 5 when averaged over two years was almost identical to that for a single age-4 population. The volume loss, and therefore profit of control, for repeated late defoliations was slightly greater for the late population and also increased in relative size as site quality decreased (Figs. 7.5 and 7.6).

Since treatments involving three or more consecutive years of defoliation were not included in the trials described in Chapter 5, the validity of ignoring any defoliation in years prior to the previous year when determining the growth impact of the current population is difficult to verify. However, the current IPM program requires this assumption to be made since routine assessments of defoliation are not carried out.

Even if these assessments were carried out they would be of little use without a model of the long-term impact of uncontrolled populations (i.e. those below the operational threshold) on growth that has been calibrated using permanent growth plots that also monitor *C. bimaculata* population densities.

Break-even versus operational action thresholds

An 'operational' action threshold of $\mu_0 = 0.5$ OLPS has been assumed throughout this study because this value represents the lowest achievable threshold (D. Bashford, FT *pers. comm.*) given that, on average, it requires approximately 28% of monitored compartments to be sprayed each season. This lower limit is due to the restriction on the maximum number of control operations that can be carried out in any one or two-week period given the number of aircraft that are appropriately equipped and available. In this case, a cost-benefit analysis may indicate that, over the long term, putting additional aircraft on 'standby' is profitable. This analysis would be based on the rate of expansion of the plantation estate, the average threshold achieved (i.e. which may be higher than 0.5 OLPS), and the economic losses accumulated from failure to control populations above break-even thresholds.

Nevertheless, despite direct economic losses resulting from the use of a conservative threshold of 0.5 OLPS there is a benefit that has not been considered so far. That benefit is that some allowance is made for costs of control that are difficult to quantify and were therefore excluded from (7.1). These 'costs' include negative environmental effects of broad-spectrum insecticides. Examples of such environmental costs are (a) the reduction in populations of beneficial insects which help control *C. bimaculata* populations through predation or parasitism, (b) reduction in populations of other non-target invertebrates, and (c) public concerns over insecticide application. It is beyond the scope of this study to consider these 'indirect' costs of the current control tactic of broad-spectrum insecticide use. However, cost-benefit analysis can easily be carried out for the considerably more 'environmentally benign' control strategy of applying the bio-insecticide Novodor FC. The method and software implementation (Appendix A10) of carrying out this analysis have been described above.

Economic value of the population monitoring/control decision component of the IPM

All three sampling schemes/decision rules returned a substantial profit, $EB(\mu_0)$, for each site quality (Fig. 7.9, Table 7.1) and age of infestation (Fig. 7.10c) for both break-even and operational thresholds (μ_0). This was still the case when considering lower 95% confidence limits for $EB(\mu_0)$. Therefore, since population monitoring is economically justified a decision is required on which sampling scheme should be used and at what sampling intensity.

Given the assumptions used, the average value of the sample information was found to be reasonably insensitive to sampling intensity for each of the three schemes. This suggests that the gain in economic value from the increased reliability of decisions largely compensated for the extra cost of more intensive sampling. From Fig. 7.9 it can be seen for OLC sampling that the degree of compensation decreases with site quality as a result of the decreasing loss in yield (Fig. 7.3) and thus lower cost of damage. For the lower-cost binomial and double sampling schemes the 'value of sampling/sample intensity' relationship gives even less guidance on the choice of an optimum sampling intensity.

The decision on what sampling intensity to use rests on whether a saving in sampling costs in the current year is preferred to gains in harvest revenue in the future as a result of better control decisions. A similar comparison can be made between sampling schemes. The cheapest scheme is the binomial and although the profit is less than the other two schemes it gives the greatest return on investment (195%).

These results reflect the long-term average population density over a large forest resource where the resources available to carry out sampling can be limiting. In this case the cheapest sampling scheme, and therefore most conservative in use of resources, would be preferred. For a non-industrial grower (e.g. a farmer) with a relatively small compact area of plantation to manage, resources to carry out sampling may not be as limiting. Also, with less ability to spread the risk of lost production, a greater priority for the non-industrial grower may be to ensure the plantation is adequately protected. In this case the higher-cost double sampling scheme may be preferable to the binomial scheme. The single-phase OLC sample gives the lowest risk of an incorrect control decision but it also gives the lowest

return on investment. The high cost of this scheme may discourage population monitoring if the effort is seen as unproductive particularly after a series of years when pest activity is low.

The expected economic value of monitoring given the distribution of site quality

Strictly, when calculating expected profit of the population monitoring/control component of the IPM program site quality should be treated as a random variable rather than the fixed values used here of. *S*=20,24,28 m. The expected loss function that takes the effect of variable site quality into account and uses a fixed, operational threshold is given by

$$EL(\mu_0) = \int_s \int_u Loss\{u, \mu_0\} f_\mu(u) f_S(s) \, du \, ds$$

where *S* is site index with long-term PDF across existing and future compartments of $f_S(.)$. A further degree of complexity is added if there is a dependency of population density on site quality, expressed as a function such as $\mu = g(S)$ so that $f_\mu(.)$ is replaced by the conditional PDF $f_{\mu|S}(.)$. For example, higher site quality may result in higher leaf nitrogen levels resulting in higher larval survival. Also a high site quality may produce a greater recuperative ability of the trees after defoliation allowing high population levels to be sustained. Alternatively, the population density and site quality distributions may be simply correlated due to common dependence on site factors such as altitude and aspect so that the product of density functions $f_\mu(.)$ and $f_S(.)$ is replaced by the joint PDF $f_{\mu,S}(.)$.

There is insufficient data at this time to investigate possible forms for $f_{\mu|S}(.)$ or $f_{\mu,S}(.)$ given existing plantations. In addition, since the plantation estate is in a stage of rapid expansion the long-term average site quality is difficult to predict. The range in site quality used here of *S*=20 to 28 should include this long-term average with high probability. Therefore, the results given here should realistically reflect the economic benefits of the IPM program over the long term.

Should sample sizes be proportional to compartment size?

The results described here and in Chapter 2 have assumed an average compartment size of 22 ha. This was based on a time-and-motion study for OLC sampling that used a compartment of this size (Table 2.3) (D. Bashford, FT *unpublished data*). The average walking time to traverse a compartment when selecting sample trees will increase approximately linearly with increasing compartment size. Therefore the relationship between this 'fixed' cost of sampling and variable sampling costs will change with compartment size unless the time taken to collect samples is adjusted in proportion to compartment size. However, the guiding principle in setting a sample size for an individual compartment is that which achieves the nominal reliability for the control decision for the area of plantation to be managed as a unit in terms of aerial application of insecticide. The variation in population density for a given plantation area (i.e. a function of the spatial pattern of density) and the specification of appropriate management units is complex and insufficient information is available to make definite recommendations at this time. A possible solution though is to, where practical for the purposes of population monitoring and control operations, amalgamate small compartments and divide large compartments to give pest management units of the order of 20 ha in size.

Predicting the time of population initiation from population monitoring

It could be argued that the numerator in the estimate of *p* in (7.9) should include some proportion of the N_{el} leaves. However, without further research it is difficult to provide a value for the proportion *p* that gives, on average, the best prediction of t_1. Until such research is carried out, the observation that a second, later oviposition rarely occurs on the same leaf (D. Bashford, *pers. comm.*) can be applied. Thus, in general, only a single cohort occupies the leaf so that when neonate or older L1 larvae are observed on a leaf with unhatched eggs it is usually only a matter of hours or at most another full day before the remaining eggs hatch. Therefore, a more accurate estimate of t_1 is obtained if N_{el} is completely excluded from the numerator.

The effect of defoliation on wood supply

In Fig. 7.1 the potential impact of compartment-level population monitoring/control on wood supply level at the resource level is indicated. As mentioned in the introduction, an aspect of forest pest management that is the main focus of forest

planners is the prediction of the impact of forest pests on sustainable wood production strategies.

For example, a crude approximation of the impact of uncontrolled *C. bimaculata* larval populations under the IPM with insecticidal control (i.e. those below the operational threshold) on wood supply can be obtained from the above results. For example, given a 15-year pulpwood rotation, a 0.5 OLPS threshold, and average site index of 24 m, then over the 5 years of the rotation that the IPM program operates an average loss of production of the order of almost 7 m^3ha^{-1} (i.e. 5x1.35) could be expected. If insecticidal control is not used the corresponding lost production would be of the order of 22 m^3ha^{-1} (i.e. 5x4.35). For a 15,000 ha plantation estate harvested on a 15-year rotation this last figure would represent a total loss in production of 22,000 m^3yr^{-1} out of an expected harvest of around 280, 000 m^3yr^{-1}. Discounting the corresponding average loss in stumpage to age 4 using an 8% discount rate and \$30 m^{-3} stumpage gives a loss of nearly \$56 ha yr^{-1} ($=30x4.35/1.08^{11}$) compared to the average cost for the IPM program of binomial sampling and control of \$14.77 ha yr^{-1} (=\$4.32+\$10.45 respectively).

A more sophisticated approach would be to use predictions of long-term average population density for each compartment stored on Forestry Tasmania's Geographic Information System (GIS) to predict lost wood production given the compartment's nominal silvicultural regime and estimated site index. However, a method of predicting population density has not as yet been developed.

The impact on wood supply and economics given above is probably conservative given the exclusion of the impact of disbudding on growth. In addition, the estimates of apparent defoliation as a function of population size may be conservative given that this relationship was based on the estimate of 'effective leaf area loss per larvae' (ELAL) from the simulation model in Section 4.3 and only 60% of the growth loss was explained by this model (see Fig. 4.17b).

As well as the above, the impact of adult feeding over the rotation and the impact of larval feeding on compartments where the stand is too tall for monitoring to be carried out are yet to be quantified.

7.11 SUMMARY

1. The application of the suite of predictive models, described in previous chapters, for decision support within the Leaf Beetle IPM system was demonstrated. For a typical 15-year rotation pulpwood regime on a site of average quality with a discount rate of 8%, a cost of control of $35/ha, and a stumpage of $30/$m^3$, a value of 0.3 occupied leaves per shoot would be the recommended action threshold.

2. Given the low costs of insecticidal control of pest populations and population monitoring compared to the relatively high cost of predicted average damage levels from larval browsing, the population monitoring/control decision component of the Leaf Beetle IPM program is profitable with the best sampling scheme giving a 195% return on investment.

3. There would be some direct economic benefit in lowering the action threshold from the current operational value of 0.5 to 0.3 OLPS of the order of $2.40 ha^{-1} but this lower threshold may not be achievable given the large increase in the number of control operations required from approximately 28% to 45% of monitored compartments. In addition, lowering the threshold would reduce the 'buffer' which accounts to some degree for unquantified economic costs of insecticidal control such as the reduction in populations of beneficial insects.

4. For a large industrial forest grower such as Forestry Tasmania, the binomial sampling scheme is recommended as a cheap, effective, and easily implemented method of population monitoring suitable for large areas of plantation. For non-industrial growers with a smaller forest estate the greater sampling effort required by the double sampling scheme may be worthwhile in order to obtain the greater degree of reliability of control decisions it affords.

5. A method for carrying out the cost-benefit analysis of a decision to control using insecticide given an estimate of population density and site quality was described and its implementation in *The Farm Forestry Toolbox* software program was outlined. This software program is available free of charge.

6. A method of predicting the latest date at which insecticide should be applied given daily minimum and maximum temperatures and date of mass oviposition or a sample estimate of the proportion of occupied leaves which are occupied only by egg batches is described.

7.11 RECOMMENDATIONS FOR FUTURE RESEARCH AND CONCLUSIONS

In the process of carrying out the research in this study a number of areas requiring further research have been identified. The studies of highest priority in the opinion of the author are:

1. Collection of a calibration data set for binomial sampling using occupancy and population density based on egg batches alone for a wide range of population densities. This dataset would be used to calibrate model (2.19) and should result in improved reliability for binomial sampling of egg populations, the recommended operational method of monitoring for a large-scale plantation estate.

2. Studies of *E. nitens* within-leaf pattern of expansion and average within- and between-leaf patterns of *C. bimaculata* larval feeding when combined with a leaf expansion model described in Section 3.2 and laboratory-based feeding studies (e.g. Baker *et al*., 1999) would allow more robust models of the growth impact of larval feeding to be constructed than those described in Section 4.4. Such models would have the additional benefit of being easily re-calibrated for different pests and/or feeding behaviour (e.g. reduced *C. bimaculata* larval feeding rates caused by sub-lethal doses of Novodor FC).

3. A series of permanent sample plots (PSPs) which measure tree growth and, for ages 2 to 6, incorporate population monitoring and defoliation assessments are required to estimate the long-term growth losses from consecutive seasons of uncontrolled leaf beetle browsing. It would be important to measure population density and defoliation for adults separately to that for larvae. A large number of

PSPs for measuring tree growth are to be established for the purpose of developing growth models for forest planning (E. Baalman, FT *unpublished report*). Therefore, for the marginal increase in cost required to carry out population monitoring and defoliation assessments, these plots would provide valuable data for strategic pest management.

4. Predicting likely times of mass oviposition for a given compartment from landscape-level predictive models, such as that described in Schaub *et al*. (1995) and Régnière (1996), would assist in planning when to carry out population monitoring. These models require calibration using long-term results from population monitoring combined with data on site-specific factors that influence population densities. This approach, if sufficiently accurate, would result in a reduction in the number of times population monitoring is required over the current fixed monitoring period of December and January.

Despite the limited nature of some of the datasets in this study, the predictive models developed have important practical applications in the Leaf Beetle IPM program. The improved decision making that can be obtained by using these models within the DSS system outlined in Fig. 7.2 and implemented in The Farm Forestry Toolbox elevates the current IPM to the status of a true level-I IPM using Kogan's (1998) classification. These predictive models and their application need further refinement, for example as outlined in points (1) to (4) above. However, the most urgent research is the search for a cost-effective, selective insecticide as an alternative to the broad-spectrum pyrethroid in current operational use.

The implementation of the predictive models developed in this study into the current Leaf Beetle IPM program makes it, even if not the 'holy-grail' of forest pest management in Australia (Clarke, 1997), the most comprehensive and scientifically-based IPM for an insect defoliator of eucalypt forests.